Dear Editor,

We would like to warmly thank you for editing our manuscript. We have updated it according to the comments of the reviewers as suggested in our responses. You can find here below the point-by-point response to reviewers comments, where the lines correspond to the revised manuscript and where slight changes in wording have been made, as well as the final version of our manuscript with track changes.

On behalf of all Co-Authors,

Jeanne Rezsöhazy

Dear editor and reviewers, we would like first to thank you for your useful feedbacks and comments on our manuscript. You can find here below the Referee's comments in *italics* and our answer in blue. In **bold**, you can find the modifications that will be made to the manuscript.

Referee#1 Vladimir Shishov

The paper "Application and evaluation of the dendroclimatic process-based model MAIDEN during the last century in Canada and Europe" by Rezsöhazy et al. is a good example to explain specifics of MAIDEN model application taking into account a complexity of such multidimensional tool to simulate tree growth under climatic influence in different environments. The overall impression of the paper is very good. The logical structure of the manuscript, a detailed description of the parametrization procedure of the model itself and skills comparison of two models: VS-Lite and MAIDEN are noteworthy. I want to underline that the parametrization of such models, their calibration and verification is a key point to apply correctly a tree-growth simulation in different habitats.

We would like to warmly thank the Referee for this very positive general feedback, for the careful evaluation of our manuscript as well as for the useful comments that will be addressed in the revised version as specified here below.

The authors mentioned that their "results provide a protocol for the application of MAIDEN to potentially any site with tree-ring width data in the extratropical region". I am wondering did the authors make the MAIDEN code available in some open-access depository to use it for wider group of researchers. I am sure the tables of optimal parameter values for some sites as well as corresponded climate data and tree-ring chronologies putting on-line will allow to make the model itself more applicable in the research community.

I suggest that the paper can be published after minor revision.

We agree with the Referee that an open-access depository with results and data from the paper would be worthwhile. Currently, all climatic data are publicly available (except NRCAN that is available on request) and the links for downloading them will be added to the manuscript. The links to access the European tree-ring width data will also be added. For the Eastern Canadian taiga sites from Nicault et al. (2014) and Boucher et al. (2017) that has been used in the paper, an online reference will be provided in the paper, that links to a web site under development to share the tree-ring network of Québec-Labrador from which the Canadian data in the manuscript come: http://dendro-qc-lab.ca/trw.html. Finally, the parameters values will be added in the supplementary material, following to another comment from the Referee (see below).

The structure of the MAIDEN model is visible online (https://figshare.com/articles/MAIDEN_ecophysiological_forest_model/5446435/1) and its modules are available upon request.

Specific comments

Section 100 "...the ongoing phenological phase (five phases per year: winter 1, winter 2, budburst, summer and fall)" Could the authors explain what is the difference between winter1 and winter 2 phenological phases?

The explanation will be added to the text on lines 103-104 (p.4), as follows: "(five phases per year: **winter 1 with no accumulation of growing degree days (GDD), winter 2 with active GDD accumulation**, budburst, summer and fall)".

Section 125 "Those chronologies have been standardized using the Age-Band Regional Curve Standardization (or RCS) method". Did the authors use pith estimations for individual tree-ring series? Did the authors split fast and slow growing trees to avoid end-effect bias?

We would like to highlight that the tree-ring series were compiled before this article. All trees were dated and measured on cross-sections sampled at breast height (1.3m). The pith offset was done one for all trees. All samples were collected on dominant trees growing in homogeneous forests and it was not necessary to separate fast-growing trees from slow growing trees in such conditions.

Accordingly, we will add the following information to the manuscript, on lines 129-133 (p.5):
"A network of tree-ring width chronologies of Picea mariana collected in similar conditions is available for the Eastern Canadian taiga (Nicault et al., 2014; Boucher et al., 2017, http://dendro-qc-lab.ca/trw.html). **We use here the tree-ring series directly derived from this compilation, without any modification.** The chronologies have been **previously** standardized using the Age-Band Regional Curve Standardization (or RCS) method **proposed by Briffa et al. (2001) and further applied to a similar boreal dataset by Nicault et al. (2014).**"

Similarly, the same information will be added on lines 160-161 (p.6) for the European sites:
"**Similarly to the Eastern Canadian taiga chronologies, the tree-ring series were not modified here.**"

Section 135 "...we get five aggregated sites (Table 1)" What are intersite correlations (Rbar) between tree-ring chronologies at the same one-degree grid? Could the authors clarity this point in the paper?

Proximity between sites was used as a criterion for building our aggregated chronologies because we assume that we can reduce the non-climatic noise in low-replicated chronologies by averaging close chronologies. A one degree grid appears to us as an objective way to merge sites together. The intersite correlations between tree-ring chronologies (chronologies inside the same one-degree grid have the same colour) is presented here below (all significant at a confidence level of 99%).

The average intersite correlations for all aggregated sites will be added to the manuscript on lines 143-144 (p.5), as follows: "**The aggregation allows us to get relatively good inter-sites correlations inside the same one-degree grid, ranging from 0.442 to 0.732 with an average of 0.558.**".

	WCORPL	WNFL1V	WNFLR1	WDA1R	WTHH	WROZM	WROZX	WHER	WHH1	WHM1	WHM2
WCORILE	0.692	0.539	0.624	0.626	0.643	0.653	0.588	0.472	0.374	0.586	0.461
WCORPL		0.492	0.577	0.537	0.329	0.497	0.731	0.504	0.587	0.581	0.570
WNFL1V			0.509	0.235	0.239	0.466	0.400	0.241	0.135	0.280	0.456
WNFLR1				0.541	0.177	0.541	0.662	0.389	0.313	0.429	0.333
WDA1R					0.442	0.621	0.586	0.303	0.548	0.579	0.493
WTHH						0.494	0.140	0.222	0.025	0.535	0.296
WROZM							0.582	0.331	0.349	0.598	0.499
WROZX								0.548	0.641	0.528	0.518
WHER									0.485	0.501	0.454
WHH1										0.589	0.593
WHM1											0.732
WHM2											

Section 135 "This observational network represents an archetypal example of a singular species that covers an important hydroclimatic gradient" Why is the gradient important? Could the authors explain it?

Sites located along the western (near James Bay, WNFL1V) and eastern (near Labrador sea, WL32) margins of the study area present the warmest growing seasons in the network (864 growing degree-days >5°C for the 1976-2005 period, Hutchinson et al., 2009). Sites located in the center of the Quebec-Labrador peninsula (WHM2) present a much shorter growing season (692 growing degree-days >5°C) much like the sites located further north (WLECA, 573 growing degree-days >5°C). Annual precipitation increase from west to east, passing from 668 mm (WNFL1V) to 907 mm (WL32) but significantly decrease with latitude, reaching only 567 mm (WLECA) for the 1976-2005 period (Hutchinson et al, 2009).

The manuscript will be modified accordingly on lines 144-152 (p.5), as follows: "This observational network represents an archetypal example of a singular species that covers an important hydroclimatic gradient. **Sites located along the western (near James Bay, WNFLV1, Fig. 1a) and eastern (near Labrador sea, WL32, Fig. 1a) margins of the study area present the warmest growing seasons in the network (864 growing degree-days above 5° for the 1976-2005 period, Hutchinson et al., 2009). Sites located in the center of the Quebec-Labrador peninsula (WHM2, Fig. 1a) present a much shorter growing season (692 growing degree-days above 5°), much like the sites located further north (WLECA, Fig. 1a, 573 growing degree-days above 5°). Annual precipitation increases from west to east, passing from 668 mm (WNFLV1, Fig. 1a) to 907 mm (WL32, Fig. 1a), and significantly decreases with latitude, reaching only 567 mm at WLECA (Fig. 1a) for the 1976-2005 period (Hutchinson et al., 2009). This makes it a relevant candidate for our calibration and validation exercises.**"

Section 170 "The comparison relies on the computation of the model likelihood defined as the sum of the logarithms of the normal probability densities of the residuals between the model simulation and the observations". Why the authors use the logarithms of the normal probability densities of the residuals? Are the residuals non-normal distributed? It seems to me by such transformation the authors tried to adopt the Markov chains procedure to their parametrization taking into account strong requirement of data normality in Markov processes.

The logarithmic transformation appears to us as a common operation to maximise likelihood in Bayesian statistics for reasons of algebraic simplicity as well as numerical stability, as mentioned in Vrugt (2016, p.275, just before equation (8)). This paper also presents the DREAM software that we use for the Bayesian calibration of our selected parameters.

Vrugt, J.A.: Markov chain Monte Carlo simulation using the DREAM sofware package: Theory, concepts, and MATLAB implementation, Environmental Modelling & Software, 75, 273-316, 2016.

Section 190 "Pearson correlation coefficients between observed TRW and simulated Dstem were computed, as well as the corresponding confidence level" Pearson correlation is not enough to guarantee a convergence of simulated curve with initial chronology. Why did not the authors use an additional criterion such as RMSE minimising or others?

We agree with the Referee that other indicators could have been used for the analysis. We wanted to only use one indicator in order to simplify the message but in the future, other statistical measures could be considered for a more careful evaluation of our method. We also would like to highlight that because of the normalization of both observations and simulations (due to different units), some indicators like RMSE do not bring much new information compared to correlations.

Section 200 "The VS-Lite parameters are calibrated at each location..." How many parameters were optimized keeping in mind that overall 11 of them were used in the VS-lite? Could the authors describe them more precisely in the ms.

Four VS-Lite parameters, corresponding to the lower and upper temperature (T_1 and T_2 in Tolwinski-Ward et al., 2011) and soil moisture (M_1 and M_2 in Tolwinski-Ward et al., 2011) thresholds of the model, have been optimized using the Matlab code from Tolwinski-Ward et al. (2013). The other parameters have been kept to default values. This information will be added to the manuscript on lines 224-227 (p.10), as follows: "The VS-Lite parameters are calibrated at each location following a bayesian approach described in Tolwinski-Ward et al. (2013). **In this study, four VS-Lite parameters, corresponding to the lower and upper temperature (respectively T_1 and T_2 in Tolwinski-Ward et al., 2011) and soil moisture (respectively M_1 and M_2 in Tolwinski-Ward et al., 2011) thresholds of the model, have been optimized. The other parameters were fixed to default values**."

Supplementary materials. Could the authors include the table with the optimal MAIDEN and VS-lite parameter values for all sites in Canada and Europe?

We will add the tables in the supplementary materials for all 21 Canadian sites, 5 aggregated Canadian sites and three European sites (1950-2000).

Supplementary materials. Among with Fig. S2, S3 could the authors include the obtained distributions of the MAIDEN parameters?

We will add the figures in the supplementary materials for all 21 Canadian sites, 5 aggregated Canadian sites (NRCAN high-resolution dataset) and three European sites (GHCN high-resolution dataset). The high-resolution dataset is the most relevant considering our results and adding more distributions to the supplementary materials will result in a high number of pages.

Supplementary materials. Could the authors include the obtained distribution of the VS-lite *parameters?*

For technical reasons, and as the paper focusses on MAIDEN, we are unfortunately not able to provide the distributions that would correspond to several additional figures in an already long supplement.

Dear editor and reviewers, we would like first to thank you for your useful feedbacks and comments on our manuscript. You can find here below the Referee's comments in *italics* and our answer in blue. In **bold**, you can find the modifications that will be made to the manuscript.

Referee#2

This manuscript presents a useful analysis of the use of the model MAIDEN as a PSM for potential paleoclimatic reconstructions. I have some minor comments, corrections, and requests for clarification.

We would like to deeply thank the Referee for the positive evaluation of our manuscript and the interesting comments. They will all be accounted for in the revised manuscript, as described here below.

I think it would be important to state more prominently that the results here come with the caveat that they are done over a limited range of climate regimes. In my experience using VS-lite, I have found large differences for Eastern North America vs. Western North America, where Eastern North America (the primary region used here) did clearly worse than Western North America. It's therefore possible that MAIDEN will be less clearly the winner in certain climate regimes.

We totally agree with the reviewer that the results come with the caveat that they are done over a limited range of climate regimes and that an analysis on a broader scale is needed to have a complete view on the performance of both models under various climate conditions. The objective here is clearly not to present an exhaustive evaluation of the two models or of our calibration method but to test our methodology on a few sets of tree-ring sites with different configurations (a network and few individual sites in Europe), so as to present our methodology. We are currently testing the methodology exemplified in the manuscript to a wider range of environmentally different sites to test the applicability of our calibration method for the MAIDEN model.

Therefore, we will state this again on lines 366-369 (p.18), as follows: "**As our objective is to provide a first test of our calibration methodology using only a few sets of tree-ring sites, the obtained results only give an incomplete view of the MAIDEN model performance and its comparison with VS-Lite, focussing over a limited range of climate regimes. More experiments in different conditions are required in the future to exhaustively evaluate and compare the performance of both models.**"

All of the validations are done with only the correlation metric. Correlation will miss potentially important differences like a variance bias. Is this not a concern here because the time series being compared are all standardized to have no mean and unit variance?

We agree with the reviewer that our analysis do not allow estimating the variance bias. Ideally, an exhaustive quantitative evaluation of MAIDEN would require a comparison of the variable simulated by MAIDEN to represent tree-growth (which is the annual quantity of carbon allocated to the stem in $gC.m^2$ of forest per year) directly with observations. In this case, all biases (including on the variance) can be estimated. Unfortunately, this would, for example, imply to have observations such as tree-ring density measurements, which are less widely distributed than tree-ring widths, and to account for biases in tree-ring observations due to the chronology building process. Those biases may indeed deteriorate the comparison with what MAIDEN simulates, i.e forest carbon accumulation and not tree-ring indexes. In specific cases, we are able to compare outputs variables from MAIDEN with observations, as it is the case for example for simulated gross primary

production with eddy covariance stations measurements of gross ecosystem production (Gennaretti et al., 2017) but this is not possible in most paleoclimate applications.
Consequently, such as VS-Lite which produces a unitless tree-growth index, we have to use a simple normalization procedure, assuming that annual quantity of carbon allocated to the stem is proportional to tree-ring width observations, as stated in our original manuscript on lines 106-108 (p.4). The disadvantage is that this normalization forbids us to assess error in the variance. This is why we only analyse the correlations for simplicity as using other metrics like the RMSE would not help us in this aspect. Similarly, studies on VS-Lite such as Breitenmoser et al. (2014) or Tolwinski-Ward et al. (2011) have used correlation as a unique statistical indicator.

This will be mentioned more explicitly in the revised version of the manuscript on lines 215-222 (p.9-10):"To compare observed and simulated tree-ring growth data after the optimization of the model parameters, both observed tree-ring width series and simulated time series have been normalized to unitless indexes. **Ideally, an exhaustive quantitative evaluation of MAIDEN would require a comparison of the variable simulated by MAIDEN to represent tree-growth directly with observations. However, this would imply the use of other tree-growth observations such as tree-rings density measurements, while tree-ring width represents the most widely available tree-growth observations which makes it a relevant candidate given our global scale goals. The disadvantage is that this normalization forbids us to assess error in the variance. This is why we only analyse the correlations for simplicity as using other metrics like the RMSE would not help us in this aspect.**".

I'm confused about the use of NRCAN data in the VS-lite model. If I've understood the manuscript correctly, the NRCAN data provides daily max-min temperature and precip data. But I believe that VS-lite is designed for monthly mean data. Is NRCAN (and daily max/min values) the right data to be using for VS-lite? I'm wondering if this might contribute to the reduced skill of VS-lite.

We agree with the reviewer that using daily maximum and minimum values could be a source of bias for VS-Lite. This problem has been highlighted in the PhD thesis of Alexandre Devers available online (https://www.theses.fr/2019GREAU029), on p.56 for example, where for France the average difference between daily average temperature and daily average temperature calculated from minimum and maximum temperature has been estimated to be around 0.5°C. The bias should be relatively weak and thus not impact so much the skill of VS-Lite.

The following information will be added in the revised manuscript on lines 166-167 (p.7), as follows:"**Note that monthly average temperature has been computed by averaging daily maximum and minimum temperature, which could lead to a small bias.**"

Alexandre Devers. Vers une réanalyse hydrométéorologique à l'échelle de la France sur les 150 dernières années par assimilation de données dans des reconstructions ensemblistes. Hydrologie. Université Grenoble Alpes, 2019. Français. NNT: 2019GREAU029. tel-02506254

Can the authors comment on the computation cost of running MAIDEN vs VS-lite? This is particularly relevant for paleoclimate DA where an expensive PSM might be justification enough for not using it if something else is much faster.

We agree that it is an important information to add in the manuscript. This information will be added on lines 233-236 (p.10), as follows: "**Running MAIDEN takes around 2.5 seconds on one CPU for a 50 years time span while running VS-Lite takes around 0.30 seconds. Currently, calibrating MAIDEN with our method takes around 18 hours on one CPU for a site due to the**

high number of iterations and calibrated parameters, while the calibration method used for VS-Lite and developed by Tolwinski-Ward et al. (2013) takes only a few seconds. "

p2.l51-53 This isn't actually true. Several reconstructions have assimilated proxy values directly using linear statistical "PSMs" (e.g., Hakim et al. 2016, Steiger et al. 2018, Tardif et al. 2018). While these are not physically-based, they still are a kind of PSM and the proxy values are not converted to temperature and then assimilated. Additionally there are reconstructions methods that have tested the direct assimilation of real isotope data using isotope GCMs (Steiger et al. 2017, Okazaki and Yoshimura 2019), and thus employed fully physically-based PSMs.

We agree with the reviewer that it has not been stated clearly in our manuscript. In the introduction, we are only talking about physically-based PSMs and this will be corrected in the revised manuscript accordingly. Also, there are indeed examples where physically-based GCMs have been used with direct assimilation but for other variables (isotopes) and not for tree-rings.

We will revise the manuscript on lines 52-53 (p.2) as follows: "**However, so far, physically-based tree-rings PSMs have not been used in published reconstructions based on data assimilation using actual data.**"

p3.l62-64 Is the inclusion of CO2 influences needed for Common Era paleoclimate though? Over most of the Common Era CO2 changes very little. Then when CO2 does start to matter, we have plentiful observations? Maybe there's some other aspect of the MAIDEN model that would be more beneficial to highlight for paleoclimatic applications? It just seems like the use of MAIDEN might not be sufficiently motivated here.

We think that the inclusion of CO_2 influences is very important as models are calibrated over the recent period where CO_2 concentration has changed a lot. If we do not take the CO_2 effect into account, then it could potentially induce stationarity problems which can, ultimately, have an impact on other parameters, such as the ones related to temperature that can covariate with CO_2.

The following sentence will be added to the revised manuscript on lines 64-66 (p.3): "**As models are calibrated over this recent period, not taking into account CO_2 concentration could potentially induce stationarity problems which can, ultimately, have an impact on the calibration of parameters, such as the ones related to temperature or water use efficiency that can covariate with CO_2.**"

Application and evaluation of the dendroclimatic process-based model MAIDEN during the last century in Canada and Europe

Jeanne Rezsöhazy[1,2], Hugues Goosse[1], Joël Guiot[2], Fabio Gennaretti[3], Etienne Boucher[4], Frédéric André[5], and Mathieu Jonard[5]

[1]Université catholique de Louvain (UCLouvain), Earth and Life Institute (ELI), Georges Lemaître Centre for Earth and Climate Research (TECLIM), Place Louis Pasteur, B-1348 Louvain-la-Neuve, Belgium
[2]Aix Marseille University, CNRS, IRD, INRA, College de France, CEREGE, Aix-en-Provence, France
[3]Institut de recherche sur les forêts, UQAT, Rouyn-Noranda, Québec, J9X 5E4, Canada
[4]Université du Québec à Montreal, Dépt. of Geography and GEOTOP, Montreal, H2V 1C7, Canada
[5]Université catholique de Louvain (UCLouvain), Earth and Life Institute (ELI), Croix du Sud 2, L7.05.09, B-1348 Louvain-la-Neuve, Belgium

Correspondence: J. Rezsöhazy (jeanne.rezsohazy@uclouvain.be)

Abstract. Tree-ring archives are one of the main sources of information to reconstruct climate variations over the last millennium with annual resolution. The links between tree-ring proxies and climate have usually been estimated using statistical approaches, assuming linear and stationary relationships. Both assumptions may be inadequate but this issue can be overcome by ecophysiological modelling based on mechanistic understanding. In this respect, the model MAIDEN (Modeling and Analysis In DENdroecology) simulating tree ring growth from daily temperature and precipitation, considering carbon assimilation and allocation in forest stands, may constitute a valuable tool. However, the lack of local meteorological data and the limited characterisation of tree species traits can complicate the calibration and validation of such complex model, which may hamper paleoclimate applications. The goal of this study is to test the applicability of the MAIDEN model in a paleoclimate context using as a test case tree ring observations covering the twentieth century from twenty-one Eastern Canadian taiga sites and three European sites. More specifically, we investigate the model sensitivity to parameters calibration and to the quality of climatic inputs and evaluate the model performance using a validation procedure. We also examine the added value of using MAIDEN in paleoclimate applications compared to a simpler tree-growth model, VS-Lite. A bayesian calibration of the most sensitive model parameters provides good results at most of the selected sites with high correlations between simulated and observed tree-growth. Although MAIDEN is found to be sensitive to the quality of the climatic inputs, simple bias-correction and downscaling techniques of these data improve significantly the performance of the model. The split-sample validation of MAIDEN gives encouraging results but requires long tree-ring and meteorological series to give robust results. We also highlight a risk of overfitting in the calibration of model parameters that increases with short series. Finally, MAIDEN has shown higher calibration and validation correlations in most cases compared to VS-Lite. Nevertheless, this latter model turns out to be more stable over calibration and validation periods. Our results provide a protocol for the application of MAIDEN to potentially any site with tree-ring width data in the extratropical region.

1 Introduction

Instrumental data inform on past climate only back to the nineteenth century because few continuous records exist before this period (Harris et al., 2014; University of East Anglia Climatic Research Unit (CRU), 2017). Complementary, indirect climate records from natural archives such as tree rings offer a longer-term perspective. In this context, dendroclimatology, defined as the science that allows the inference of past climates from tree-rings, enables climate reconstructions at high temporal resolution (annual), over several centuries or millennia (Fritts, 1976; Hughes et al., 2011). Thanks to the availability of tree-ring observations in many regions, they represent the main data source in most large scale hemispheric reconstructions covering the last millennium (e.g. Cook et al., 1999; Jones et al., 2009; Mann et al., 2009; Anchukaitis et al., 2017; Wilson et al., 2016; PAGES 2k Consortium, 2017; St. George and Esper, 2019; Esper et al., 2018).

Reconstructing past climate on the basis of tree-rings first requires to establish a relationship between measured variables, such as tree ring width or density, and climate. This has been classically done using statistical approaches (Fritts, 1976; Cook and Kairiukstis, 1990), often reducing the problem to empirical linear relationships. Consequently, numerous temperature reconstructions are based on multiple linear regressions, calibrated using temperature during the instrumental period (e.g. Fritts, 1991; Jones et al., 1998; Mann et al., 1999, 2008). When using those statistical models for the entire period covered by dendroclimatic data, we assume both linear and stationary relationships (Guiot et al., 2014), while those assumptions may be inadequate for many records (Briffa et al., 1998; Wilson and Elling, 2004; Wilson et al., 2007; D'Arrigo et al., 2008).

Process-based tree-growth models are able to overcome those limitations of statistical models, by explicitly representing the processes at the origin of the recorded signal (Guiot et al., 2014). They are also one kind of a larger group of models called Proxy System Models (PSM). PSMs simulate the development of measured variables (here, in tree rings) based on climatic variables as inputs. They integrate a simplified representation of the mechanisms governing the relationship between climate and observations used to capture paleoclimatic information (Evans et al., 2013). These models can be applied in an inverse mode to estimate the climatic conditions that gave rise to the measured characteristics (Guiot et al., 2014; Boucher et al., 2014). Alternatively, they can be forced by climate model results (direct mode), allowing thereby to compare model results with indirect climate records, without the need to reconstruct the climate from these observations (Evans et al., 2013; Dee et al., 2016). In addition to major advantages for model-data comparisons, proxy system models can facilitate the assimilation of proxy data in long climate model runs (Dee et al., 2016; Goosse, 2016). In paleoclimatology, the objective of data assimilation is to optimally combine the results of one climate model and the observations to obtain an estimate of the state of the climate system as accurate as possible (Kalnay, 2003). This technique is now used regularly to obtain reanalysis providing estimates of different climatic variables, such as temperature, precipitations, atmospheric and ocean circulation for the last decades. Similar procedures are being developed in palaeoclimatology (e.g Goosse et al., 2012; Franke et al., 2017; Tardif et al., 2018)~~but~~. However, so far, ~~all tests using actual data have been based on temperature reconstructions derived from proxies, not on proxies~~

~~themselves~~physically-based tree-rings PSMs have not been used in published reconstructions based on data assimilation using actual data. This implies additional uncertainties when reconstructing temperatures.

Several models developed to simulate tree growth have been applied in dendroclimatology (Guiot et al., 2014). Among them, the VS-Lite model is a deterministic numerical model that simulates the primary response of ring width to climate based on the principle of limiting climatic factors (i.e. temperature and soil moisture; Tolwinski-Ward et al., 2011). Because of its simplicity and the small number of inputs required, it has been used in a wide range of conditions in a large number of paleoclimate studies (e.g Breitenmoser et al., 2014; Lavergne et al., 2015; Dee et al., 2016; Steiger and Smerdon, 2017; Seftigen et al., 2018; Fang and Li, 2019). However, VS-Lite is not able to reproduce tree-growth observations for numerous sites, particularly when the dependence on climatic conditions is complex (Breitenmoser et al., 2014). More comprehensive models such as the full Vaganov-Shashkin model (Vaganov et al., 2006) or MAIDEN (Modeling and Analysis In DENdroecology; Misson, 2004) could be more adapted to those conditions. One of the strenghts of the MAIDEN model is to include the influence of atmospheric CO_2 concentration on growth. This is essential when we know that the atmospheric concentration of CO_2 increased by 30% during the last fifty years (Myhre et al., 2013; Boucher et al., 2014). As models are calibrated over this recent period, not taking into account CO_2 concentration could potentially induce stationarity problems which can, ultimately, have an impact on the calibration of parameters, such as the ones related to temperature or water use efficiency that can covariate with CO_2. Unfortunately, those more comprehensive models including explicitly complex biological processes such as photosynthesis and carbon allocation may need careful initialisation and calibration for each set. They may thus require specific information on the sites that may not be available. This may then hamper a systematic application of the model on a large number of sites as done for instance with VS-Lite (Breitenmoser et al., 2014).

Before applying a mechanistic model to a wide range of tree ring records covering the past centuries, testing its applicability over the twentieth century when data allow an estimation of the model skill appears necessary, which is the goal of our study. For a specific study site, local meteorological data and measurements of several ecophysiological variables allow a precise calibration of many individual processes included in the model. However, this is a rare case and likely one of the main limitations in the application of the model to a wide range of sites and soil conditions or when driven by climate model results that have known biases (Flato et al., 2013). We first present in Sect. 2.1 the two dendroclimatic models that are compared in this study, namely the complex model MAIDEN and the more simple model VS-Lite. MAIDEN and VS-Lite are applied to selected sites of the Northern Hemisphere (described in Sect. 2.2), covering a range of environmental conditions and tree species. A first set of data consists of a large number of sites from the same region with similar environmental conditions but with low in situ replication, while a second set only contains a few sites but with good replication. In this way, we test the applicability of MAIDEN to two datasets contrasted in terms of site documentation that allow us to evaluate the extent to which MAIDEN can be applied. We compare the calibration methods adopted for VS-Lite (Tolwinski-Ward et al., 2013) and MAIDEN (Hartig et al., 2019) in Sect. 2.3. Different strategies to select the value for the most sensitive parameters of the MAIDEN model as well as the sensitivity of parameters calibration to the quality of climatic inputs are tested in Sect. 3.1, 3.2 and 3.3. Finally, we compare calibration and validation statistics of both models and discuss their applicability to a wide range of sites and species in Sect. 3.4 and 3.5.

2 Material and Methods

2.1 Tree growth models

2.1.1 The MAIDEN model

The dendroclimatic model MAIDEN has initially been developed by Misson (2004). It explicitly includes biological processes, namely photosynthesis and carbon allocation to different tree compartments, to simulate an annual tree growth increment. The model uses daily climatic inputs (i.e. CO_2 atmospheric concentration, precipitations and minimum and maximum air temperature). Up to now, MAIDEN has been applied in the Mediterranean (Gea-Izquierdo et al., 2015) and temperate regions (Misson, 2004; Boucher et al., 2014), in the Eastern Canadian taiga (Gennaretti et al., 2017) and in Argentina (Lavergne et al., 2017). Currently, there are two versions of the model from Gea-Izquierdo et al. (2015), developed for the Mediterranean forests, and Gennaretti et al. (2017) for boreal tree species. A unified version from those two versions has also been developed by Fabio Gennaretti (unpublished). In this study, all tests have been conducted using the unified version of MAIDEN. This unified version gives the opportunity to choose between the version from Gennaretti et al. (2017) and from Gea-Izquierdo et al. (2015) and, if needed, to test equations from both versions to evaluate their impact. However, here, only the version from Gennaretti et al. (2017) is used as it is the most adapted to the selected sites.

MAIDEN simulates photosynthesis on a daily basis and allocates the daily available carbon from photosynthesis and stored non-structural carbohydrates to different pools (leaves, roots, stem and storage). The allocation is based on functionnal rules defined following the ongoing phenological phase (five phases per year: winter 1 with no accumulation of growing degree days (GDD), winter 2 with active GDD accumulation, budburst, summer and fall). At the end of the year, the model sums all the daily carbon inputs allocated to the stem to get an annual tree growth increment (yearly Dstem, hereafter Dstem, in grams of carbon per square meter of stand per year). Dstem is assumed to be proportional to tree-ring growth so that we can build simulated tree-ring index time series and compare it with tree-ring width (hereafter TRW) observations (Sect. 2.3.1) (Gea-Izquierdo et al., 2015; Gennaretti et al., 2017). The structure of the MAIDEN model is provided online (https://figshare.com/articles/MAIDEN_ecophysiological_forest_model/5446435/1) and its modules are available upon request.

Tree-ring observations site and climate station (corresponding to a single location or grid cell as a function of the climatic dataset) constants of the MAIDEN model (Table S1) are derived from observations, as far as possible. For practical reasons, we were not able to retrieve slope and aspect informations from a Digital Elevation Model, for example, because it requires field knowledge of the site and for each sample, that we cannot systematically obtain, given our global scale goals. Thus, slope and aspect constants are set to zero. The soil is divided in four layers (1-15cm; 15-30cm; 30-65cm; 65-100cm). Clay and sand fractions are extracted from the Harmonized World Soil Database (hereafter HWSD) v1.2 at 30 arc-second resolution (FAO/IIASA/ISRIC/ISSCAS/JRC, 2012) at the nearest cell with observed value which is always at a distance smaller than 100 km to the site and assigned as follows: 1-30cm parameters from the HWSD for the two first soil layers in MAIDEN; 30-100cm parameters from the HWSD for the two deepest soil layers in MAIDEN. Soil layers thickness is fixed at the same values for all sites, as for fine roots fractions.

2.1.2 The VS-Lite model

VS-Lite was developed by Tolwinski-Ward et al. (2011) as a simplified version of the full Vaganov-Shashkin model (Vaganov et al., 2006). The model reproduces the primary response of ring width to climate using an approach based on the limiting factors principle (i.e. temperature and soil moisture) and on threshold growth response functions. It does not model any biological processes explicitly so that it cannot be considered fully mechanistic. The model needs monthly climate data (cumulated precipitations and average temperature) as inputs as well as latitude of the study site. The main output of VS-Lite used here is a unitless annual tree-growth increment (Tolwinski-Ward et al., 2011).

2.2 Study sites and climate data

2.2.1 Study sites

A network of tree-ring width chronologies of *Picea mariana* collected in similar conditions is available for the Eastern Canadian taiga ~~(Nicault et al., 2014; Boucher et al., 2017). Those~~ (Nicault et al., 2014; Boucher et al., 2017, http://dendro-qc-lab.ca/trw.html). We use here the tree-ring series directly derived from this compilation, without any modification. The chronologies have been previously standardized using the Age-Band Regional Curve Standardization (or RCS) method ~~(Briffa et al., 2001)~~ proposed by Briffa et al. (2001) and further applied to a similar boreal dataset by Nicault et al. (2014). We also use the Eastern Canadian taiga chronology for *Picea mariana* from Gennaretti et al. (2017) (hereafter *QC_taiga*), standardized using a site-specific RCS (Gennaretti et al., 2014b). The latter is highly replicated (Gennaretti et al., 2014b) compared to the other Eastern Canadian sites from Nicault et al. (2014) and Boucher et al. (2017), which cover a broader spatial range, and provides additional observations to calibrate the model. From this network, we have only selected sites from Nicault et al. (2014) and Boucher et al. (2017) ending at least in 2000, with an expressed population signal (defined as the amount of variance of a population chronology infinitely replicated explained by a finite subsample; Buras, 2017) equal to or above 0.8 and replication equal to or above 15. We have also kept the site from Gennaretti et al. (2017) as a control site. At the end of the selection process, we get twenty-one sites (Fig. 1a). In order to increase replication, the Canadian sites from Nicault et al. (2014) and Boucher et al. (2017) are aggregated based on ~~an~~ a one degree grid by averaging tree-ring width chronologies (Fig. 1b). From this, we get five aggregated sites (Table 1). Note that *QC_taiga* is not included into the aggregation process to keep it as a reference. The aggregation allows us to get relatively good inter-sites correlations inside the same one-degree grid, ranging from 0.442 to 0.732 with an average of 0.558. This observational network represents an archetypal example of a singular species that covers an important hydroclimatic gradient~~, which makes it~~. Sites located along the western (near James Bay, WNFLV1, Fig. 1a) and eastern (near Labrador sea, WL32, Fig. 1a) margins of the study area present the warmest growing seasons in the network (864 growing degree-days above 5°C for the 1976-2005 period, Hutchinson et al. (2009)). Sites located in the center of the Quebec-Labrador peninsula (WHM2, Fig. 1a) present a much shorter growing season (692 growing degree-days above 5°C), much like the sites located further north (WLECA, Fig. 1a, 573 growing degree-days above 5°C). Annual precipitation increases from west to east, passing from 668 mm (WNFLV1, Fig. 1a) to 907 mm (WL32, Fig. 1a), and significantly decreases with latitude, reaching only 567 mm at WLECA (Fig. 1a) for the 1976-2005 period (Hutchinson et al., 2009). This makes this network a relevant candidate for our calibration and validation exercises.

Three additionnal tree-ring width chronologies (hereafter European sites) are used to perform tests on sites with good replication, especially at the European Alps site, and long nearby series from meteorological stations (Fig. 2): EALP (47N/10.7E; 2050m; European Alps; *Pinus cembra* and *Larix decidua*; Büntgen et al., 2011; processed data available in the PAGES2k database (PAGES 2k Consortium, 2017)); SWIT179 (46.77N/9.82E; 1800m; *Picea abies*; standardized with a cubic-smoothing spline with a 50% frequency cut-off at 35 years; Seftigen et al., 2018; unprocessed data archived at the International Tree Ring Data Bank, https://www.ncdc.noaa.gov/data-access/paleoclimatology-data) and FINL045 (68.07N/27.2E; *Pinus sylvestris*; standardized using a spline with a 50% frequency cut-off response at 32 years; Babst et al., 2013~~).~~; processed data available in the supplementary materials of Babst et al. (2013)). Similarly to the Eastern Canadian taiga chronologies, the tree-ring series were not modified here. Those three European sites exemplify a situation where we only have access to individual sites with different species and from different environmental conditions that are not part of a larger network of tree-ring width observations.

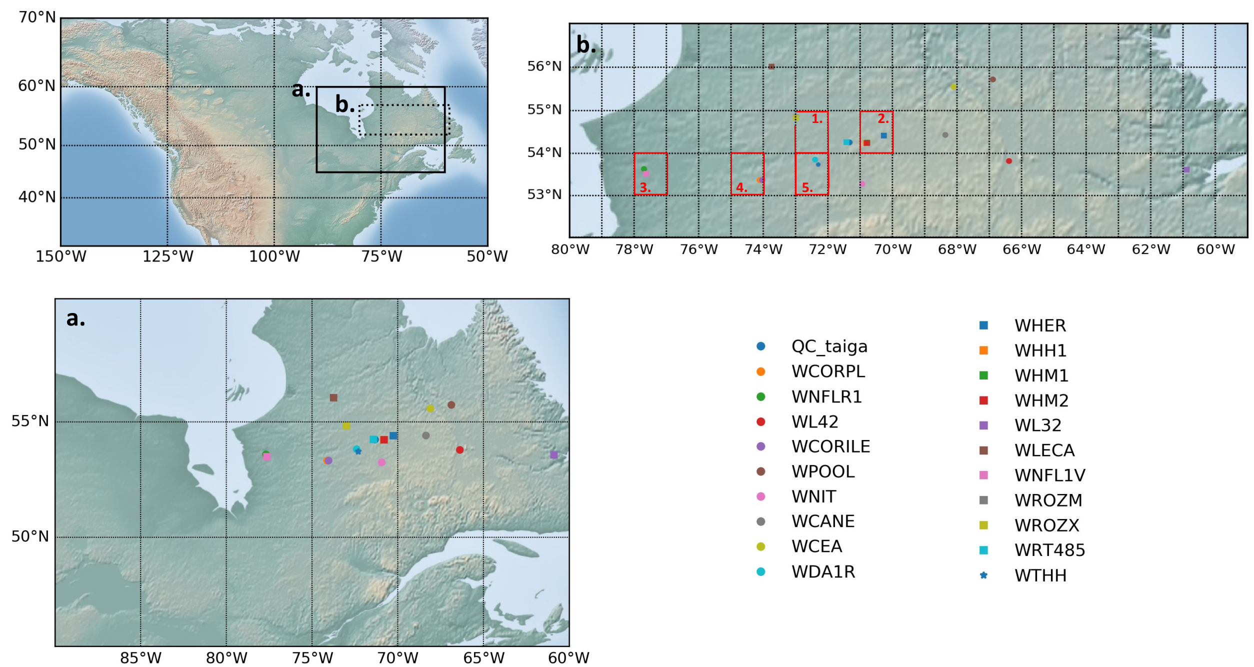

Figure 1. Location of (a) twenty-one Eastern Canadian taiga sites (20 sites from Nicault et al. (2014) and Boucher et al. (2017); 1 site called here *QC_taiga* from Gennaretti et al. (2017)) (b) aggregated Eastern Canadian taiga sites from Nicault et al. (2014) and Boucher et al. (2017) based on a 1°grid (red numbered grid cells). Background map from Hunter (2007).

Table 1. Aggregated Eastern Canadian taiga sites based on the individual sites from Nicault et al. (2014) and Boucher et al. (2017) (Fig. 1a and b).

Aggregated site name	Individual sites	Grid cell number
WROZ	WROZM, WROZX	1
WH	WHER, WHH1, WHM1, WHM2	2
WNFL	WNFL1V, WNFLR1	3
WCOR	WCORILE, WCORPL	4
WDA1R_WTHH	WDA1R, WTHH	5

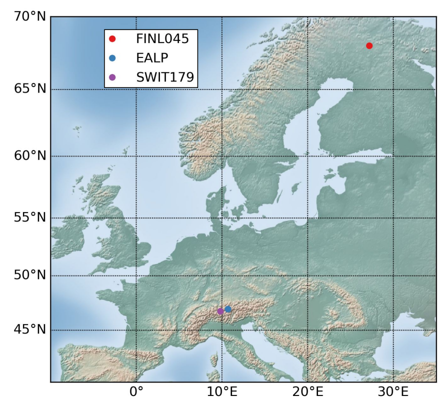

Figure 2. Location of three European sites with tree-ring width observations used in this study. Background map from Hunter (2007).

2.2.2 Climate data

Daily climatic inputs are needed to run MAIDEN (Sect. 2.1.1). Monthly climatic inputs for VS-Lite are computed from those daily data. Note that monthly average temperature has been computed by averaging daily maximum and minimum temperature, which could lead to a small bias. Three daily climatic datasets with different spatial resolution (Table 2) were selected for our analysis on the Eastern Canadian taiga network (Fig. 1a and b). First, a dataset at a high spatial resolution of 5 minutes from the gridded interpolated Canadian database of daily minimum-maximum temperature and precipitation (Hutchinson et al., 2009, hereafter NRCAN). The *Global Meteorological Forcing Dataset for land surface modeling* (http://hydrology.princeton.edu/data.php; Sheffield et al., 2006) at 1° resolution is used as a mid-resolution climatic dataset (hereafter GMF). The NOAA-CIRES 20th Century Reanalysis V2c (https://www.esrl.noaa.gov/psd/data/gridded/data.20thC_ReanV2c.monolevel.html) at 2° resolution is used as a low-resolution dataset (hereafter 20CRv2c). Finally, the 20CRv2c dataset was modified to match the monthly mean seasonal cycle of the high-resolution dataset NRCAN (hereafter 20CRv2c corr.). This simple bias correction and downscaling to the location of the site is done by removing the difference between the monthly mean seasonal cycle of

20CRv2c (2°) and NRCAN (5') from the maximum and minimum temperature data. In order to avoid negative values, daily precipitations are multiplied by the ratio between the monthly mean seasonal cycle of NRCAN (5') and 20CRv2c (2°). The time series are extracted from the grid cells nearest to the studied individual sites. The climatic data are averaged over the individual sites data for the aggregated Eastern Canadian sites (Table 1).

The Global Historical Climate Network Daily (Table 2; see Table S2 for details on selected stations; Menne et al., 2012a, b; hereafter GHCN) is used to perform analysis on the European sites (FINL045, EALP, SWIT179, Fig. 2).

Daily atmospheric CO_2 concentration data are linearly interpolated from the annual data from Sato and Schmidt (https://data.giss.nasa.gov/modelforce/ghgases/).

Table 2. Description of all daily climatic datasets used in this study (Abbreviation, Climatic dataset, Spatial resolution and Source), time periods on which MAIDEN and VS-Lite simulations are performed with each specific climatic dataset (Time period) and sites where climate data are used (Sites). European and Canadian sites refer to Fig. 1 and 2 respectively.

Abbreviation	Climatic dataset	Spatial resolution	Source	Time period	Sites
GHCN	Global Historical Climate Network Daily	station	Menne et al., 2012a, b	1909-1944 or 1910-1949;1950-2000	European sites
NRCAN	Canadian database of daily minimum-maximum temperature and precipitation	5 minutes	Hutchinson et al., 2009	1950-2000	Canadian sites
GMF	Global Meteorological Forcing Dataset for land surface modeling	1 degree	Sheffield et al., 2006	1950-2000	Canadian sites
20CRv2c	NOAA-CIRES 20th Century Reanalysis V2c	2 degrees	NOAA-CIRES	1950-2000;1900-2000	Canadian sites
20CRv2c corr.	NOAA-CIRES 20th Century Reanalysis V2c corrected for bias in the mean seasonal cycle based on NRCAN	2 degrees	-	1950-2000;1900-2000	Canadian sites

2.3 Calibration

2.3.1 The MAIDEN model

We have developed a protocol to systematically and automatically calibrate the model, through a bayesian procedure with Markov Chain Monte Carlo sampling carried out using the DREAMzs algorithm (Hartig et al., 2019). The calibration procedure focusses on the most sensitive parameters of the model identified in Gennaretti et al. (2017): six parameters influencing the simulated stand growth primary production and twelve parameters involved in the modelling of the daily quantity of carbon allocated to different tree compartments (Table S3). Those 6+12 parameters are calibrated by comparison between simulated Dstem and tree-ring width observations. The comparison relies on the computation of the model likelihood defined as the sum of the logarithms of the normal probability densities of the residuals between the model simulation and the observations. The prior distributions of the 6+12 parameters are assumed to be uniform over an acceptable range, as in Gennaretti et al. (2017). The calibration procedure is made up of three steps. During the first step, we calibrate the twelve carbon allocation parameters, while fixing the six photosynthesis parameters to arbitrary values in their acceptable ranges. We run three Markov chains of 10 000 iterations with a five iterations thinning (i.e. we only consider one random sample out of five) to calibrate the parameters. During the second step, we fix the twelve carbon allocation parameters at the values obtained from the first step. We calibrate the six photosynthesis parameters by also running three Markov chains of 10 000 iterations with a five iterations thinning. Finally, during the third step, the six photosynthesis parameters are fixed at the values obtained from the second step and the twelve carbon allocation parameters are calibrated, by running three Markov chains of 30 000 iterations, with a five iterations thinning as well. Each of those nine chains starts from random initial values of the parameters in their acceptable ranges. At the end of each calibration step, we select the set of parameters with the highest posterior (Maximum A Posteriori value or MAP, Hartig et al., 2019) from all iterations considering a burn-in period (i.e. the number of initial iterations of a chain that are not considered in the calibration) of 1000 iterations (first and second steps) and 3000 iterations (third step). At the end of the calibration process, we thus have six calibrated parameters from the second calibration step and twelve carbon allocation parameters from the third one. The calibration method has been tested for convergence of Markov chains with Gelman-Rubin statistical indicators (Hartig et al., 2019).

The MAIDEN model was calibrated at the twenty-one Eastern Canadian taiga sites and at the five aggregated sites over the 1950-2000 time period using the high- (NRCAN), mid- (GMF) and low-resolution (20CRv2c) datasets as inputs, as well as the bias-corrected low-resolution dataset (20CRv2c corr.), and over the 1900-2000 time period using the 20CRv2c and 20CRv2c corr. datasets as climatic inputs. MAIDEN was also calibrated at the three European sites using GHCN station data over 1950-2000 (FINL045; EALP; SWIT179), 1909-1944 (FINL045) and 1910-1949 (EALP and SWIT179). Calibrated parameters values for the 1950-2000 time period are available in Tables S4–S7. Parameter posterior frequency distributions for the NRCAN (5') high-resolution climatic dataset are available on Fig. S6–S63. Pearson correlation coefficients between observed TRW and simulated Dstem were computed, as well as the corresponding confidence level. To compare observed and simulated tree-ring growth data after the optimization of the model parameters, both observed tree-ring width series and simulated time series have been normalized to unitless indexes. Ideally, an exhaustive quantitative evaluation of MAIDEN would require a comparison of the variable simulated by MAIDEN to represent tree-growth directly with observations. However, this would imply the use of other tree-growth observations such as tree-rings density measurements, while tree-ring width represents the most widely available tree-growth observations which makes it a relevant candidate given our global scale goals . The disadvantage is that this normalization forbids us to assess error in the variance. This is why we only analyse the correlations for simplicity as using other metrics like the RMSE would not help us in this aspect.

2.3.2 ~~The VS-Lite model~~

2.3.2 The VS-Lite model

The VS-Lite parameters are calibrated at each location following a bayesian approach described in Tolwinski-Ward et al. (2013). In this study, four VS-Lite parameters, corresponding to the lower and upper temperature (respectively T_1 and T_2 in Tolwinski-Ward et al. (2011)) and soil moisture (respectively M_1 and M_2 in Tolwinski-Ward et al. (2011)) thresholds of the model, have been optimized. The other parameters were fixed to default values. The method is based on a standard Markov chain Monte Carlo approach, a Metropolis-Hastings algorithm embedded within a Gibbs sampler. The VS-Lite model was calibrated at the same sites and over the same time periods as MAIDEN, using the same climatic data (Sect. 2.3.1). Calibrated parameters values for the 1950-2000 period are available in Tables S8–S11. Pearson correlation coefficients between TRW observations and simulated tree-growth indexes were also computed. Observed time series have been normalized to unitless indexes as well.

Running MAIDEN takes around 2.5 seconds on one CPU for a 50 years time span while running VS-Lite takes around 0.30 seconds. Currently, calibrating MAIDEN with our method takes around 18 hours on one CPU for a site due to the high number of iterations and calibrated parameters, while the calibration method used for VS-Lite and developed by Tolwinski-Ward et al. (2013) takes only a few seconds.

2.4 Validation

Split-sample validation are performed by dividing the available data into two subperiods, one for calibration and one for validation, and vice-versa. In order to test the influence of time series length, we validate the ~~model~~ two models for both short (1950-1974 and 1975-2000) and long (1909-1944 and 1950-2000 or 1910-1949 and 1950-2000) time periods. For each validation experiment, pearson correlation coefficients between observed TRW and simulated ~~Dstem~~ tree-growth indexes were computed, as well as the corresponding confidence level.

Split-sample validation was preferred over other validation methods such as h-block Jack-knife which are computationally intensive. Additionally, removing years may be inapropriate for the validation because of the autocorrelation charaterizing yearly TRW observations. Similar problems arise from a bootstrap technique (Gea-Izquierdo et al., 2017).

Table 3. Description of each experiment performed in our study: experiment name; sites and climate dataset used for the experiment; time period of the experiment; short description of the experiment. Information on climate datasets can be found in Table 2. Individual and aggregated Eastern Canadian taiga sites refer to Fig. 1 and European sites refer to Fig. 2.

Experiment name	Sites	Climate dataset	Time period	Description
Calibration strategies for MAIDEN				
Application of prior MAIDEN parameters to all Canadian sites (Sect. 3.1)	Individual and aggregated Eastern Canadian taiga sites	NRCAN	1950-2000	We apply *QC_taiga* parameters as calibrated by Gennaretti et al. (2017) to all Eastern Canadian taiga sites
Site-specific calibration of the MAIDEN parameters and sensitivity to the quality of climatic inputs (Sect. 3.2)	Individual and aggregated Eastern Canadian taiga sites	NRCAN, GMF, 20CRv2c, 20CRv2c corr.	1950-2000 ;1900-2000 (20CRv2c and 20CRv2c corr. only)	We calibrate each Eastern Canadian taiga sites with a bayesian procedure and evaluate the sensitivity of the calibration to the climate inputs quality
Regional calibration of MAIDEN (Sect. 3.3)	Individual and aggregated Eastern Canadian taiga sites	NRCAN	1950-2000	We evaluate the performance of MAIDEN at the Eastern Canadian taiga sites using a regional calibration
Validation of MAIDEN				
Split-sample validation of MAIDEN calibration (Sect. 3.4)	Aggregated Eastern Canadian taiga sites (AC) and European sites (E)	NRCAN (AC); GHCN (E)	1950-1974/1975-2000 (AC, E); 1909-1944 or 1910-1949/1950-2000 (E)	We validate our calibration procedure for MAIDEN using a split-sample method
Comparison between models				
Comparison between VS-Lite and MAIDEN (Sect. 3.5)	Individual Eastern Canadian taiga sites (IC) and European sites (E)	NRCAN (IC); GHCN (E)	1950-1974/1975-2000 (E); 1909-1944 or 1910-1949/1950-2000 (E); 1950-2000 (IC)	We compare VS-Lite and MAIDEN calibration and validation statistics

3 Results and Discussion

Our results and discussion are structured into five sections that allow together to fulfil our objective of testing the applicability of MAIDEN over the twentieth century (Table 3). At first, we want to determine the best set of parameters for MAIDEN at our study sites and test the sensitivity of calibration to the quality of climatic inputs (Sect. 3.1, 3.2 and 3.3). In a context of paleoclimate model-data comparison where MAIDEN will be driven by climate models outputs at low resolution, this is a crucial point of our analysis. For example, bias-correction and downscaling techniques could be good options to improve the robustness of the model calibration if the model is sensitive to the quality of climatic inputs.

We first test the possibility of using calibrated parameters from a well-documented site at other similar sites in terms of environment (here, the Eastern Canadian taiga) and tree species (here, *Picea mariana*), in Sect. 3.1. Another option is to calibrate each site individually, as in Sect. 3.2 following the calibration protocol detailed in Sect. 2.3.1. We thirdly test in Sect. 3.3 an alternative calibration method which consists in calibrating the MAIDEN model over the mean of a tree-ring width observations network with similar environmental conditions and then applying the resulting calibrated parameters to the individual sites. From another perspective, this experiment could also be seen as an alternative method for the validation of the MAIDEN model when the climate and/or tree-ring width observations time-series are too short for a split-sample validation. In this case, the individual sites are considered as nearly independent validation data. To test the sensitivity of the model to the quality of climatic inputs, we have selected four climatic datasets at different spatial resolution (Sect. 2.2.2, Table 2) that will be used in Sect. 3.2 to drive MAIDEN at the Eastern Canadian taiga sites. As a second sensitivity experiment, we have applied the parameters calibrated with MAIDEN using the high-resolution climatic data (NRCAN) to the Eastern Canadian taiga sites driven by the low-resolution data without or with bias-correction (20CRv2c and 20CRv2c corr.).

The validation of MAIDEN in Sect. 3.4 is essential to evaluate the robustness of the calibration. The last section of our study consists in comparing the performance of the complex model MAIDEN with the performance of the simple model VS-Lite so as to assess the benefits of using a complex tree-growth model as MAIDEN for past climate reconstruction compared to a simple one (Sect. 3.5).

3.1 Application of prior MAIDEN parameters to all Canadian sites

At first, the *QC_taiga* parameters as calibrated by Gennaretti et al. (2017) (twelve carbon allocation and six photosynthesis parameters) were applied to the other twenty Eastern Canadian sites and five aggregated sites from Nicault et al. (2014) and Boucher et al. (2017) using the NRCAN (5’) climate data (Table 2) over the 1950-2000 time period. Correlations between observations and simulations with MAIDEN using *QC_taiga* calibrated parameters (Fig. 3) are low and non-significant at most sites. Several reasons can explain the low skill of MAIDEN using those parameters. These results could be linked to the lower replication level at the sites from Nicault et al. (2014) and Boucher et al. (2017) - even when aggregated - compared to the site from Gennaretti et al. (2017), that weakens the climatic signal in the series. This may also be due to a high sensitivity of parameters calibration to an unstable climate-species relationship among sites that are different from each other in many aspects (such as soil type, vegetation, nutrient availibility, for example). Additionally, the long-term trends of forest growth in the Eastern Canadian taiga mostly depend on the past fire history (e.g. Payette et al., 2008; Gennaretti et al., 2014a; Erni et al., 2017). This represents the main natural disturbance factor that has shaped the North American boreal ecosystem by determining forest structure and composition as well as carbon stocks, and interacting with climate on a long time-scale. Yet, MAIDEN does not account for disturbances. To evaluate the effect of those disturbances on our experiment, the long-term decadal trends have been removed in both observations and simulations following Gennaretti et al. (2017) (Fig. S1). With only the high frequency signal, the agreement between TRW observations and simulations with MAIDEN using *QC_taiga* calibrated parameters is far better for most individual and aggregated sites.

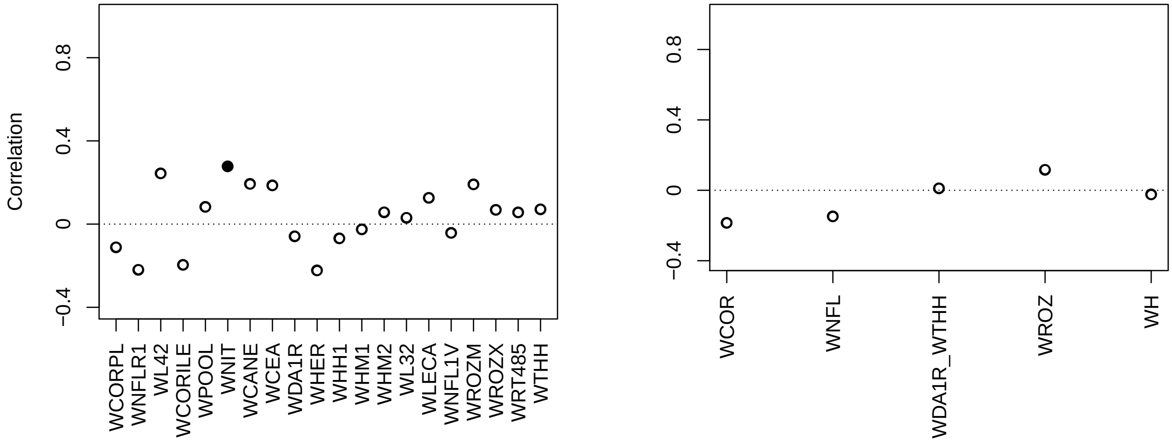

Figure 3. Pearson correlation coefficients between tree growth observations and simulations at the Eastern Canadian taiga sites (Fig. 1) with MAIDEN using NRCAN (5') as climatic inputs (Table 2) for the 1950-2000 period with *QC_taiga* calibrated parameters from Gennaretti et al. (2017). Individual (left) and aggregated sites (right). White inner circles stand for non-significant correlations (p-value > 0.05). Plain circles stand for significant correlations (p-value < 0.05).

3.2 Site-specific calibration of the MAIDEN parameters and sensitivity to the quality of climatic inputs

A second option is to calibrate each of the twenty-one Eastern Canadian taiga sites as well as the five aggregated Eastern Canadian taiga sites (Fig. 1) using the calibration procedure detailed in Sect. 2.3.1. Correlations between tree growth observations and simulations with MAIDEN for the 1950-2000 calibration period at the Eastern Canadian taiga sites are good and significant for all the climatic datasets (Fig. 4a). Correlations are in general slightly higher for the higher resolution datasets (NRCAN (5') and GMF (1°) datasets, with an average correlation of 0.62 and 0.65 respectively compared with 0.57 for 20CRv2c (2°) and 0.61 for 20CRv2c corr. (2°)). At the aggregated sites (Fig. 5a), correlations for each dataset increase a little bit compared to the average of individual correlations but the general picture is the same. The bias-correction (20CRv2c corr. (2°)) can slightly improve correlations for the 20CRv2c (2°) climatic dataset in some cases (e.g. WL42 and WROZM). Consequently, those results do not indicate that using higher resolution datasets increase effectively correlations. This is likely due to the calibration procedure that might be able to compensate for specific biases in each climatic dataset. This implies large variations of calibrated parameters between experiments (Fig. S2 and S3), questionning the robustness of the selected values. The calibration method can also compensate potential biases of tree-ring observations and of sampling procedures which have important impacts on long-term decadal trends (e.g. biases due to disturbance origin and tree selection criteria) (Johnson and Abrams, 2009; Gennaretti et al., 2014a; Duchesne et al., 2019).

Many potential biases of tree-ring observations due to the specific physiology of selected trees – that may not be representative of forest processes – and the chronology building process exist that may dampen the comparison with what MAIDEN simulates, i.e forest carbon accumulation and not forest demographic processes (Johnson and Abrams, 2009; Duchesne et al., 2019). Ideally, considering those biases, we should find a better way to transform tree-ring data in time series with meaningful units to improve model-data comparisons. For example, Gennaretti et al. (2018) compute a wood biomass production index, which is closer to what MAIDEN simulates. This implies to have access to both tree-ring width and density measurements. ~~However, given our global scale goals, this approach may be difficult to consider due to the lower availability of tree-ring density data (e.g. PAGES 2k Consortium, 2017).~~

Pearson correlations coefficients between TRW observations and tree-growth index simulations by MAIDEN for the 1900-2000 calibration period (Fig. 4b) are in most cases lower than those of the 1950-2000 calibration period. The bias-correction can slightly improve correlations in some cases but the latter stay smaller. At the aggregated sites (Fig. 5b), correlations for each dataset decrease slightly compared to the mean of individual correlations. The low correlation for the whole twentieth century can be explained by the large uncertainty of the 20CRv2c (2°) climatic dataset before 1950 there, as measured by the large spread of the 20CRv2c ensemble spread at that time (Fig. S4).

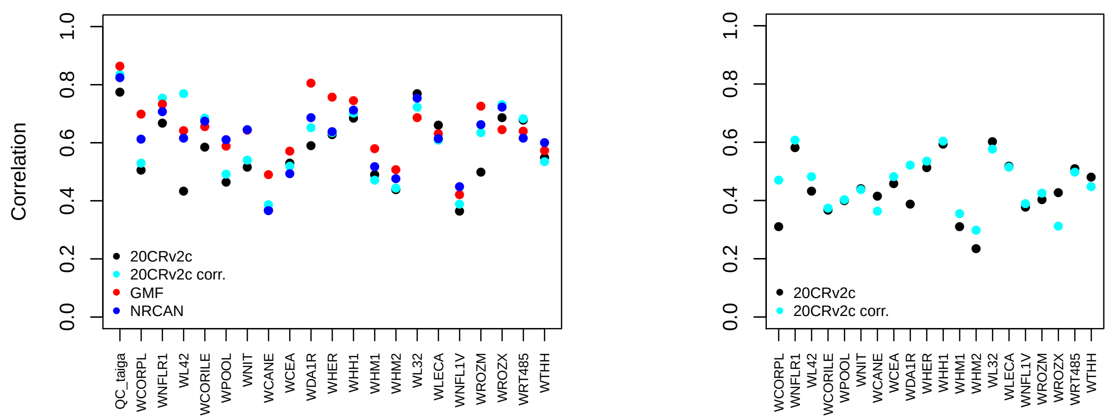

(a) 1950-2000

(b) 1900-2000

Figure 4. Pearson correlation coefficients between tree growth observations and simulations at the Eastern Canadian taiga sites (Fig. 1a) with MAIDEN using the different climatic datasets described in Table 2 as inputs for the 1950-2000 (a) and 1900-2000 (b) calibration periods. White inner circles stand for non-significant correlations (p-value > 0.05). Here, all circles are plain because correlations are all significant.

When applying the parameters calibrated using the highest resolution dataset NRCAN (5') as climatic inputs to the Eastern Canadian taiga sites driven by 20CRv2c (2°) dataset (Fig. 6, right, in red), correlations are in average much lower. Mean correlation is 0.17 in that case compared to 0.57 when the parameters are calibrated using 20CRv2c (2°) as climatic inputs. With the 20CRv2c corr. (2°) dataset as climatic inputs – i.e. the low-resolution dataset corrected for bias in the mean seasonal cycle – (Fig. 6, left, in red) we see that the performance of the MAIDEN model when applying NRCAN (5') parameters

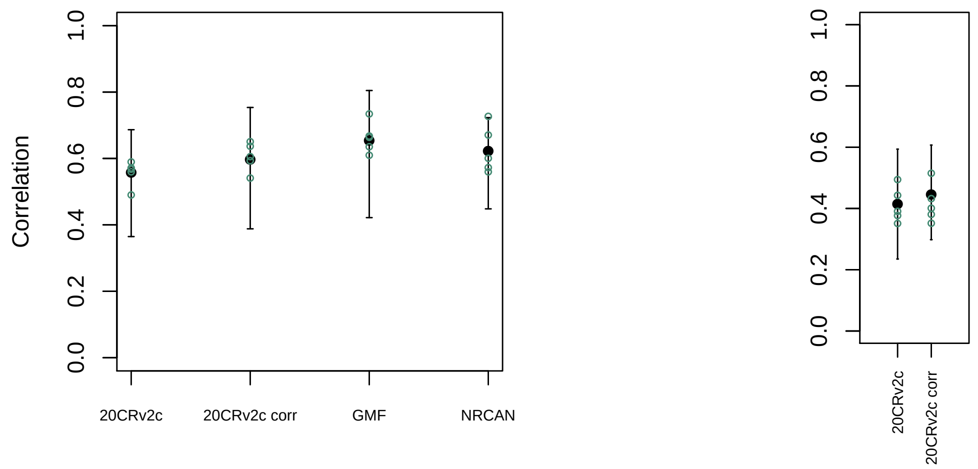

(a) 1950-2000

(b) 1900-2000

Figure 5. Pearson correlation coefficients (aggregated Eastern Canadian taiga sites (Fig. 1b), green circles), and mean and range of correlations (individual Eastern Canadian taiga sites used in aggregation (Fig. 1a and b), in black) between tree growth observations and simulations with MAIDEN using the different climatic datasets described in Table 2 as inputs for the 1950-2000 (a) and 1900-2000 (b) calibration periods.

is less good compared to the case when the parameters are calibrated using 20CRv2c corr. (2°) as climatic inputs (in black). Nevertheless, correlations are far better than with 20CRv2c (2°) (Fig. 6, right, in red). Indeed, the mean correlation is 0.36 when applying NRCAN (5') parameters and 0.61 when applying 20CRv2c corr. (2°) parameters. Consequently, the bias-correction of the 20CRv2c (2°) increases the robustness of the calibration of the MAIDEN parameters. Additionally, this shows that the MAIDEN model parameters calibration is highly sensitive to the quality of the climatic dataset used as inputs.

At the aggregated sites (Fig. 7), the general picture is the same but with far lower correlations. The mean correlations are 0.07 when applying the parameters calibrated using NRCAN (5') to the aggregated sites driven by 20CRv2c (2°) dataset and 0.56 when the parameters are calibrated using 20CRv2c (2°). With the 20CRv2c corr. (2°) dataset as climatic inputs, mean correlations are respectively 0.18 and 0.61 with NRCAN (5') and 20CRv2c corr. (2°) parameters. Those results would require a case-by-case analysis as it seems that higher replication does not provide better performance in this specific experiment.

3.3 Regional calibration of MAIDEN

At last, we apply the parameters calibrated against the mean of TRW observations from the twenty Eastern Canadian taiga sites (Fig. 8) to the five aggregated sites (Fig. 8, right) and to the individual sites used in the aggregation procedure (Fig. 8, left). For this experiment, we use the NRCAN (5') climate data (Sect. 2.2.2, Table 2) averaged over individual sites for each aggregated site (Table 1). The main parameters linked to site conditions and control parameters (Table S1) are fixed to their mode (soil parameters), mean (site latitude, elevation and isohyet, station elevation and isohyet) or common value (*exp_site*,

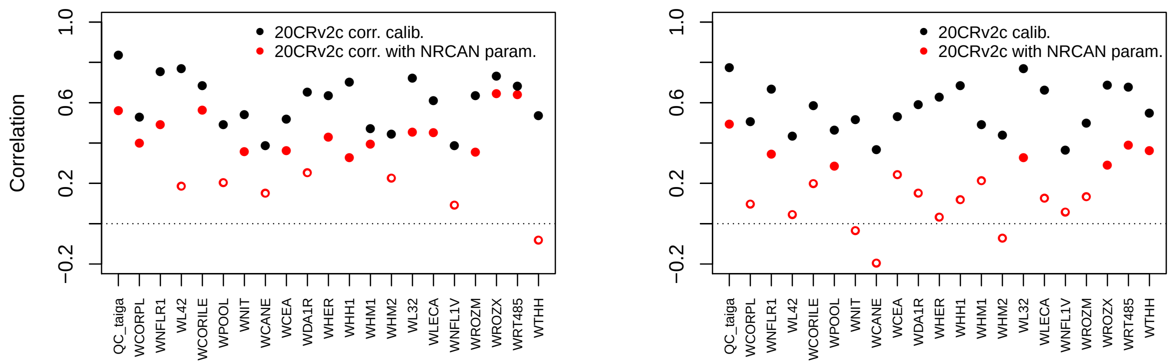

Figure 6. Pearson correlation coefficients between tree growth observations and simulations at the Eastern Canadian taiga sites (Fig. 1a) with MAIDEN using the 20CRv2c corr. (2°) (left) or 20CRv2c (2°) (right) climatic dataset for the 1950-2000 period with parameters calibrated using NRCAN (5') (with NRCAN param.) climatic inputs and with parameters calibrated using 20CRv2c corr. (2°) (left) or 20CRv2c (2°) (right) (calib.) climatic inputs (Table 2). White inner circles stand for non-significant correlations (p-value > 0.05).

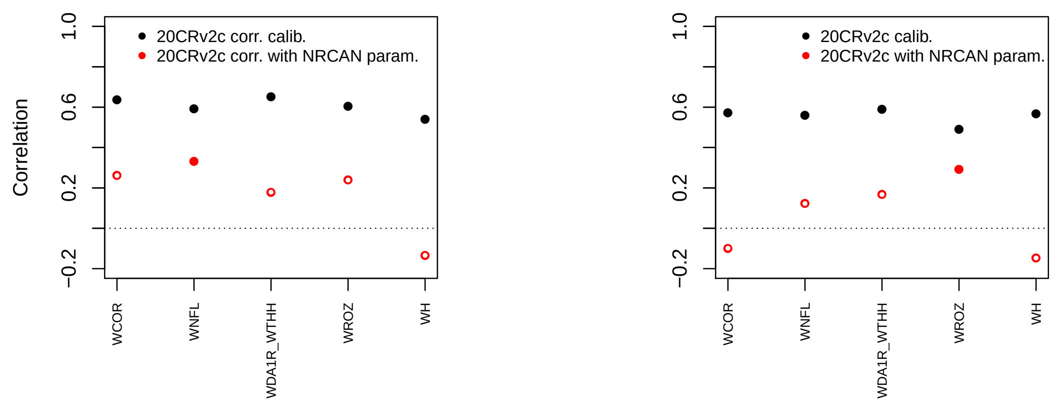

Figure 7. Pearson correlation coefficients between tree growth observations and simulations at the aggregated Eastern Canadian taiga sites (Fig. 1b) with MAIDEN using the 20CRv2c corr. (2°) (left) or 20CRv2c (2°) (right) climatic dataset for the 1950-2000 period with parameters calibrated using NRCAN (5') (with NRCAN param.) climatic inputs and with parameters calibrated using 20CRv2c corr. (2°) (left) or 20CRv2c (2°) (right) (calib.) climatic inputs (Table 2). White inner circles stand for non-significant correlations (p-value > 0.05).

slope and aspect parameters). Overall, correlations between TRW observations and simulations by MAIDEN with parameters calibrated based on the mean of the observed TRW time series are low and non-significant for the individual sites (Fig. 8, left). At the more replicated aggregated sites (Fig. 8, right), correlations between TRW observations and simulations get better with three significant correlations out of five sites. However, this result should be viewed in parallel with the individual correlations (Fig. 8, left) and sites implied in the aggregation (Table 1). Indeed, aggregated sites with higher correlations are made up of individual sites with higher correlations as well. It means that probably not only higher replication is at the origin of higher correlations for most aggregated sites but also the specific conditions at each individual site as well as site ecological history, as previously mentioned (Sect. 3.1).

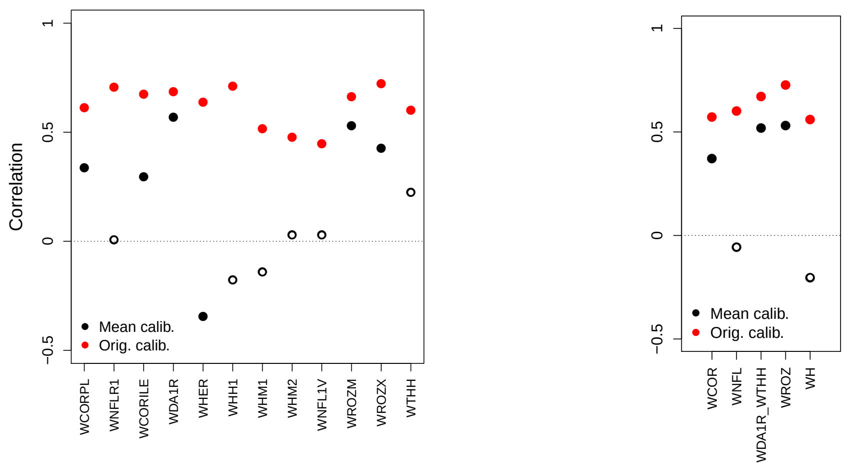

Figure 8. Pearson correlation coefficients between tree growth observations and simulations at the individual (left) and aggregated Eastern Canadian taiga sites (right) (Fig. 1a and b) with MAIDEN using the NRCAN (5') climatic dataset (Table 2) with site-specific calibration of the parameters (Orig. calib., in red) and with parameters calibrated based on the mean of the observed TRW time series (Mean calib.) for the 1950-2000 period. White inner circles stand for non-significant correlations (p-value > 0.05).

3.4 Split-sample validation of MAIDEN calibration

Depending on the available years, we have selected different time periods at the European sites (Table 4) and at the aggregated Eastern Canadian taiga sites (Table 5), using each period once for the calibration and once for the validation. At the European sites, twenty-five years is clearly a too short period of time to get robust results while the validation is generally successful for the longer period as indicated by the significant correlations – except in one case – (Table 4). Similarly, at the aggregated Eastern Canadian sites – where we only have fifty years of reliable climate data (see Sect. 3.2) – , a twenty-five years subperiod is not enough for a robust calibration and validation (Table 5). However, even on the long time period (Table 4), we can see a clue of some overfitting, especially at the SWIT179 site, where the correlation for the validation period is far lower compared to the correlation for the calibration period. Those results show that because of the large number of parameters, the validation of MAIDEN is difficult. It requires long observation series but the skill of the model still decreases significantly for the validation period.

3.5 Comparison with VS-Lite

In average, over the 1950-2000 calibration period at the individual Eastern Canadian taiga sites, VS-Lite has lower correlations for the highest resolution dataset (NRCAN) compared with MAIDEN, i.e. 0.106 and 0.62 mean correlations for VS-Lite and MAIDEN respectively (Fig. 9). Results for the other climatic datasets over the 1950-2000 (GMF (1°), 20CRv2c (2°) and

Table 4. Pearson correlation coefficients between tree growth observations and simulations at the European sites (Fig. 2) with MAIDEN and VS-Lite using GHCN as climatic inputs (Table 2) for the 1950-1974 and 1975-2000 and for the 1910-1949 (EALP, SWIT179) or 1909-1944 (FINL045) and 1950-2000 calibration and validation periods and vice-versa. Asterisks stand for significant correlations (p-value < 0.05).

European sites	Model	1950-1974		1975-2000	
		Calibration	Validation	Calibration	Validation
EALP	MAIDEN	0.831*	0.443*	0.886*	0.546*
	VS-Lite	0.629*	0.618*	0.603*	0.599*
SWIT179	MAIDEN	0.744*	0.284	0.783*	0.325
	VS-Lite	0.260	0.181	0.435*	0.396*
FINL045	MAIDEN	0.827*	0.0358	0.610*	0.135
	VS-Lite	0.415*	0.209	0.271	0.143

		1910-1949 or 1909-1944		1950-2000	
		Calibration	Validation	Calibration	Validation
EALP	MAIDEN	0.880*	0.626*	0.856*	0.569*
	VS-Lite	0.491*	0.487*	0.656*	0.656*
SWIT179	MAIDEN	0.721*	0.163	0.659*	0.306*
	VS-Lite	0.490*	0.489*	0.350*	0.353*
FINL045	MAIDEN	0.751*	0.428*	0.670*	0.394*
	VS-Lite	0.320	0.304	0.315*	0.263

20CRv2c corr. (2°)) and over the 1900-2000 calibration periods (20CRv2c (2°) and 20CRv2c corr. (2°) climatic datasets) also show lower correlations compared to MAIDEN (Fig. S5). As for split-sample validation over the long time period, the performance of VS-Lite is more stable (less fall of validation ~~than~~ from calibration correlation) compared with MAIDEN (Table 4) even if correlations are, except for SWIT179, lower than MAIDEN. Similarly, over the short time period, the performance of VS-Lite is less good than over the long time period but still more stable than MAIDEN (Table 4). Compared to VS-Lite, MAIDEN has shown lower skill over short time period validation that indicates that we should only use MAIDEN when a long enough period is available for validation. As for long validation period, MAIDEN has shown a stronger decrease in correlations compared to VS-Lite but still with higher correlations than VS-lite on average. This would indicate that MAIDEN calibration is not always prone to overfitting.

As our objective is to provide a first test of our calibration methodology using only a few sets of tree-ring sites, the obtained results only give an incomplete view of the MAIDEN model performance and its comparison with VS-Lite, focussing over a

Table 5. Pearson correlation coefficients between tree growth observations and simulations at the aggregated Eastern Canadian sites (Fig. 1b) with MAIDEN using NRCAN (5') as climatic inputs (Table 2) for the 1950-1974 and 1975-2000 calibration and validation periods and vice-versa. Asterisks stand for significant correlations (p-value < 0.05).

Canadian sites	1950-1974		1975-2000	
	Calibration	Validation	Calibration	Validation
WCOR	0.693*	0.146	0.783*	0.589*
WNFL	0.619*	0.103	0.804*	0.429*
WDA1R_WTHH	0.480*	0.737*	0.610*	0.332
WROZ	0.674*	0.577*	0.841*	0.270
WH	0.549*	0.008	0.718*	-0.011

limited range of climate regimes. More experiments in different conditions are required in the future to exhaustively evaluate and compare the performance of both models.

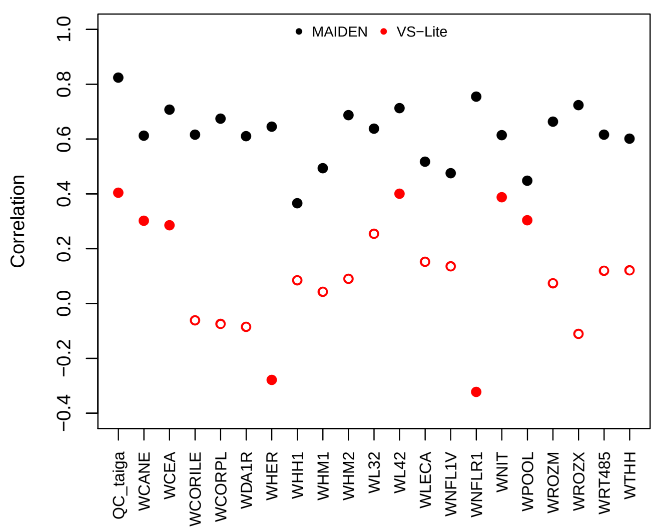

Figure 9. Pearson correlation coefficients between tree growth observations and simulations at the Eastern Canadian taiga sites (Fig. 1a) with VS-Lite (in red) and MAIDEN (in black) using NRCAN (5') as climatic inputs (Table 2) for the 1950-2000 calibration period. White inner circles stand for non-significant correlations (p-value > 0.05).

4 Conclusions

In this paper we have tested the applicability of the ecophysiological tree-growth model MAIDEN for potential dendroclimatological applications during the twentieth century at twenty-one Eastern Canadian taiga sites and three European sites using tree-ring width observations. Our results provide a protocol for the application of MAIDEN to potentially any site with tree-ring width data in the extratropical region, from climatic data selection to validation step, through automatised bayesian calibration of the most sensitive parameters. As the ultimate goal is to use MAIDEN in a context of paleoclimatic reconstruction, forced by low-resolution climate models outputs, we also analysed the sensitivity of the model to parameters calibration and to the quality of climatic inputs. The performance of MAIDEN was compared to the one of a simple tree-growth model, VS-Lite, to evaluate the advantages of using a complex tree-growth model for past climate reconstruction.

Different strategies have been tested to select the value for the most sensitive parameters of the MAIDEN model. When applying calibrated parameters from a well-documented site at other sites with same species and similar environmental conditions, very low correlations between tree-ring width observations and simulations by the MAIDEN model are found. However, when removing the long-term trend to account for the past disturbance-history of these sites that is not represented in MAIDEN, correlations get higher. In the future, this strategy can be used by selecting sites carefully to avoid disturbances. At our study sites, the bayesian calibration of the most sensitive parameters of the model can provide good and significant correlations between tree-growth observations and simulations.

Secondly, sensitivity of the MAIDEN model parameters calibration to the quality of the climatic data used as inputs has been highlighted. In a context of paleoclimatic applications, where MAIDEN will be used driven by climate models outputs at low resolution, bias-correction and downscaling techniques could be good options to improve climate inputs and calibration quality, leading thereby to reasonable correlations with observed tree-ring width.

Our split-sample validation experiments are encouraging. However, when a calibration interval of only a few decades is available, the calibration display large overfitting for individual sites as indicated by the very low correlation with observations over the validation period. Similar split-sample experiments on longer series show much better results, with potentially some overfitting but still with relatively high and generally significant correlations over the validation period. When working with a network of similar sites, the alternative validation technique, i.e. applying calibrated parameters from the mean of a network of tree-ring width observations series with same species and environmental conditions to the individual sites, should be preferred if not enough data (climate and TRW observations) are available for split-sample validation.

Lastly, at our study sites, MAIDEN has shown higher calibration and validation correlations in most cases compared to VS-Lite. VS-Lite correlations over the calibration period are especially far lower for sites with low replication (i.e. the Eastern Canadian taiga sites from Nicault et al. (2014) and Boucher et al. (2017)). However, VS-Lite stays more stable over both calibration and validation periods. Consequently, VS-Lite has a lower ability to reproduce tree growth at our sites but is ~~prone to a lower risk of~~ less prone to overfitting than MAIDEN. Most importantly, we have shown that, to limit overfitting, MAIDEN should not be used with short and low-replicated tree-ring width observations time series. VS-Lite is less risky to use in such situations as there is potentially less overfitting in the calibration and probably easier to apply over a large network of tree-ring width time series. However, VS-Lite does not include neither CO_2 nor biological processes and may thus not be able to take into account changes in conditions between the recent calibration period and the more distant past.

In the future, MAIDEN will be applied at a larger spatial scale in a systematic way using the protocol that has been developed here, by selecting hundreds of sites from the commonly used databases in paleoclimate reconstruction based on tree-ring proxies, covering a wide range of environmental conditions and tree species, such as PAGES2k (PAGES 2k Consortium, 2017) and NTREND (Anchukaitis et al., 2017; Wilson et al., 2016). This broader analysis will allow us to refine the protocol developed here in order to identify the sites where MAIDEN can be successfully applied and estimate the uncertainty associated with the use of MAIDEN for many more different sites.

Although some limitations could remain in our calibration protocol, we have shown the ability of MAIDEN to simulate tree-growth index time series that can fit robustly tree-ring width observations under certain conditions (well-replicated tree-ring width observations time series, high-resolution or downscaled climate data, long time period), as well as its potential to be used as a complex mechanistic proxy system model in paleoclimatic applications and more specifically in data assimilation.

Competing interests. The authors declare that there is no conflict of interest.

Acknowledgements. JR is F.R.S-FNRS Research Fellow, Belgium; HG is Research Director at F.R.S.-FNRS, Belgium; JG is Research Director at CNRS, France. This publication has received partial funding from Laboratory of Excellence OT-Med (project ANR-11- LABEX-0061, A*MIDEX project 11-IDEX-0001-02) as well as from F.R.S-FNRS and Fonds de recherche Société et culture Québec through the ClimHuNor project. Computational resources have been provided by the supercomputing facilities of the Université catholique de Louvain (CISM/UCL) and the Consortium des Équipements de Calcul Intensif en Fédération Wallonie Bruxelles (CÉCI) funded by the Fond de la Recherche Scientifique de Belgique (F.R.S.-FNRS) under convention 2.5020.11 and by the Walloon Region.

References

Anchukaitis, K. J., Wilson, R., Briffa, K. R., Büntgen, U., Cook, E. R., D'Arrigo, R., Davi, N., Esper, J., Frank, D., Gunnarson, B. E., Hegerl, G., Helama, S., Klesse, S., Krusic, P. J., Linderholm, H. W., Myglan, V., Osborn, T. J., Zhang, P., Rydval, M., Schneider, L., Schurer, A., Wiles, G., and Zorita, E.: Last millennium Northern Hemisphere summer temperatures from tree rings: Part II, spatially resolved reconstructions, Quaternary Science Reviews, 163, 1–22, https://doi.org/10.1016/j.quascirev.2017.02.020, 2017.

Babst, F., Poulter, B., Trouet, V., Tan, K., Neuwirth, B., Wilson, R., Carrer, M., Grabner, M., Tegel, W., Levanic, T., Panayotov, M., Urbinati, C., Bouriaud, O., Ciais, P., and Frank, D.: Site- and species-specific responses of forest growth to climate across the European continent, Global Ecology and Biogeography, 22, 706–717, https://doi.org/10.1111/geb.12023, 2013.

Boucher, E., Guiot, J., Hatté, C., Daux, V., Danis, P. A., and Dussouillez, P.: An inverse modeling approach for tree-ring-based climate reconstructions under changing atmospheric CO2 concentrations, Biogeosciences, 11, 3245–3258, https://doi.org/10.5194/bg-11-3245-2014, 2014.

Boucher, E., Nicault, A., Arseneault, D., Bégin, Y., and Karami, M. P.: Decadal variations in Eastern Canada's taiga wood biomass production forced by ocean-atmosphere interactions, Scientific Reports, 7, 1–13, https://doi.org/10.1038/s41598-017-02580-9, 2017.

Breitenmoser, P., Brönnimann, S., and Frank, D.: Forward modelling of tree-ring width and comparison with a global network of tree-ring chronologies, Climate of the Past, 10, 437–449, https://doi.org/10.5194/cp-10-437-2014, 2014.

Briffa, K. R., Schweingruber, F. H., Jones, P. D., Osborn, T. J., Harris, I. C., Shiyatov, S. G., Vaganov, E. A., and Grudd, H.: Trees tell of past climates: but are they speaking less clearly today?, Philosophical Transactions of the Royal Society of London. Series B: Biological Sciences, 353, 65–73, https://doi.org/10.1098/rstb.1998.0191, https://doi.org/10.1098/rstb.1998.0191, 1998.

Briffa, K. R., Osborn, T. J., Schweingruber, F. H., Harris, I. C., Jones, P. D., Shiyatov, S. G., and Vaganov, E. A.: Low-frequency temperature variations from a northern tree ring density network, Journal of Geophysical Research Atmospheres, 106, 2929–2941, https://doi.org/10.1029/2000JD900617, 2001.

Büntgen, U., Tegel, W., Nicolussi, K., McCormick, M., Frank, D., Trouet, V., Kaplan, J. O., Herzig, F., Heussner, K.-U., Wanner, H., Luterbacher, J., and Esper, J.: 2500 Years of European Climate Variability and Human Susceptibility, Science, 331, 578 – 582, https://doi.org/10.1126/science.1197175, http://science.sciencemag.org/content/331/6017/578.abstract, 2011.

Buras, A.: A comment on the expressed population signal, Dendrochronologia, 44, 130–132, https://doi.org/10.1016/j.dendro.2017.03.005, http://dx.doi.org/10.1016/j.dendro.2017.03.005, 2017.

Cook, E. R. and Kairiukstis, L.: Methods of dendrochronology: Applications in the Environmental Sciences, Kluwer Academic, Boston, https://doi.org/10.1016/0048-9697(91)90076-q, 1990.

Cook, E. R., Meko, D. M., Stahle, D. W., and Cleaveland, M. K.: Drought reconstructions for the continental United States, Journal of Climate, 12, 1145–1163, https://doi.org/10.1175/1520-0442(1999)012<1145:drftcu>2.0.co;2, 1999.

D'Arrigo, R., Wilson, R., Liepert, B., and Cherubini, P.: On the 'Divergence Problem' in Northern Forests: A review of the tree-ring evidence and possible causes, Global and Planetary Change, 60, 289–305, https://doi.org/10.1016/j.gloplacha.2007.03.004, 2008.

Dee, S. G., Steiger, N. J., Emile-Geay, J., and Hakim, G. J.: On the utility of proxy system models for estimating climate states over common era, Journal of Advances in Modeling Earth Systems, 8, 1164–1179, https://doi.org/10.1002/2013MS000282.Received, 2016.

Duchesne, L., Houle, D., Ouimet, R., Caldwell, L., Gloor, M., and Brienen, R.: Large apparent growth increases in boreal forests inferred from tree-rings are an artefact of sampling biases, Scientific Reports, 9, 1–9, https://doi.org/10.1038/s41598-019-43243-1, 2019.

Erni, S., Arseneault, D., Parisien, M. A., and Bégin, Y.: Spatial and temporal dimensions of fire activity in the fire-prone eastern Canadian taiga, Global Change Biology, 23, 1152–1166, https://doi.org/10.1111/gcb.13461, 2017.

Esper, J., George, S. S., Anchukaitis, K., D'Arrigo, R., Ljungqvist, F., Luterbacher, J., Schneider, L., Stoffel, M., Wilson, R., and Büntgen, U.: Large-scale, millennial-length temperature reconstructions from tree-rings, Dendrochronologia, 50, 81–90, https://doi.org/10.1016/j.dendro.2018.06.001, http://linkinghub.elsevier.com/retrieve/pii/S1125786518300687, 2018.

Evans, M. N., Tolwinski-Ward, S. E., Thompson, D. M., and Anchukaitis, K. J.: Applications of proxy system modeling in high resolution paleoclimatology, Quaternary Science Reviews, 76, 16–28, https://doi.org/10.1016/j.quascirev.2013.05.024, http://dx.doi.org/10.1016/j.quascirev.2013.05.024, 2013.

Fang, M. and Li, X.: An Artificial Neural Networks-Based Tree Ring Width Proxy System Model for Paleoclimate Data Assimilation, Journal of Advances in Modeling Earth Systems, 11, 892–904, https://doi.org/10.1029/2018MS001525, 2019.

FAO/IIASA/ISRIC/ISSCAS/JRC: Harmonized World Soil Database (version 1.2). FAO, Rome, Italy and IIASA, Laxenburg, Austria, 2012.

Flato, G., Marotzke, J., Abiodun, B., Braconnot, P., Chou, S., Collins, W., Cox, P., Driouech, F., Emori, S., Eyring, V., Forest, C., Gleckler, P., Guilyardi, E., Jakob, C., Kattsov, V., Reason, C., and Rummukainen, M.: Evaluation of Climate Models, in: Climate Change 2013: The Physical Science Basis. Contribution of Working Group I to the Fifth Assessment Report of the Intergovernmental Panel on Climate Change, Cambridge University Press, Cambridge, United Kingdom and New York, USA., https://doi.org/10.1017/CBO9781107415324, 2013.

Franke, J., Brönnimann, S., Bhend, J., and Brugnara, Y.: A monthly global paleo-reanalysis of the atmosphere from 1600 to 2005 for studying past climatic variations, Scientific Data, 4, 1–19, https://doi.org/10.1038/sdata.2017.76, 2017.

Fritts, H. C.: Tree rings and climate, Academic Press, London, 1976.

Fritts, H. C.: Reconstructing large-scale climatic patterns from tree-ring data: A diagnostic analysis., University of Arizona Press, Tucson, Arizona, USA, 1991.

Gea-Izquierdo, G., Guibal, F., Joffre, R., Ourcival, J. M., Simioni, G., and Guiot, J.: Modelling the climatic drivers determining photosynthesis and carbon allocation in evergreen Mediterranean forests using multiproxy long time series, Biogeosciences Discussions, 12, 2745–2786, https://doi.org/10.5194/bgd-12-2745-2015, 2015.

Gea-Izquierdo, G., Nicault, A., Battipaglia, G., Dorado-Liñán, I., Gutiérrez, E., Ribas, M., and Guiot, J.: Risky future for Mediterranean forests unless they undergo extreme carbon fertilization, Global Change Biology, 23, 2915–2927, https://doi.org/10.1111/gcb.13597, 2017.

Gennaretti, F., Arseneault, D., and Bégin, Y.: Millennial disturbance-driven forest stand dynamics in the Eastern Canadian taiga reconstructed from subfossil logs, Journal of Ecology, 102, 1612–1622, https://doi.org/10.1111/1365-2745.12315, 2014a.

Gennaretti, F., Arseneault, D., Nicault, A., Perreault, L., and Begin, Y.: Volcano-induced regime shifts in millennial tree-ring chronologies from northeastern North America, Proceedings of the National Academy of Sciences, 111, 10 077–10 082, https://doi.org/10.1073/pnas.1324220111, http://www.pnas.org/cgi/doi/10.1073/pnas.1324220111, 2014b.

Gennaretti, F., Gea-Izquierdo, G., Boucher, E., Berninger, F., Arseneault, D., and Guiot, J.: Ecophysiological modeling of the climate imprint on photosynthesis and carbon allocation to the tree stem in the North American boreal forest, Biogeosciences, 14, 4851–4866, https://doi.org/10.5194/bg-2017-51, 2017.

Gennaretti, F., Boucher, E., Nicault, A., Gea-Izquierdo, G., Arseneault, D., Berninger, F., Savard, M. M., Bégin, C., and Guiot, J.: Underestimation of the Tambora effects in North American taiga ecosystems, Environmental Research Letters, 13, https://doi.org/10.1088/1748-9326/aaac0c, 2018.

Goosse, H.: An additional step toward comprehensive paleoclimate reanalyses, Journal of Advances in Modeling Earth Systems, 6, 1501–1503, https://doi.org/10.1002/2013MS000282.Received, 2016.

Goosse, H., Crespin, E., Dubinkina, S., Loutre, M. F., Mann, M. E., Renssen, H., Sallaz-Damaz, Y., and Shindell, D.: The role of forcing and internal dynamics in explaining the "Medieval Climate Anomaly", Climate Dynamics, 39, 2847–2866, https://doi.org/10.1007/s00382-012-1297-0, 2012.

Guiot, J., Boucher, E., and Gea-Izquierdo, G.: Process models and model-data fusion in dendroecology, Frontiers in Ecology and Evolution, 2, 1–12, https://doi.org/10.3389/fevo.2014.00052, http://journal.frontiersin.org/article/10.3389/fevo.2014.00052/abstract, 2014.

Harris, I., Jones, P. D., Osborn, T. J., and Lister, D. H.: Updated high-resolution grids of monthly climatic observations - the CRU TS3.10 Dataset, International Journal of Climatology, 34, 623–642, https://doi.org/10.1002/joc.3711, 2014.

Hartig, F., Minunno, F., and Paul, S.: BayesianTools: General-Purpose MCMC and SMC Samplers and Tools for Bayesian Statistics. R package version 0.1.6., https://github.com/florianhartig/BayesianTools, 2019.

Hughes, M. K., Swetnam, T. W., and Diaz, H. F.: Dendroclimatology: Progress and Prospects, vol. 11, New York, springer edn., 2011.

Hunter, J. D.: Matplotlib: A 2D graphics environment, Computing in Science and Engineering, 9, 90–95, https://doi.org/10.1109/MCSE.2007.55, 2007.

Hutchinson, M. F., McKenney, D. W., Lawrence, K., Pedlar, J. H., Hopkinson, R. F., Milewska, E., and Papadopol, P.: Development and testing of Canada-wide interpolated spatial models of daily minimum-maximum temperature and precipitation for 1961-2003, Journal of Applied Meteorology and Climatology, 48, 725–741, https://doi.org/10.1175/2008JAMC1979.1, 2009.

Johnson, S. E. and Abrams, M. D.: Age class, longevity and growth rate relationships: Protracted growth increases in old trees in the eastern United States, Tree Physiology, 29, 1317–1328, https://doi.org/10.1093/treephys/tpp068, 2009.

Jones, P. D., Briffa, K. R., Barnett, T. P., and Tett, S. F. B.: High-resolution palaeoclimatic records for the last millennium, The Holocene, 4, 455–471, 1998.

Jones, P. D., Briffa, K. R., Osborn, T. J., Lough, J. M., Van Ommen, T. D., Vinther, B. M., Luterbacher, J., Wahl, E. R., Zwiers, F. W., Mann, M. E., Schmidt, G. A., Ammann, C. M., Buckley, B. M., Cobb, K. M., Esper, J., Goosse, H., Graham, N., Jansen, E., Kiefer, T., Kull, C., Küttel, M., Mosley-Thompson, E., Overpeck, J. T., Riedwyl, N., Schulz, M., Tudhope, A. W., Villalba, R., Wanner, H., Wolff, E., and Xoplaki, E.: High-resolution palaeoclimatology of the last millennium: A review of current status and future prospects, Holocene, 19, 3–49, https://doi.org/10.1177/0959683608098952, 2009.

Kalnay, E.: Atmospheric Modeling, Data Assimilation and Predictability, Cambridge University Press, 2003.

Lavergne, A., Daux, V., Villalba, R., and Barichivich, J.: Temporal changes in climatic limitation of tree-growth at upper tree-line forests: Contrasted responses along the west-to-east humidity gradient in Northern Patagonia, Dendrochronologia, 36, 49–59, https://doi.org/10.1016/j.dendro.2015.09.001, http://dx.doi.org/10.1016/j.dendro.2015.09.001, 2015.

Lavergne, A., Gennaretti, F., Risi, C., Daux, V., Savard, M., Naulier, M., Villalba, R., Begin, C., Lavergne, A., Gennaretti, F., Risi, C., Daux, V., Boucher, E., Lavergne, A., Gennaretti, F., Risi, C., Daux, V., Boucher, E., and Savard, M. M.: Modelling tree ring cellulose δ 18 O variations in two temperature-sensitive tree species from North and South America, Climate of the Past, pp. 1515–1526, 2017.

Mann, M. E., Bradley, R. S., and Hughes, M. K.: Northern Hemisphere temperatures during the past millennium, Climate Change: Evaluating recent and future climate change, 26, 759–762, 1999.

Mann, M. E., Zhang, Z., Hughes, M. K., Bradley, R. S., Miller, S. K., Rutherford, S., and Ni, F.: Proxy-based reconstructions of hemispheric and global surface temperature variations over the past two millennia, Proceedings of the National Academy of Sciences, 105, 13 252–13 257, https://doi.org/10.1073/pnas.0805721105, 2008.

Mann, M. E., Zhang, Z., Rutherford, S., Bradley, R. S., Hughes, M. K., Shindell, D., Ammann, C., Faluvegi, G., and Ni, F.: Global Signatures and Dynamical Origins of the Little Ice Age and Medieval Climate Anomaly, Science, 326, 1256–1260, https://doi.org/10.1126/science.1166349, 2009.

Menne, M., Durre, I., Korzeniewski, B., McNeal, S., Thomas, K., Yin, X., Anthony, S., Ray, R., Vose, R., Gleason, B., and Houston, T.: Global Historical Climatology Network - Daily (GHCN-Daily), Version 3.24. NOAA National Climatic Data Center., 2012a.

Menne, M. J., Durre, I., Vose, R. S., Gleason, B. E., and Houston, T. G.: An overview of the global historical climatology network-daily database, Journal of Atmospheric and Oceanic Technology, 29, 897–910, https://doi.org/10.1175/JTECH-D-11-00103.1, 2012b.

Misson, L.: MAIDEN: a model for analyzing ecosystem processes in dendroecology, Canadian Journal of Forest Research, 34, 874–887, https://doi.org/10.1139/x03-252, http://www.nrcresearchpress.com/doi/abs/10.1139/x03-252, 2004.

Myhre, G., Shindell, D., Bréon, F.-M., Collins, W., Fuglestvedt, J., Huang, J., Koch, D., Lamarque, J.-F., Lee, D., Mendoza, B., Nakajima, T., Robock, A., Stephens, G., Takemura, T., and Zhang, H.: Anthropogenic and Natural Radiative Forcing, in: Climate Change 2013: The Physical Science Basis. Contribution of Working Group I to the Fifth Assessment Report of the Intergovernmental Panel on Climate Change, Cambridge University Press, Cambridge, United Kingdom and New York, USA., https://doi.org/10.1017/CBO9781107415324.018, 2013.

Nicault, A., Boucher, E., Tapsoba, D., Arseneault, D., Berninger, F., Bégin, C., DesGranges, J., Guiot, J., Marion, J., Wicha, S., and Bégin, Y.: Spatial analysis of black spruce (Picea mariana (Mill.) B.S.P.) radial growth response to climate in northern Québec – Labrador Peninsula, Canada , Canadian Journal of Forest Research, 45, 343–352, https://doi.org/10.1139/cjfr-2014-0080, 2014.

PAGES 2k Consortium: A global multiproxy database for temperature reconstructions of the Common Era, Scientific Data, 4, 1–33, https://doi.org/DOI: 10.1038/sdata.2017.88, 2017.

Payette, S., Filion, L., and Delwaide, A.: Spatially explicit fire-climate history of the boreal forest-tundra (Eastern Canada) over the last 2000 years, Philosophical Transactions of the Royal Society B: Biological Sciences, 363, 2301–2316, https://doi.org/10.1098/rstb.2007.2201, 2008.

Seftigen, K., Frank, D. C., Björklund, J., Babst, F., and Poulter, B.: The climatic drivers of normalized difference vegetation index and tree-ring-based estimates of forest productivity are spatially coherent but temporally decoupled in Northern Hemispheric forests, Global Ecology and Biogeography, 27, 1352–1365, https://doi.org/10.1111/geb.12802, 2018.

Sheffield, J., Goteti, G., and Wood, E. F.: Development of a 50-year high-resolution global dataset of meteorological forcings for land surface modeling, Journal of Climate, 19, 3088–3111, https://doi.org/10.1175/JCLI3790.1, 2006.

St. George, S. and Esper, J.: Concord and discord among Northern Hemisphere paleotemperature reconstructions from tree rings, Quaternary Science Reviews, 203, 278–281, https://doi.org/S0277379118307170, 2019.

Steiger, N. J. and Smerdon, J. E.: A pseudoproxy assessment of data assimilation for reconstructing the atmosphere-ocean dynamics of hydroclimate extremes, Climate of the Past, 13, 1435–1449, https://doi.org/10.5194/cp-13-1435-2017, 2017.

Tardif, R., Hakim, G. J., Perkins, W. A., Horlick, K. A., Erb, M. P., Emile-Geay, J., Anderson, D. M., Steig, E. J., and Noone, D.: Last Millennium Reanalysis with an expanded proxy database and seasonal proxy modeling, Climate of the Past Discussions, pp. 1–37, https://doi.org/10.5194/cp-2018-120, https://www.clim-past-discuss.net/cp-2018-120/, 2018.

Tolwinski-Ward, S. E., Evans, M. N., Hughes, M. K., and Anchukaitis, K. J.: An efficient forward model of the climate controls on interannual variation in tree-ring width, Climate Dynamics, 36, 2419–2439, https://doi.org/10.1007/s00382-010-0945-5, 2011.

Tolwinski-Ward, S. E., Anchukaitis, K. J., and Evans, M. N.: Bayesian parameter estimation and interpretation for an intermediate model of tree-ring width, Climate of the Past, 9, 1481–1493, https://doi.org/10.5194/cp-9-1481-2013, 2013.

University of East Anglia Climatic Research Unit (CRU): CRU TS4.01: Climatic Research Unit (CRU) Time-Series (TS) version 4.01 of high-resolution gridded data of month-by-month variation in climate (Jan. 1908 - Dec. 2016), Centre for Environmental Data Analysis (CEDA), 2017.

Vaganov, E. A., Hughes, M. K., and Shashkin, A.: Growth dynamics of conifer tree rings, New York, springer edn., 2006.

Wilson, R. and Elling, W.: Temporal instability in tree-growth/climate response in the Lower Bavarian Forest region: Implications for dendroclimatic reconstruction, Trees - Structure and Function, 18, 19–28, https://doi.org/10.1007/s00468-003-0273-z, 2004.

Wilson, R., D'Arrigo, R., Buckley, B., Büntgen, U., Esper, J., Frank, D., Luckman, B., Payette, S., Vose, R., and Youngblut, D.: A matter of divergence: Tracking recent warming at hemispheric scales using tree ring data, Journal of Geophysical Research Atmospheres, 112, 1–17, https://doi.org/10.1029/2006JD008318, 2007.

Wilson, R., Anchukaitis, K., Briffa, K. R., Büntgen, U., Cook, E., D'Arrigo, R., Davi, N., Esper, J., Frank, D., Gunnarson, B., Hegerl, G., Helama, S., Klesse, S., Krusic, P. J., Linderholm, H. W., Myglan, V., Osborn, T. J., Rydval, M., Schneider, L., Schurer, A., Wiles, G., Zhang, P., and Zorita, E.: Last millennium northern hemisphere summer temperatures from tree rings: Part I: The long term context, Quaternary Science Reviews, 134, 1–18, https://doi.org/10.1016/j.quascirev.2015.12.005, 2016.

S1: Supplementary materials

Table S1. Main constants linked to site conditions and control parameters in the MAIDEN model.

Parameter	Meaning	Units
exp_site	Indicates if the species at the site is a deciduous (1) or evergreen (2) tree	no unit (1 or 2)
base_elev_cst	Station elevation	meters
base_isoh_cst	Station isohyet	centimeters
site_lat_cst	Site latitude	degrees
site_elev_cst	Site elevation	meters
site_slp_cst	Site slope	degrees
site_asp_cst	Site aspect	degrees
site_isoh_cst	Site isohyet	centimeters
site_ehoriz_cst	Site East slope	degrees
site_whoriz_cst	Site West slope	degrees
thick1-2-3 or 4	Soil layer thickness	meters
finefrac1-2-3 or 4	% of fine roots in the soil layer	Coeff. between 0-1
clay1-2-3 or 4	% of clay in the soil layer	%
sand1-2-3 or 4	% of sand in the soil layer	%

Table S2. GHCN (Table 2) stations used for daily climate data at the European sites (Fig. 2).

Site	Time period	Station name	Station lat/lon	Station elevation
FINL	1900-1944/1950-2000	Sodankyla	67.37N26.65E	179m
EALP	1950-2000	Zugspitze	47.42N10.99E	2964m
	1910-1949	Innsbruck	47.27N11.4E	577m
SWIT179	1910-2000	Saentis	47.25N9.35E	2502m

Table S3. Calibrated parameters of the MAIDEN model (Gennaretti et al., 2017).

	Process		Parameter	Units
Photosynthesis	Temperature dependence of photosynthesis	Asymptote	V_{max}	μmol C.m^{-2} of leaves . s^{-1}
		Slope	V_b	$^{\circ}$C^{-1}
		Inflection point	V_{ip}	$^{\circ}$C
	Water stress dependence of stomatal conductance	Slope	$soil_b$	mm^{-1}
		Inflection point	$soil_{ip}$	mm
	Acclimation to temperature of photosynthesis	Needed days	τ	days
Carbon allocation	Definition of canopy maximum amount of carbon	Slope of temperature dependence	*CanopyT*	$^{\circ}$C^{-1}
		Slope of precipitation dependence	*CanopyP*	mm^{-1}
	Start of the growing season (budburst)	GDD sum threshold	GDD_1	$^{\circ}$C
		Day before the later start	*vegphase23*	day of the year
		Acclimation to changing GDD sums	*day23_flex*	~~day of the year~~ years
	Daily available carbon from buds reservoir	Storage C used by the tree	C_{bud}	gC.m^{-2} of stand . day^{-1}
	Partition of carbon to different tree compartments during growing season	Portion allocated to canopy and roots	*h3*	fraction (0-1)
	Partition of carbon to different tree compartments during summer period	Inflection point of the temperature dependence	st_{4temp}	$^{\circ}$C
	Photoperiod for transition from summer to fall season	Photoperiod threshold	*photoper*	hours
	Carbon losses from the canopy	Yearly canopy turnover rate	*PercentFall*	fraction (0-1)
		Approximate day of the year with maximum losses	*OutMax*	day of the year
		Index proportional to the length of the period with losses	*OutLength*	NA

Table S4. ~~GHCN~~ MAIDEN calibrated parameters values (Table ~~2~~S3) ~~stations used~~ over the 1950-2000 period for ~~daily climate data at~~ the twenty-one Eastern Canadian taiga sites, five aggregated Eastern Canadian taiga sites (NRCAN (5') climatic dataset, Fig. 1, Table 2) and three European sites (GHCN station data, Fig. 2, Table 2).

Dataset	Site	GDD1	vegphase23	day23_flex	CanopyP	CanopyT	PercentFall	OutMax	OutLength	Cbud	h3	st4temp	photoper	Vmax	Vb	Vip	soilb	soilip	tau
NRCAN	QC_taiga	63.403	155.321	7.441	1.104	1.309	0.137	170.266	9.378	1.892	0.970	99.921	13.743	33.246	-0.135	20.301	-0.014	236.251	10.986
NRCAN	WCORPL	19.049	171.896	5.481	15.869	16.044	0.122	181.651	8.325	1.500	0.690	15.565	13.367	58.559	-0.229	11.111	-0.020	318.724	6.964
NRCAN	WNFLR1	74.008	170.197	8.624	16.625	17.049	0.099	177.628	11.309	1.983	0.324	42.883	13.348	26.483	-0.136	10.839	-0.023	260.840	6.672
NRCAN	WL42	86.427	176.503	3.561	1.425	1.644	0.091	199.670	11.317	1.384	0.506	17.047	13.128	61.034	-0.193	14.804	-0.018	300.386	13.380
NRCAN	WCORILE	97.375	168.303	4.367	19.023	4.940	0.108	159.102	9.390	1.390	0.285	7.698	12.889	71.462	-0.135	13.767	-0.013	368.213	2.123
NRCAN	WPOOL	17.709	167.718	6.990	3.910	9.930	0.097	172.567	10.908	1.299	0.124	45.731	12.300	28.358	-0.197	16.832	-0.016	119.184	1.510
NRCAN	WNIT	34.580	165.366	1.194	14.719	9.647	0.124	163.836	11.716	1.082	0.167	82.783	13.256	123.684	-0.176	19.069	-0.014	353.154	9.761
NRCAN	WCANE	28.189	178.133	3.459	7.511	1.942	0.114	181.293	9.072	1.135	0.023	94.195	13.767	128.890	-0.294	20.993	-0.024	202.876	1.249
NRCAN	WCEA	102.804	177.515	7.770	3.976	8.212	0.107	186.967	8.398	1.340	0.076	43.256	12.936	125.486	-0.163	23.795	-0.018	374.543	6.827
NRCAN	WDA1R	17.256	159.653	5.514	15.392	0.170	0.098	165.542	10.218	1.488	0.622	15.382	13.571	84.079	-0.136	19.056	-0.021	298.486	3.694
NRCAN	WHER	24.016	180.457	9.596	10.538	10.287	0.097	175.104	10.539	1.794	0.282	56.515	13.987	16.204	-0.119	12.972	-0.015	120.703	4.005
NRCAN	WHH1	34.570	161.348	6.628	15.612	18.041	0.103	178.681	11.085	1.575	0.253	22.939	13.779	26.570	-0.133	18.467	-0.023	114.641	9.420
NRCAN	WHM1	109.541	177.636	7.965	15.971	3.851	0.096	182.295	9.734	1.711	0.225	50.227	12.500	26.902	-0.142	17.533	-0.007	288.438	2.278
NRCAN	WHM2	39.917	178.020	2.164	16.710	18.633	0.127	172.894	7.970	1.481	0.479	32.984	12.304	63.905	-0.145	14.738	-0.022	398.449	4.107
NRCAN	WL32	60.984	156.171	7.108	13.672	16.074	0.090	169.621	9.887	1.472	0.469	6.886	13.946	31.660	-0.286	15.059	-0.010	129.900	3.464
NRCAN	WLECA	111.354	167.925	8.528	2.635	10.267	0.103	193.841	11.685	1.234	0.313	16.742	12.861	51.242	-0.193	20.333	-0.008	208.170	2.746
NRCAN	WNFL1V	14.210	169.452	7.227	13.154	4.663	0.121	165.126	11.766	1.263	0.998	52.112	12.437	36.575	-0.113	19.736	-0.012	377.023	1.067
NRCAN	WROZM	21.270	167.485	1.875	18.106	16.159	0.133	160.417	4.605	1.151	0.757	30.170	13.914	67.561	-0.104	21.151	-0.023	292.789	2.247
NRCAN	WROZX	43.035	168.173	1.593	12.498	19.278	0.096	169.720	7.006	1.310	0.276	34.586	13.553	27.911	-0.105	18.322	-0.022	243.454	18.665
NRCAN	WRT485	89.048	173.233	6.517	12.051	5.321	0.094	176.983	11.824	1.231	0.201	6.992	13.247	82.030	-0.129	29.358	-0.019	126.865	2.448
NRCAN	WTHH	15.963	167.972	5.069	0.742	19.062	0.110	168.375	11.230	1.049	0.267	8.399	13.325	72.763	-0.135	28.040	-0.018	127.278	2.044
NRCAN	WCOR	14.568	154.225	9.215	4.124	8.017	0.107	159.538	11.356	2.427	0.256	41.704	13.833	66.425	-0.100	13.036	-0.014	331.144	19.299
NRCAN	WNFL	96.049	159.796	3.996	15.297	9.355	0.092	184.498	10.207	2.389	0.265	47.119	13.405	41.677	-0.177	12.018	-0.020	273.574	3.263
NRCAN	WDA1R_WTHH	18.938	174.889	6.651	1.032	2.323	0.108	150.426	6.464	1.380	0.298	8.275	12.311	110.619	-0.142	13.209	-0.023	356.216	19.803
NRCAN	WROZ	26.364	153.589	1.601	15.775	18.630	0.147	161.491	9.386	1.133	0.620	2.697	13.254	96.710	-0.124	14.956	-0.014	396.201	13.193
NRCAN	WH	54.844	155.791	4.134	5.880	15.647	0.110	171.819	10.873	1.594	0.152	5.462	12.598	43.160	-0.143	13.597	-0.017	134.855	1.872
GHCN	EALP	176.466	92.590	7.835	3.483	2.651	0.263	145.638	3.635	13.142	0.993	8.250	14.028	80.946	-0.140	24.093	-0.029	342.517	14.468
GHCN	SWIT179	43.239	158.136	2.612	6.654	7.949	0.500	224.261	12.397	9.147	0.467	15.266	9.822	54.405	-0.175	14.108	-0.056	304.582	16.755
GHCN	FINL045	56.252	152.044	3.346	6.974	8.250	0.132	242.491	8.044	4.489	0.879	44.379	11.962	117.566	-0.173	18.193	-0.054	419.557	9.348

Table S5. MAIDEN calibrated parameters values (Table S3) over the 1950-2000 period for the twenty-one Eastern Canadian taiga sites and five aggregated Eastern Canadian taiga sites (GMF (1°) climatic dataset, Fig. 1, Table 2).

Dataset	Site	GDD1	vegphase23	day23_flex	CanopyP	CanopyT	PercentFall	OutMax	OutLength	Cbud	h3	st4temp	photoper	Vmax	Vb	Vip	soilb	soilip	tau
GMF	QC_taiga	75.663	152.558	1.636	2.863	8.957	0.134	189.983	10.825	1.200	0.983	99.616	13.737	13.314	-0.133	11.010	-0.009	242.325	5.220
GMF	WCORPL	19.614	154.658	5.627	0.264	19.840	0.131	168.635	9.027	1.895	0.780	26.895	13.139	65.571	-0.121	13.440	-0.019	368.897	3.752
GMF	WNFLR1	49.391	169.826	6.628	11.234	6.101	0.113	167.168	10.788	1.771	0.335	15.850	12.424	29.047	-0.188	11.749	-0.013	305.712	10.576
GMF	WL42	58.119	172.639	7.569	16.189	7.377	0.109	179.399	8.269	1.035	0.535	1.178	13.411	18.125	-0.176	10.952	-0.011	297.743	4.432
GMF	WCORILE	26.325	164.009	5.596	17.281	8.733	0.146	169.686	9.020	1.114	0.407	11.819	13.201	16.369	-0.125	12.854	-0.020	206.164	18.014
GMF	WPOOL	77.772	173.692	7.052	2.790	15.853	0.091	184.851	11.002	1.336	0.090	30.447	13.644	42.324	-0.169	20.228	-0.023	143.943	10.72
GMF	WNIT	30.784	166.823	2.741	13.505	7.509	0.134	164.790	11.952	1.678	0.373	22.584	12.858	24.049	-0.273	13.153	-0.009	174.770	6.647
GMF	WCANE	70.119	170.101	3.273	15.928	8.959	0.144	185.114	9.475	1.087	0.105	27.563	12.575	137.905	-0.280	18.917	-0.018	381.838	11.640
GMF	WCEA	85.430	161.229	1.943	18.883	12.005	0.142	153.534	5.886	1.193	0.431	78.100	13.618	107.353	-0.230	11.551	-0.020	394.208	1.954
GMF	WDA1R	24.320	152.898	8.400	1.016	14.503	0.129	174.207	11.061	1.974	0.905	61.826	13.600	108.395	-0.103	22.824	-0.024	325.118	4.721
GMF	WHER	81.055	154.396	2.065	7.682	9.018	0.095	157.001	9.334	1.102	0.589	2.016	13.400	16.916	-0.121	11.807	-0.012	336.875	12.949
GMF	WHH1	14.275	174.618	2.949	10.268	0.171	0.093	171.613	10.146	1.223	0.292	13.350	12.947	21.290	-0.235	13.151	-0.022	222.973	13.111
GMF	WHM1	32.838	167.438	6.757	6.371	5.958	0.110	155.831	8.873	1.181	0.360	11.616	13.477	18.910	-0.104	17.042	-0.011	151.966	2.310
GMF	WHM2	91.379	152.520	3.743	1.271	17.498	0.128	151.777	9.601	1.037	0.502	10.550	12.253	13.764	-0.140	10.661	-0.011	273.032	5.109
GMF	WL32	95.642	180.031	4.224	4.193	14.564	0.098	177.032	11.805	1.861	0.073	34.838	13.185	53.737	-0.203	20.427	-0.025	143.028	5.336
GMF	WLECA	116.601	172.242	7.905	18.894	4.609	0.104	163.603	4.515	1.150	0.577	20.228	13.408	13.865	-0.118	12.874	-0.005	118.175	4.252
GMF	WNFL1V	58.951	159.826	8.953	13.153	12.897	0.114	178.394	10.591	1.169	0.480	8.190	12.041	70.906	-0.106	29.684	-0.014	246.196	10.527
GMF	WROZM	34.123	154.326	1.391	1.824	12.766	0.133	175.840	7.810	1.120	0.503	14.596	12.224	38.683	-0.147	17.125	-0.019	268.996	1.033
GMF	WROZX	61.982	157.946	3.203	7.807	13.029	0.140	176.400	8.099	1.644	0.869	72.129	13.874	112.519	-0.101	23.261	-0.025	395.291	5.423
GMF	WRT485	24.015	169.276	8.934	18.033	7.811	0.133	172.579	11.565	1.588	0.701	12.111	12.298	17.253	-0.221	11.145	-0.024	205.932	3.025
GMF	WTHH	68.680	177.619	9.452	9.448	17.848	0.119	167.538	7.717	1.080	0.571	4.714	13.603	19.948	-0.185	14.189	-0.010	212.170	6.833
GMF	WCOR	20.805	178.574	2.620	10.231	19.250	0.105	154.684	6.307	1.818	0.469	12.603	12.393	42.352	-0.117	12.343	-0.009	376.197	4.200
GMF	WNFL	47.029	161.315	3.861	6.531	8.277	0.094	182.211	10.528	2.095	0.382	16.444	12.828	45.482	-0.230	11.637	-0.014	311.371	1.951
GMF	WDA1R_WTHH	39.429	180.587	4.740	0.007	10.191	0.120	167.530	6.059	1.446	0.568	3.757	13.472	26.760	-0.124	11.530	-0.009	290.608	2.714
GMF	WROZ	29.498	180.242	3.967	0.403	9.470	0.120	175.502	8.817	1.364	0.338	8.931	13.680	44.734	-0.103	11.303	-0.009	388.244	12.917
GMF	WH	66.488	154.640	2.067	9.850	1.462	0.098	182.743	10.232	2.314	0.260	9.865	13.106	33.213	-0.103	10.300	-0.013	225.312	4.833

Table S6. MAIDEN calibrated parameters values (Table S3) over the 1950-2000 period for the twenty-one Eastern Canadian taiga sites and five aggregated Eastern Canadian taiga sites (20CRv2c corr. (2°) climatic dataset, Fig. 1, Table 2).

Dataset	Site	GDD1	vegphase23	day23_flex	CanopyP	CanopyT	PercentFall	OutMax	OutLength	Cbud	h3	st4temp	photoper	Vmax	Vb	Vip	soilb	soilip	tau
20CRv2c corr.	QC_taiga	113.370	152.798	8.744	0.222	16.280	0.147	171.699	7.445	1.342	0.998	90.354	13.635	27.746	-0.102	12.668	-0.006	142.220	11.427
20CRv2c corr.	WCORPL	67.994	167.436	7.342	11.186	15.686	0.111	167.320	11.872	1.700	0.129	87.342	12.581	32.381	-0.109	21.452	-0.010	214.488	17.015
20CRv2c corr.	WNFLR1	78.261	174.734	6.191	2.768	8.093	0.092	162.590	5.851	1.877	0.192	58.798	13.299	65.388	-0.122	15.216	-0.023	287.940	2.384
20CRv2c corr.	WL42	29.260	178.089	9.434	13.527	17.155	0.093	167.099	11.168	1.024	0.954	4.132	13.363	30.286	-0.113	11.358	-0.022	357.574	19.205
20CRv2c corr.	WCORILE	12.599	174.353	6.890	0.700	4.433	0.129	195.443	9.126	1.850	0.930	85.955	13.050	53.561	-0.296	10.832	-0.025	365.462	6.040
20CRv2c corr.	WPOOL	112.458	180.716	8.072	14.904	17.606	0.097	198.678	11.974	1.244	0.120	25.553	13.383	78.202	-0.130	29.083	-0.017	182.063	4.687
20CRv2c corr.	WNIT	19.219	176.941	6.150	12.806	9.017	0.136	151.973	11.449	2.039	0.427	35.933	13.733	134.551	-0.269	16.502	-0.024	390.727	9.147
20CRv2c corr.	WCANE	78.482	167.604	9.756	10.507	8.310	0.099	164.636	11.268	2.186	0.994	90.511	12.379	51.995	-0.289	16.932	-0.019	236.149	13.742
20CRv2c corr.	WCEA	81.167	178.414	7.441	0.210	15.923	0.116	169.741	4.922	1.348	0.389	75.341	13.536	58.210	-0.127	23.997	-0.012	382.036	5.418
20CRv2c corr.	WDA1R	104.308	160.431	3.691	5.556	7.740	0.140	161.868	10.006	1.481	0.659	1.507	13.440	104.597	-0.103	21.727	-0.023	344.532	6.344
20CRv2c corr.	WHER	63.043	166.470	2.476	17.934	16.531	0.091	177.202	10.553	1.785	0.195	61.706	13.385	15.438	-0.113	10.067	-0.021	314.001	14.469
20CRv2c corr.	WHH1	89.238	162.196	2.490	14.260	5.373	0.113	184.458	10.997	1.528	0.299	16.712	13.163	35.179	-0.100	24.270	-0.022	257.149	1.324
20CRv2c corr.	WHM1	89.658	165.179	2.332	15.537	19.911	0.097	174.207	11.409	1.661	0.047	98.363	12.489	124.366	-0.154	29.038	-0.012	233.181	3.418
20CRv2c corr.	WHM2	110.167	170.088	4.846	0.043	12.045	0.105	165.444	7.855	1.318	0.274	34.803	12.197	19.156	-0.111	16.353	-0.023	167.282	7.595
20CRv2c corr.	WL32	116.547	178.676	5.965	5.265	15.111	0.092	184.089	10.907	1.766	0.053	58.663	13.483	42.173	-0.269	16.806	-0.014	145.674	1.660
20CRv2c corr.	WLECA	90.354	180.902	5.626	11.212	8.273	0.109	199.300	7.751	1.013	0.010	49.618	12.033	22.119	-0.212	13.036	-0.015	313.818	12.315
20CRv2c corr.	WNFL1V	40.318	179.836	6.997	1.668	9.648	0.129	171.170	8.712	1.515	0.137	57.226	12.209	30.784	-0.127	20.251	-0.012	171.664	9.904
20CRv2c corr.	WROZM	63.805	164.546	2.513	2.971	13.699	0.101	169.451	11.196	1.358	0.154	70.833	12.796	15.280	-0.103	11.943	-0.017	153.426	18.963
20CRv2c corr.	WROZX	11.256	158.783	1.475	6.717	11.490	0.100	169.016	8.972	1.305	0.162	68.989	13.289	15.439	-0.129	12.107	-0.022	197.314	15.718
20CRv2c corr.	WRT485	102.122	173.485	9.331	3.189	13.364	0.121	181.631	11.174	1.024	0.318	3.755	12.111	67.786	-0.127	27.347	-0.005	366.987	3.936
20CRv2c corr.	WTHH	48.844	171.447	6.643	0.289	9.060	0.139	170.923	8.826	1.182	0.534	7.378	12.208	21.961	-0.136	16.102	-0.010	143.590	3.259
20CRv2c corr.	WCOR	56.468	179.615	3.574	16.008	1.242	0.114	157.886	7.560	2.017	0.263	14.179	13.968	102.747	-0.115	16.294	-0.019	397.049	10.996
20CRv2c corr.	WNFL	20.771	164.646	4.922	5.208	12.450	0.127	155.527	11.352	2.304	0.078	63.865	12.954	39.707	-0.116	17.774	-0.016	211.665	3.658
20CRv2c corr.	WDA1R_WTHH	59.728	175.202	8.912	7.291	15.136	0.110	168.798	10.731	1.586	0.169	25.445	12.855	72.407	-0.127	13.938	-0.019	382.916	3.795
20CRv2c corr.	WROZ	19.524	173.178	3.238	19.948	17.295	0.091	151.863	8.737	1.837	0.247	61.332	12.374	89.821	-0.107	14.736	-0.021	397.978	15.062
20CRv2c corr.	WH	119.083	165.796	1.176	2.114	8.057	0.104	184.843	11.733	2.771	0.067	18.052	13.788	76.144	-0.105	22.057	-0.006	328.383	1.022

Table S7. MAIDEN calibrated parameters values (Table S3) over the 1950-2000 period for the twenty-one Eastern Canadian taiga sites and five aggregated Eastern Canadian taiga sites (20CRv2c (2°) climatic dataset, Fig. 1, Table 2).

Dataset	Site	GDD1	vegphase23	day23_flex	CanopyP	CanopyT	PercentFall	OutMax	OutLength	Cbud	h3	st4temp	photoper	Vmax	Vb	Vip	soilb	soilip	tau
20CRv2c	QC_taiga	75.720	162.168	9.429	3.806	4.436	0.142	161.784	7.128	2.868	0.947	95.218	13.485	22.246	-0.157	13.200	-0.008	397.024	2.846
20CRv2c	WCORPL	44.431	158.330	7.142	2.826	19.045	0.099	187.010	5.206	1.043	0.026	36.677	13.618	103.760	-0.116	20.246	-0.018	374.728	19.391
20CRv2c	WNFLR1	75.809	167.038	1.718	13.416	9.042	0.111	179.207	11.314	1.385	0.099	84.442	13.892	39.007	-0.135	18.911	-0.006	369.090	2.293
20CRv2c	WL42	83.970	161.752	3.598	18.021	15.015	0.117	196.304	10.705	1.179	0.471	89.359	12.869	21.043	-0.193	11.375	-0.022	248.490	12.055
20CRv2c	WCORILE	101.474	154.897	6.015	7.926	5.971	0.099	167.905	11.464	1.061	0.057	35.086	12.627	68.195	-0.152	14.843	-0.017	397.308	11.180
20CRv2c	WPOOL	107.070	163.868	5.215	12.717	14.609	0.097	181.672	11.563	1.112	0.119	38.952	12.915	20.150	-0.206	12.698	-0.015	181.127	12.122
20CRv2c	WNIT	46.340	174.983	5.523	0.065	19.960	0.135	170.592	11.654	1.573	0.321	26.871	13.769	16.621	-0.275	10.872	-0.010	130.537	18.718
20CRv2c	WCANE	117.593	165.327	6.518	9.262	8.489	0.095	190.972	5.377	1.301	1.000	55.147	13.234	24.946	-0.191	15.154	-0.018	212.148	15.867
20CRv2c	WCEA	16.999	178.818	2.874	3.271	4.543	0.104	168.800	7.396	1.062	0.250	85.997	12.675	19.907	-0.270	10.342	-0.020	358.779	9.664
20CRv2c	WDA1R	44.501	175.164	5.003	11.839	13.155	0.108	170.377	9.474	1.092	0.243	81.989	12.506	84.785	-0.112	17.687	-0.022	348.379	1.489
20CRv2c	WHER	55.843	154.795	8.234	8.967	17.999	0.097	180.100	11.782	1.427	0.310	54.276	12.896	16.450	-0.101	13.173	-0.017	202.653	15.885
20CRv2c	WHH1	115.526	170.285	2.370	12.582	17.775	0.119	189.149	10.913	1.159	0.309	17.661	13.287	38.614	-0.139	21.284	-0.020	211.300	3.248
20CRv2c	WHM1	66.111	172.640	8.305	0.824	4.900	0.091	193.059	11.798	1.214	0.164	18.974	13.369	28.720	-0.181	16.652	-0.008	287.187	2.558
20CRv2c	WHM2	116.989	170.119	8.727	6.623	1.158	0.150	194.261	11.175	1.263	0.389	59.636	12.473	29.252	-0.129	18.507	-0.011	169.127	1.643
20CRv2c	WL32	15.396	176.894	2.706	6.839	15.526	0.122	170.542	11.614	1.120	0.182	87.455	13.711	110.276	-0.295	14.399	-0.022	353.621	1.233
20CRv2c	WLECA	100.826	174.227	3.438	17.519	17.296	0.096	186.546	10.267	1.244	0.302	37.580	12.352	27.111	-0.132	18.973	-0.023	179.091	1.122
20CRv2c	WNFL1V	79.176	173.450	1.076	16.285	11.663	0.129	158.549	7.783	1.072	0.293	85.854	12.496	57.088	-0.263	11.029	-0.021	338.566	2.186
20CRv2c	WROZM	83.289	168.105	1.265	14.963	12.219	0.094	166.930	10.533	1.808	0.291	40.019	12.166	19.213	-0.115	10.790	-0.006	306.374	3.024
20CRv2c	WROZX	24.634	167.104	2.377	4.668	10.024	0.125	174.838	11.551	1.205	0.147	93.212	13.551	47.811	-0.106	26.302	-0.013	183.486	19.587
20CRv2c	WRT485	103.114	171.036	1.519	11.590	19.660	0.098	185.015	11.226	1.171	0.134	19.026	12.543	126.788	-0.159	28.423	-0.014	238.127	1.085
20CRv2c	WTHH	45.979	154.621	7.085	13.906	8.149	0.117	195.802	11.858	1.393	0.700	63.045	13.618	41.220	-0.106	25.134	-0.006	127.995	6.676
20CRv2c	WCOR	89.792	169.235	3.771	8.555	10.056	0.110	190.627	10.764	1.682	0.433	10.341	13.024	119.892	-0.145	13.926	-0.019	357.625	16.816
20CRv2c	WNFL	81.661	173.171	2.122	18.413	9.513	0.102	180.427	11.517	1.867	0.064	57.458	13.358	36.924	-0.103	15.964	-0.006	292.632	14.260
20CRv2c	WDA1R_WTHH	118.615	156.106	2.599	0.986	19.844	0.101	176.546	11.917	1.675	0.301	14.910	12.911	100.050	-0.109	15.932	-0.015	372.220	19.135
20CRv2c	WROZ	81.338	152.814	7.145	0.332	5.040	0.117	186.358	11.717	1.722	0.214	53.164	12.543	-0.122	10.222	-0.009	394.353	15.502	
20CRv2c	WH	97.027	168.575	6.833	17.466	8.474	0.092	187.697	11.841	2.264	0.032	70.550	13.202	57.902	-0.106	17.880	-0.005	118.539	1.771

Table S8. VS-Lite calibrated parameters values (Sect. 2.3.2) over the 1950-2000 period for the twenty-one Eastern Canadian taiga sites (NRCAN (5') climatic dataset, Fig. 1a, Table 2) and three European sites (GHCN station data, Fig. 2, Table 2).

~~Site~~ Dataset	~~Time period~~ Sites	~~Station name~~ T1	~~Station lat/lon~~ T2	~~Station elevation~~ M1	M2
~~FINL~~ NRCAN	~~1900-1944/1950-2000~~ QC_taiga	~~Sodankyla~~ 2.430	~~67.37N26.65E~~15.727	~~179m~~ 0.053	0.429
~~EALP~~ NRCAN	~~1950-2000~~ WCORPL	~~Zugspitze~~ 4.612	~~47.42N10.99E~~ 12.497	~~2964m~~0.035	0.275
NRCAN	~~1910-1949~~ WNFLR1	~~Innsbruck~~ 4.914	~~47.27N11.4E~~ 11.493	~~577m~~0.033	0.357
NRCAN	WL42	7.259	11.658	0.070	0.457
NRCAN	WCORILE	3.058	12.002	0.032	0.194
NRCAN	WPOOL	7.899	11.514	0.066	0.194
NRCAN	WNIT	7.876	12.118	0.016	0.230
NRCAN	WCANE	7.264	11.557	0.077	0.171
NRCAN	WCEA	5.745	12.363	0.074	0.443
NRCAN	WDA1R	1.316	14.399	0.053	0.183
NRCAN	WHER	2.795	19.393	0.058	0.258
NRCAN	WHH1	7.490	11.677	0.007	0.190
NRCAN	WHM1	7.660	12.939	0.017	0.220
NRCAN	WHM2	8.843	12.165	0.040	0.168
NRCAN	WL32	7.642	13.785	0.013	0.231
NRCAN	WLECA	8.389	12.148	0.032	0.169
NRCAN	WNFL1V	3.575	11.542	0.086	0.465
NRCAN	WROZM	1.726	11.656	0.027	0.153
NRCAN	WROZX	6.170	11.382	0.070	0.473
NRCAN	WRT485	2.014	17.012	0.001	0.158
NRCAN	WTHH	3.996	13.065	0.020	0.119
GHCN	EALP	8.242	22.117	0.058	0.277
GHCN	SWIT179	~~1910-2000~~ 1.480	~~Saentis~~ 21.912	~~47.25N9.35E~~ 0.052	~~2502m~~0.294
GHCN	FINL045	2.517	19.159	0.007	0.120

Table S9. VS-Lite calibrated parameters values (Sect. 2.3.2) over the 1950-2000 period for the twenty-one Eastern Canadian taiga sites (GMF (1°) climatic dataset, Fig. 1a, Table 2).

Dataset	Sites	T1	T2	M1	M2
GMF	QC_taiga	7.934	20.259	0.036	0.210
GMF	WCORPL	2.574	12.366	0.027	0.233
GMF	WNFLR1	3.124	10.795	0.018	0.404
GMF	WL42	6.973	10.861	0.036	0.378
GMF	WCORILE	2.585	12.279	0.025	0.132
GMF	WPOOL	8.036	11.556	0.042	0.266
GMF	WNIT	8.193	13.365	0.028	0.219
GMF	WCANE	7.517	12.862	0.089	0.482
GMF	WCEA	6.072	11.476	0.080	0.469
GMF	WDA1R	1.613	22.429	0.003	0.318
GMF	WHER	4.808	12.558	0.040	0.439
GMF	WHH1	7.303	11.754	0.061	0.259
GMF	WHM1	2.750	13.427	0.009	0.223
GMF	WHM2	5.479	12.363	0.023	0.185
GMF	WL32	8.300	15.367	0.007	0.355
GMF	WLECA	7.638	11.770	0.017	0.464
GMF	WNFL1V	3.241	11.483	0.080	0.468
GMF	WROZM	1.867	15.193	0.060	0.386
GMF	WROZX	1.470	14.070	0.055	0.154
GMF	WRT485	1.141	17.046	0.075	0.386
GMF	WTHH	3.033	13.675	0.012	0.138

Table S10. VS-Lite calibrated parameters values (Sect. 2.3.2) over the 1950-2000 period for the twenty-one Eastern Canadian taiga sites (20CRv2c corr. (2°) climatic dataset, Fig. 1a, Table 2).

Dataset	Sites	T1	T2	M1	M2
20CRv2c corr.	QC_taiga	7.000	14.214	0.094	0.436
20CRv2c corr.	WCORPL	1.996	11.968	0.043	0.276
20CRv2c corr.	WNFLR1	2.443	19.159	0.011	0.246
20CRv2c corr.	WL42	7.672	11.259	0.080	0.447
20CRv2c corr.	WCORILE	3.102	12.325	0.056	0.254
20CRv2c corr.	WPOOL	6.812	10.631	0.005	0.221
20CRv2c corr.	WNIT	8.347	12.275	0.055	0.201
20CRv2c corr.	WCANE	8.277	12.194	0.017	0.200
20CRv2c corr.	WCEA	2.681	12.493	0.043	0.410
20CRv2c corr.	WDA1R	3.382	18.603	0.013	0.295
20CRv2c corr.	WHER	4.768	12.783	0.027	0.196
20CRv2c corr.	WHH1	7.464	11.322	0.058	0.116
20CRv2c corr.	WHM1	8.472	15.277	0.082	0.258
20CRv2c corr.	WHM2	8.383	18.934	0.053	0.218
20CRv2c corr.	WL32	8.446	14.245	0.011	0.108
20CRv2c corr.	WLECA	7.556	13.389	0.023	0.446
20CRv2c corr.	WNFL1V	3.803	15.342	0.011	0.168
20CRv2c corr.	WROZM	8.262	14.324	0.001	0.256
20CRv2c corr.	WROZX	8.633	14.984	0.017	0.262
20CRv2c corr.	WRT485	8.381	15.478	0.016	0.189
20CRv2c corr.	WTHH	3.802	15.778	0.033	0.105

Table S11. VS-Lite calibrated parameters values (Sect. 2.3.2) over the 1950-2000 period for the twenty-one Eastern Canadian taiga sites (20CRv2c (2°) climatic dataset, Fig. 1a, Table 2).

Dataset	Sites	T1	T2	M1	M2
20CRv2c	QC_taiga	8.378	13.382	0.036	0.319
20CRv2c	WCORPL	7.532	18.410	0.036	0.270
20CRv2c	WNFLR1	8.399	19.795	0.014	0.110
20CRv2c	WL42	6.012	10.591	0.031	0.314
20CRv2c	WCORILE	7.629	10.677	0.047	0.262
20CRv2c	WPOOL	7.219	10.537	0.076	0.281
20CRv2c	WNIT	7.990	12.538	0.035	0.267
20CRv2c	WCANE	7.118	10.445	0.015	0.279
20CRv2c	WCEA	5.313	15.658	0.019	0.238
20CRv2c	WDA1R	8.167	19.349	0.088	0.194
20CRv2c	WHER	3.440	17.681	0.062	0.366
20CRv2c	WHH1	6.951	19.205	0.051	0.366
20CRv2c	WHM1	7.395	22.139	0.031	0.266
20CRv2c	WHM2	7.551	18.823	0.024	0.212
20CRv2c	WL32	8.308	14.045	0.008	0.234
20CRv2c	WLECA	6.798	14.509	0.050	0.391
20CRv2c	WNFL1V	8.604	15.787	0.042	0.153
20CRv2c	WROZM	8.131	12.693	0.060	0.133
20CRv2c	WROZX	8.645	16.846	0.035	0.205
20CRv2c	WRT485	7.555	20.034	0.019	0.210
20CRv2c	WTHH	6.906	20.691	0.014	0.240

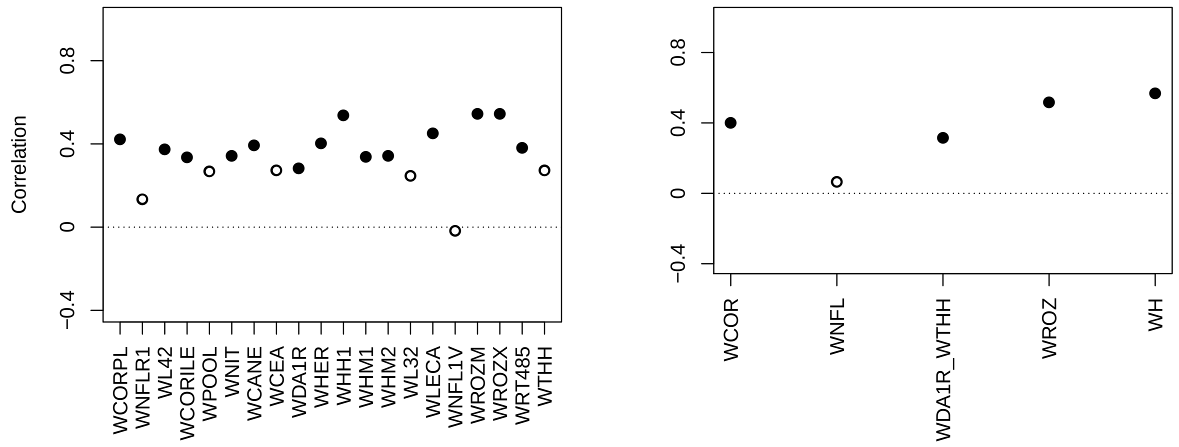

Figure S1. Pearson correlation coefficients between tree growth observations and simulations at the Eastern Canadian taiga sites (Fig. 1) with MAIDEN using NRCAN (5') as climatic inputs (Table 2) for the 1950-2000 period with *QC_taiga* calibrated parameters from Gennaretti et al. (2017). Individual (left) and aggregated sites (right). The long-term decadal trends have been removed in observations and simulations. White inner circles stand for non-significant correlations (p-value > 0.05). Plain circles stand for significant correlations (p-value < 0.05).

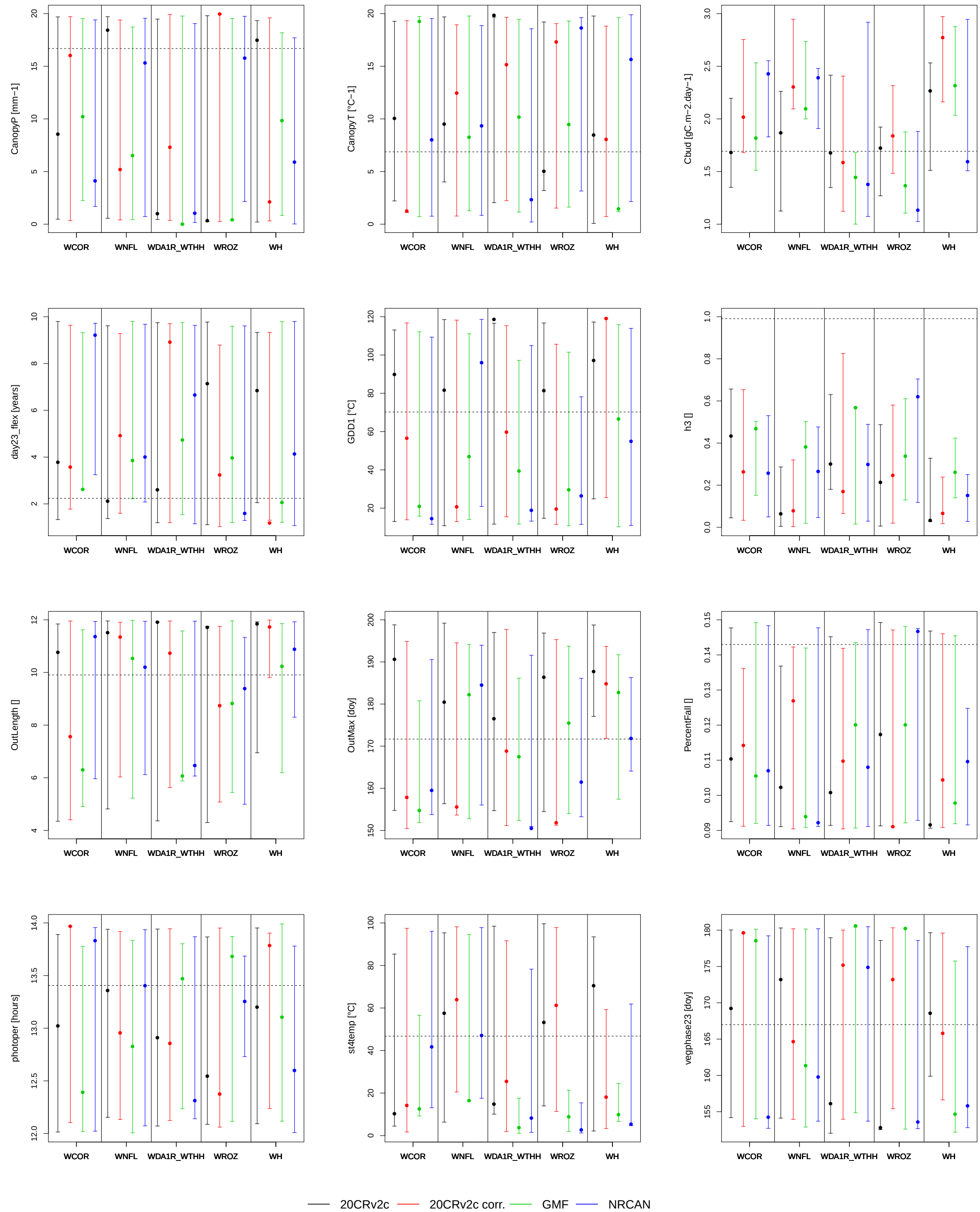

Figure S2. Selected carbon allocation parameters value (Table S3) based on the calibration procedure detailed in Sect. 2.3.1 and 95% confidence interval of each parameter (computed based on all iterations of the third step of the calibration process, with a five iterations thinning and a burn-in period of 3000 iterations, see Sect. 2.3.1) for the five aggregated Eastern Canadian sites (Fig. 1b) and for all climatic datasets (Table 2) over the 1950-2000 time period. Dashed line corresponds to the parameter value at *QC_taiga* site from Gennaretti et al. (2017).

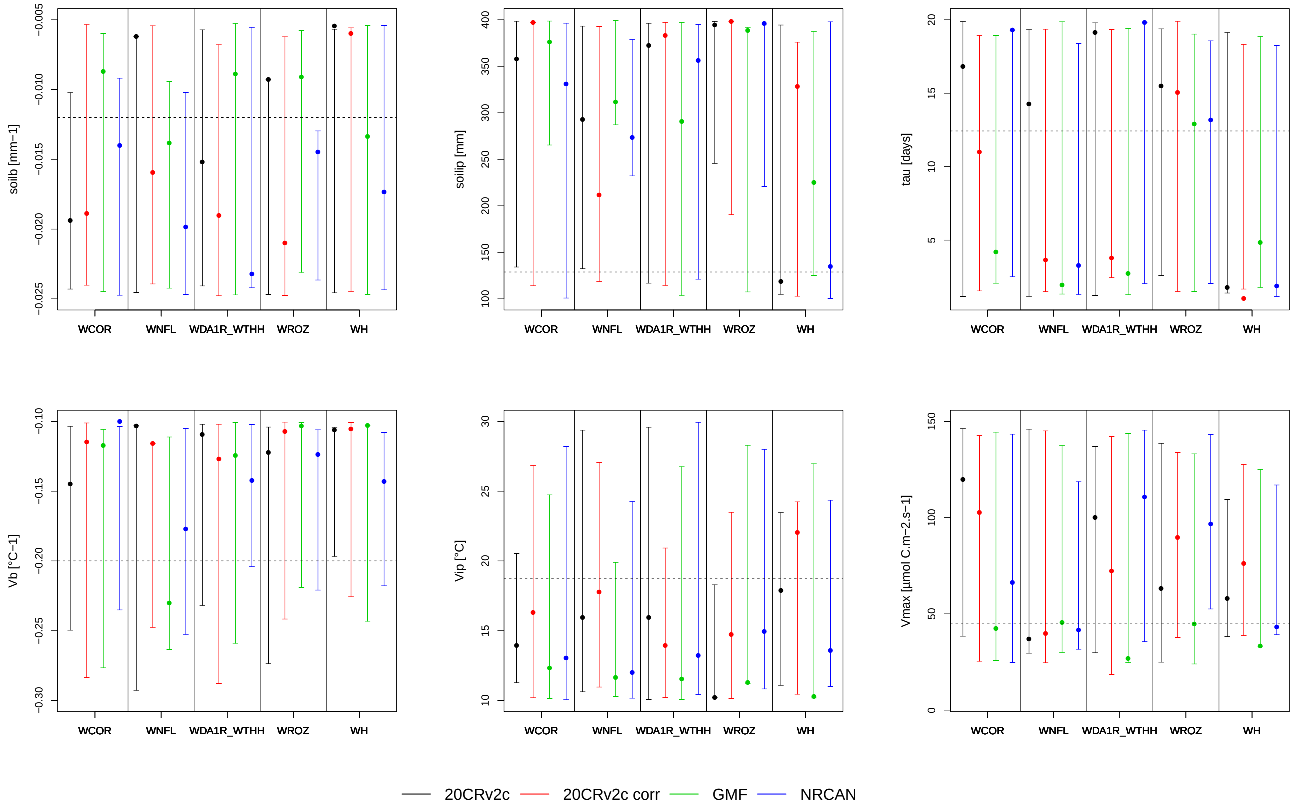

Figure S3. Selected photosynthesis parameters value (Table S3) based on the calibration procedure detailed in Sect. 2.3.1 and 95% confidence interval of each parameter (computed based on all iterations of the second step of the calibration process, with a five iterations thinning and a burn-in period of 1000 iterations, see Sect. 2.3.1) for the five aggregated Eastern Canadian sites (Fig. 1b) and for all climatic datasets (Table 2) over the 1950-2000 time period. Dashed line corresponds to the parameter value at *QC_taiga* site from Gennaretti et al. (2017).

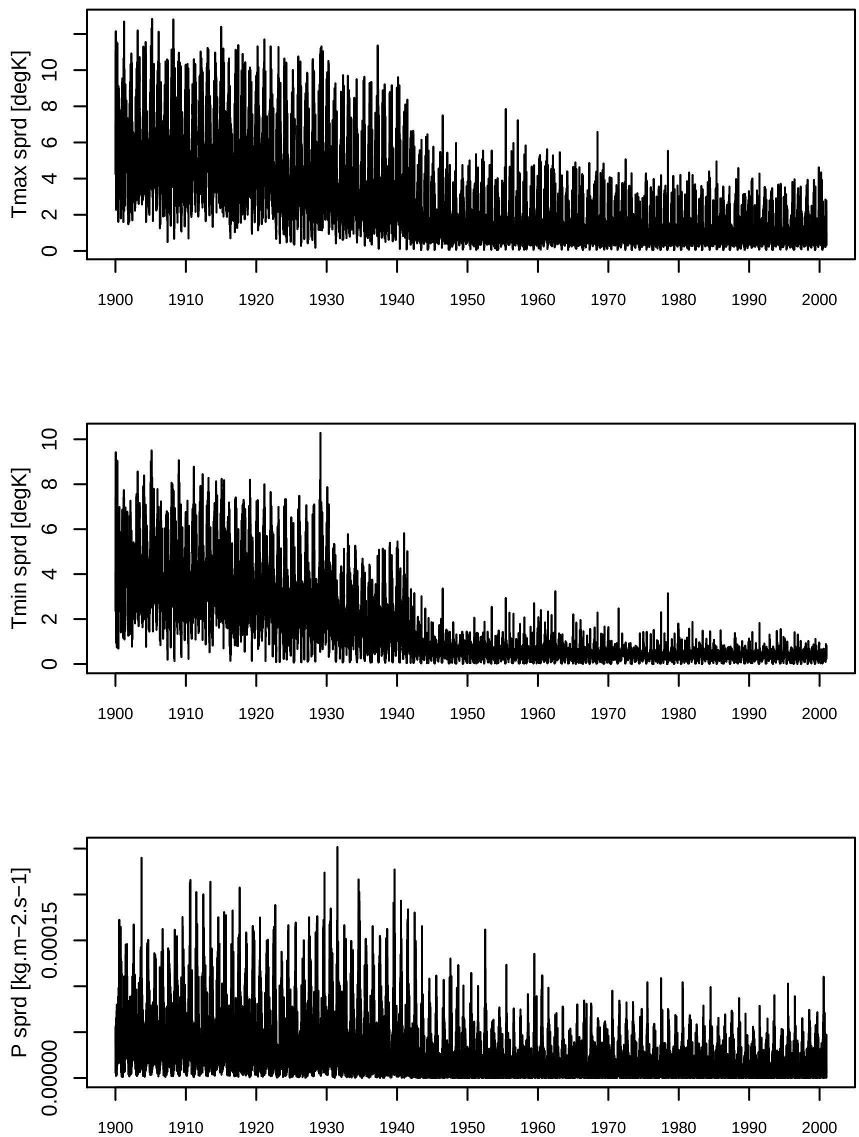

Figure S4. WL42 (Fig. 1a). Ensemble spread of maximum temperature (Tmax sprd), minimum temperature (Tmin sprd) and precipitations (P sprd) for the NOAA-CIRES 20th Century Reanalysis V2c (Table 2) for the 1900-2000 time period.

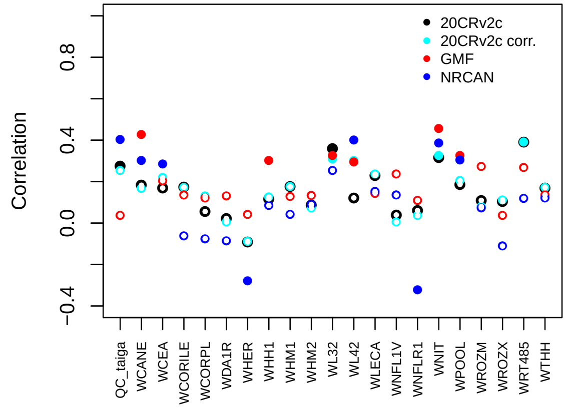

(a) 1950-2000

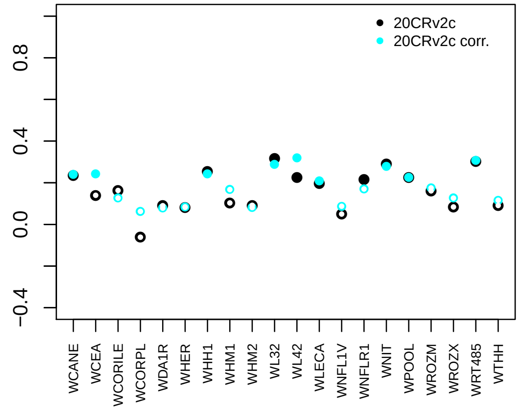

(b) 1900-2000

Figure S5. Pearson correlation coefficients between tree growth observations and simulations at the Eastern Canadian taiga sites (Fig. 1a) with VS-Lite using the different climatic datasets described in Table 2 for the 1950-2000 (a) and 1900-2000 (b) calibration periods. White inner circles stand for non-significant correlations (p-value > 0.05).

Carbon allocation parameters for QC_taiga

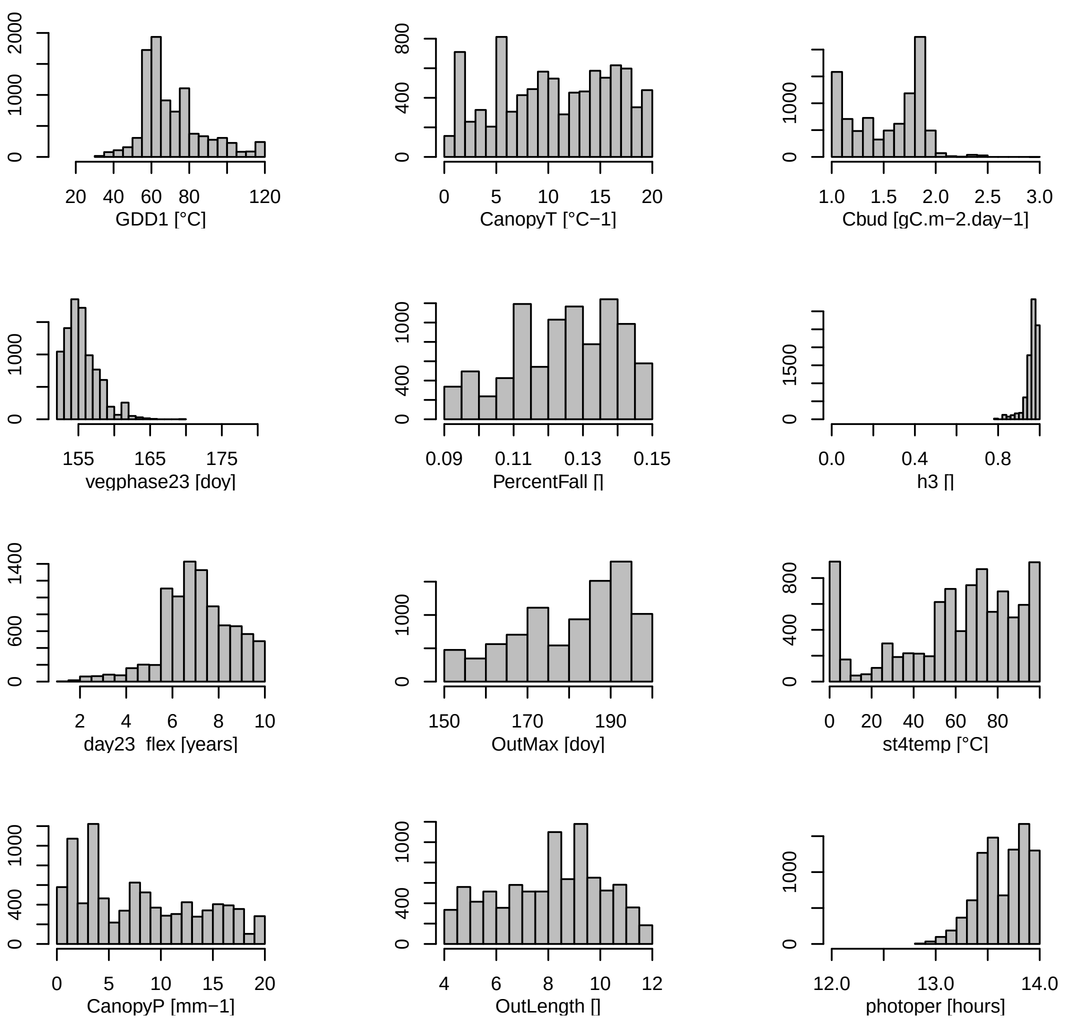

Figure S6. Posterior frequency distributions of carbon allocation parameters (Table S3) at QC_taiga site (NRCAN (5') climatic dataset) (Fig. 1a, Table 2) for the 1950-2000 calibration period.

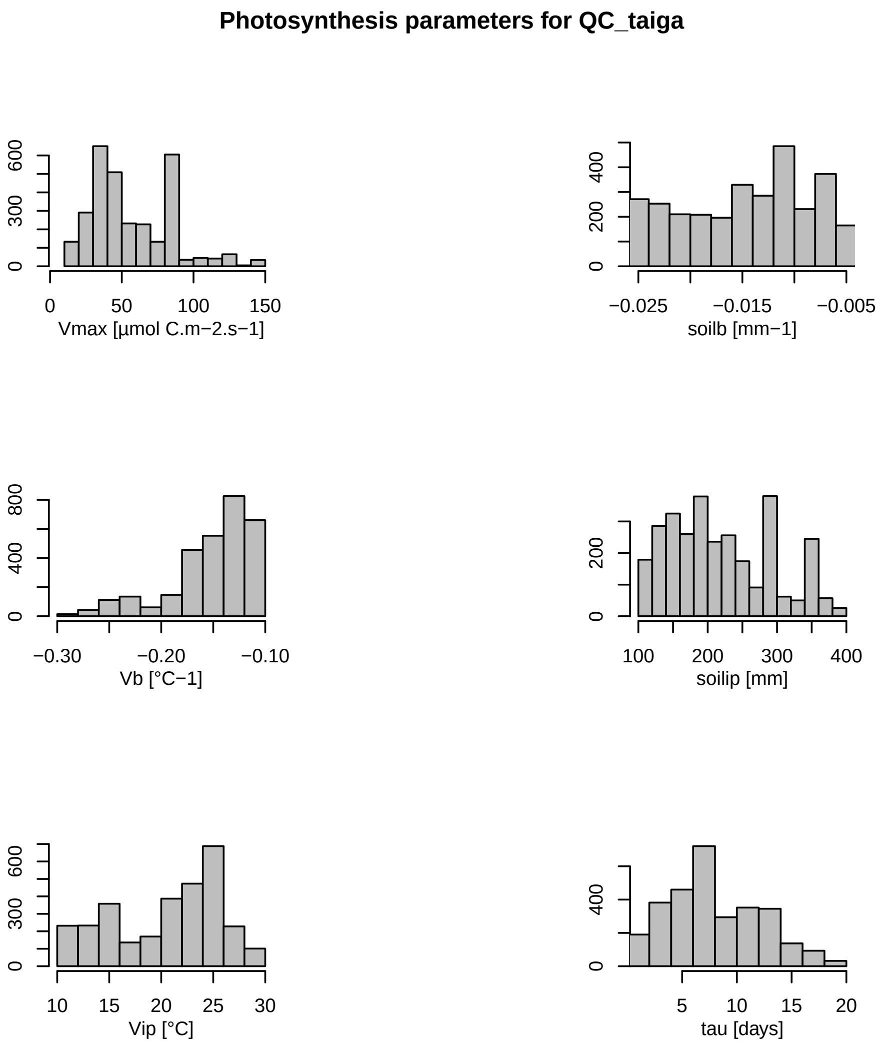

Figure S7. Posterior frequency distributions of photosynthesis parameters (Table S3) at QC_taiga site (NRCAN (5') climatic dataset) (Fig. 1a, Table 2) for the 1950-2000 calibration period.

Carbon allocation parameters for WCORPL

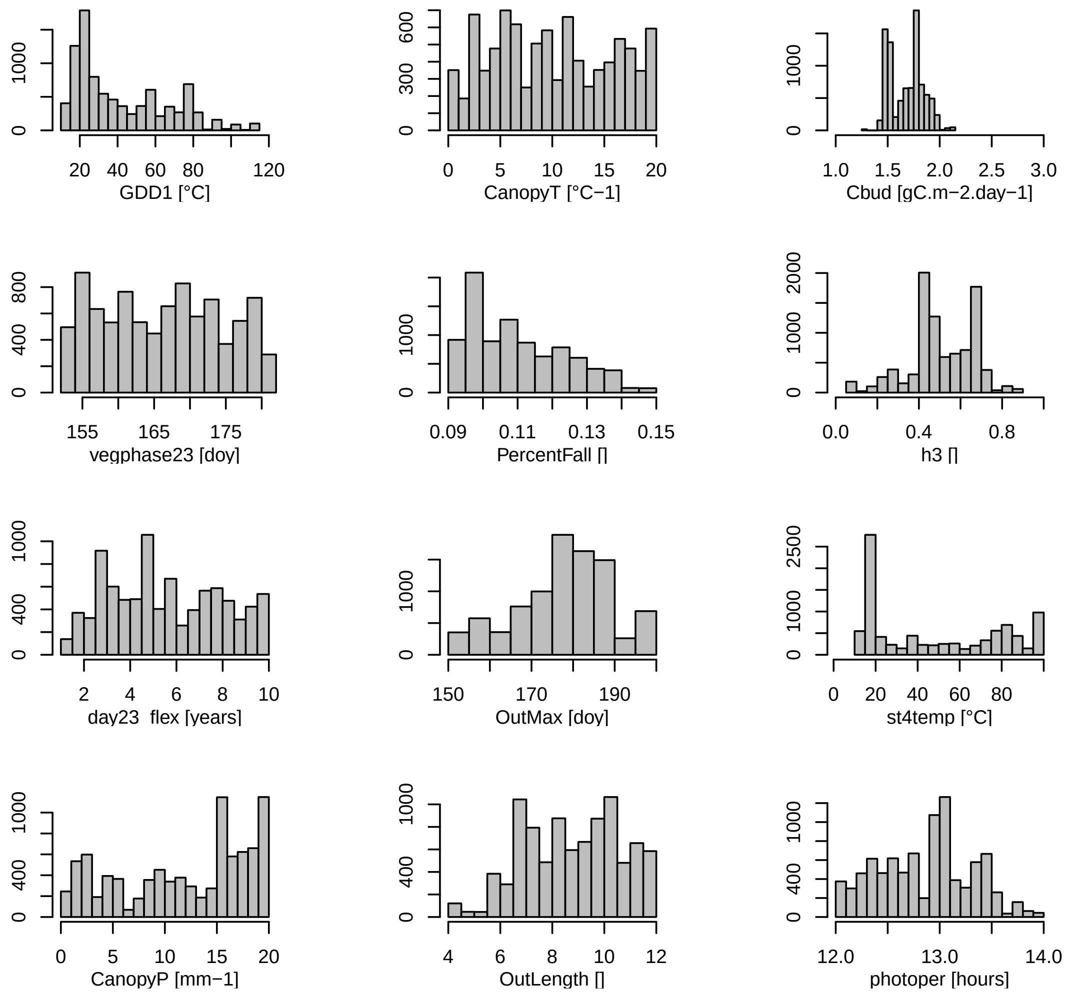

Figure S8. As in Fig. S6 at WCORPL site.

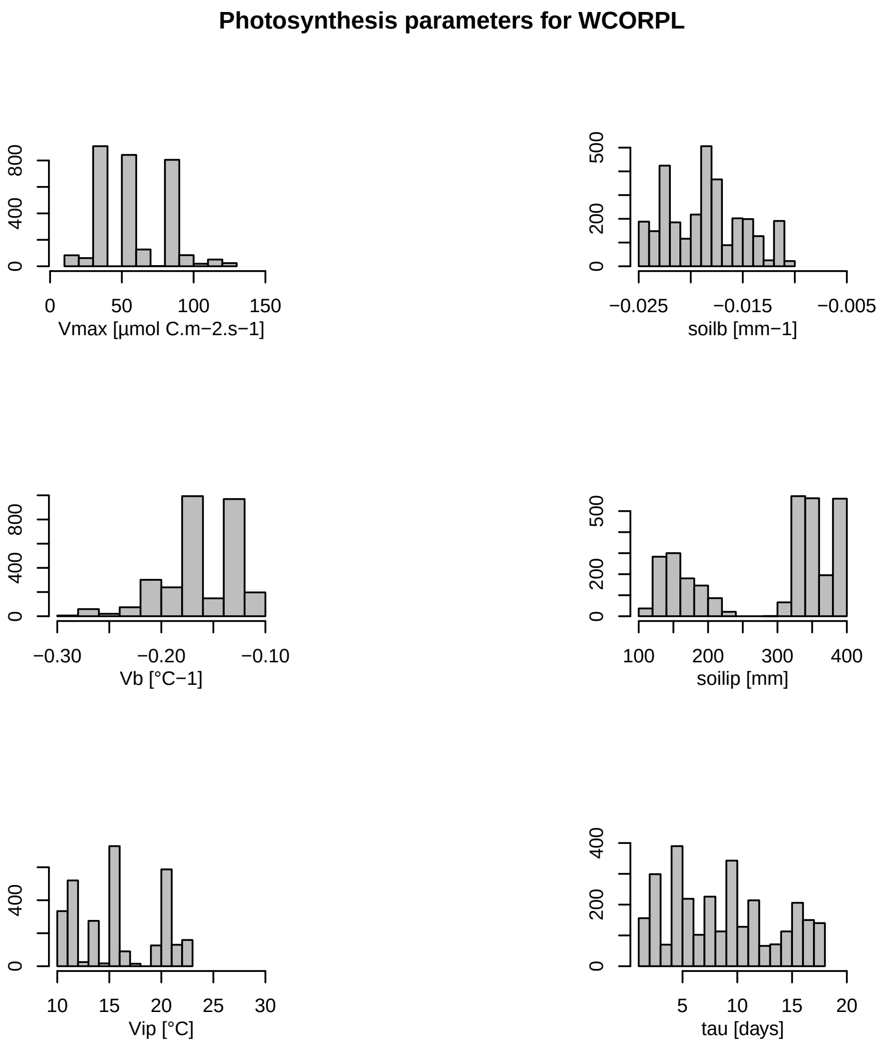

Figure S9. As in Fig. S7 at WCORPL site.

Carbon allocation parameters for WCANE

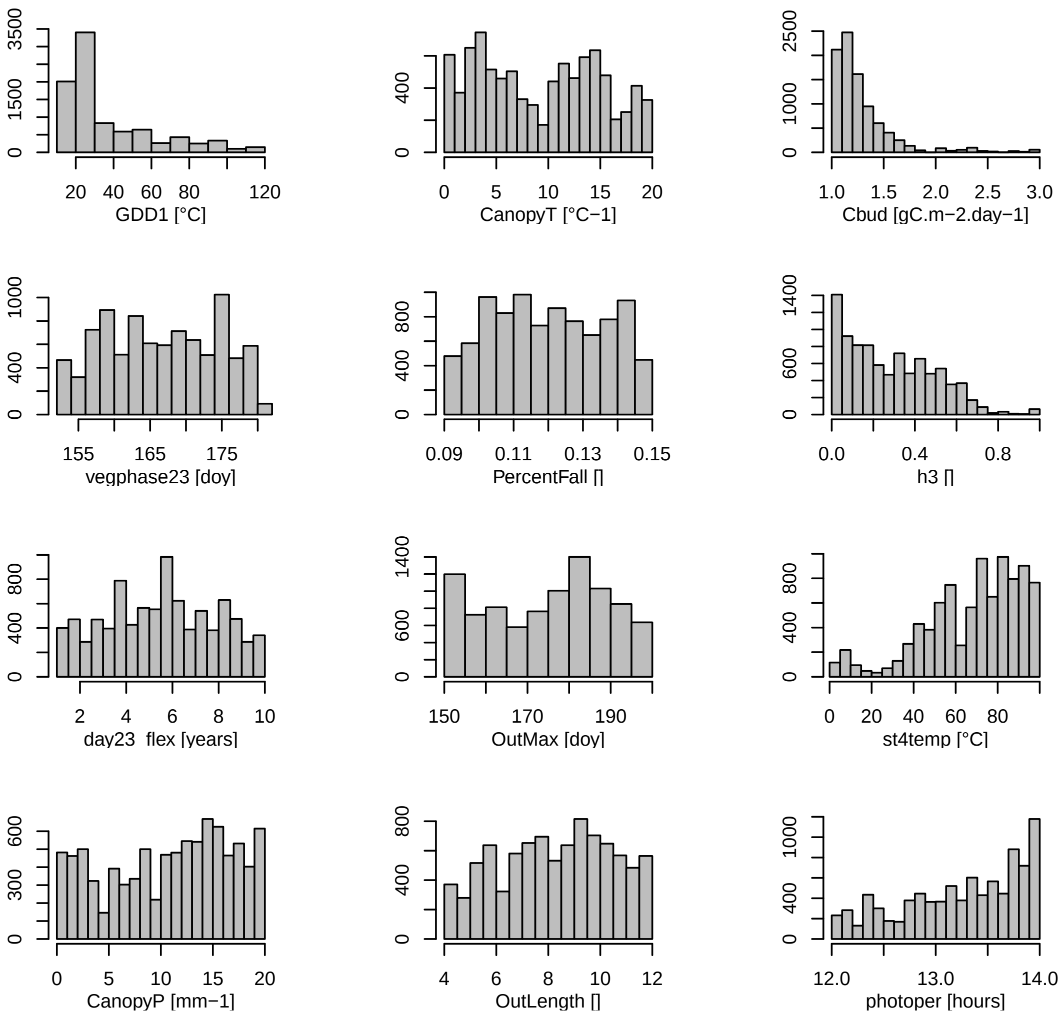

Figure S10. As in Fig. S6 at WCANE site.

Photosynthesis parameters for WCANE

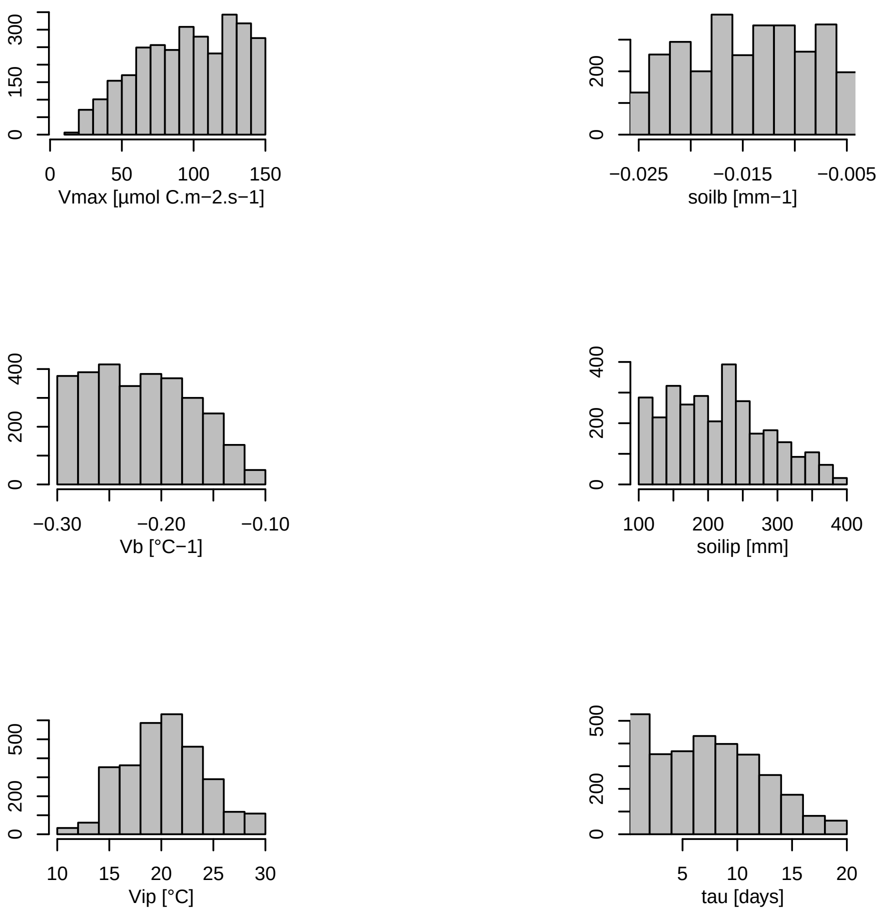

Figure S11. As in Fig. S7 at WCANE site.

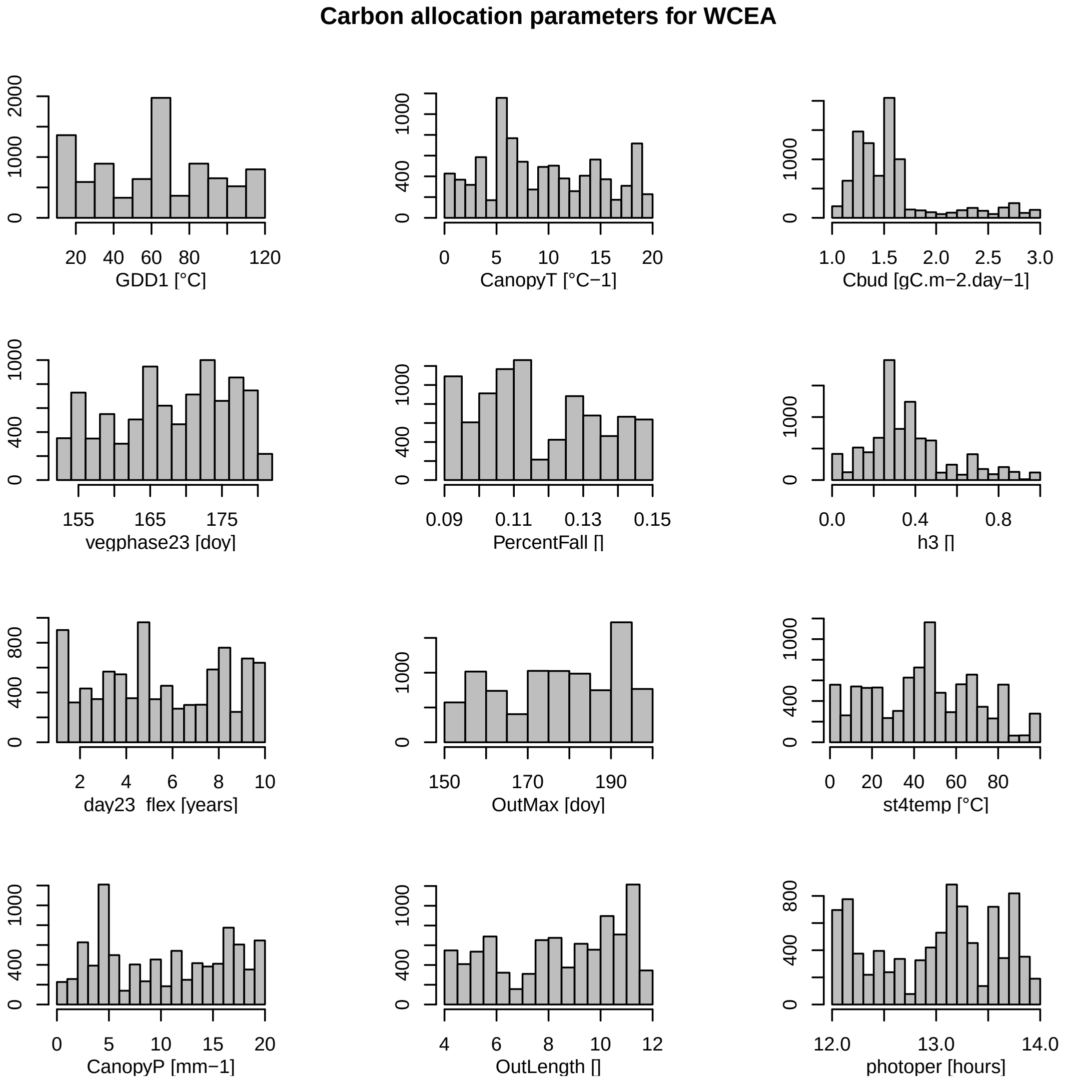

Figure S12. As in Fig. S6 at WCEA site.

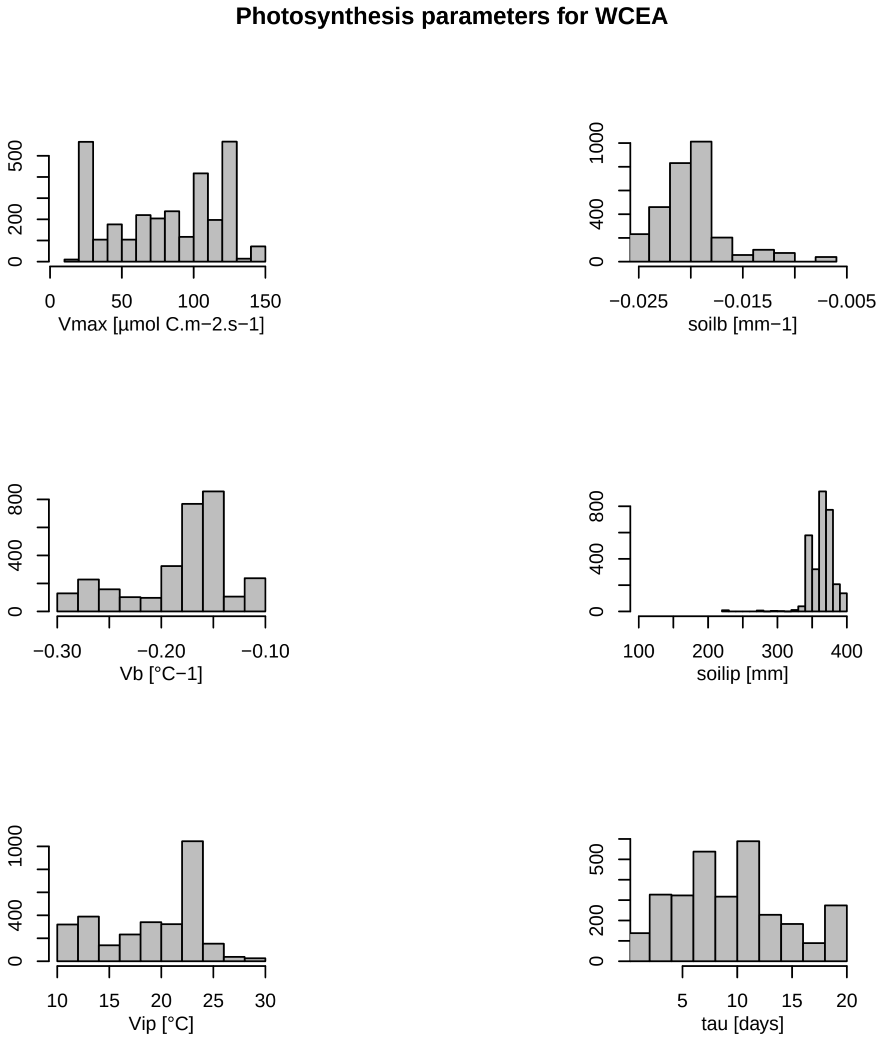

Figure S13. As in Fig. S7 at WCEA site.

Carbon allocation parameters for WCORILE

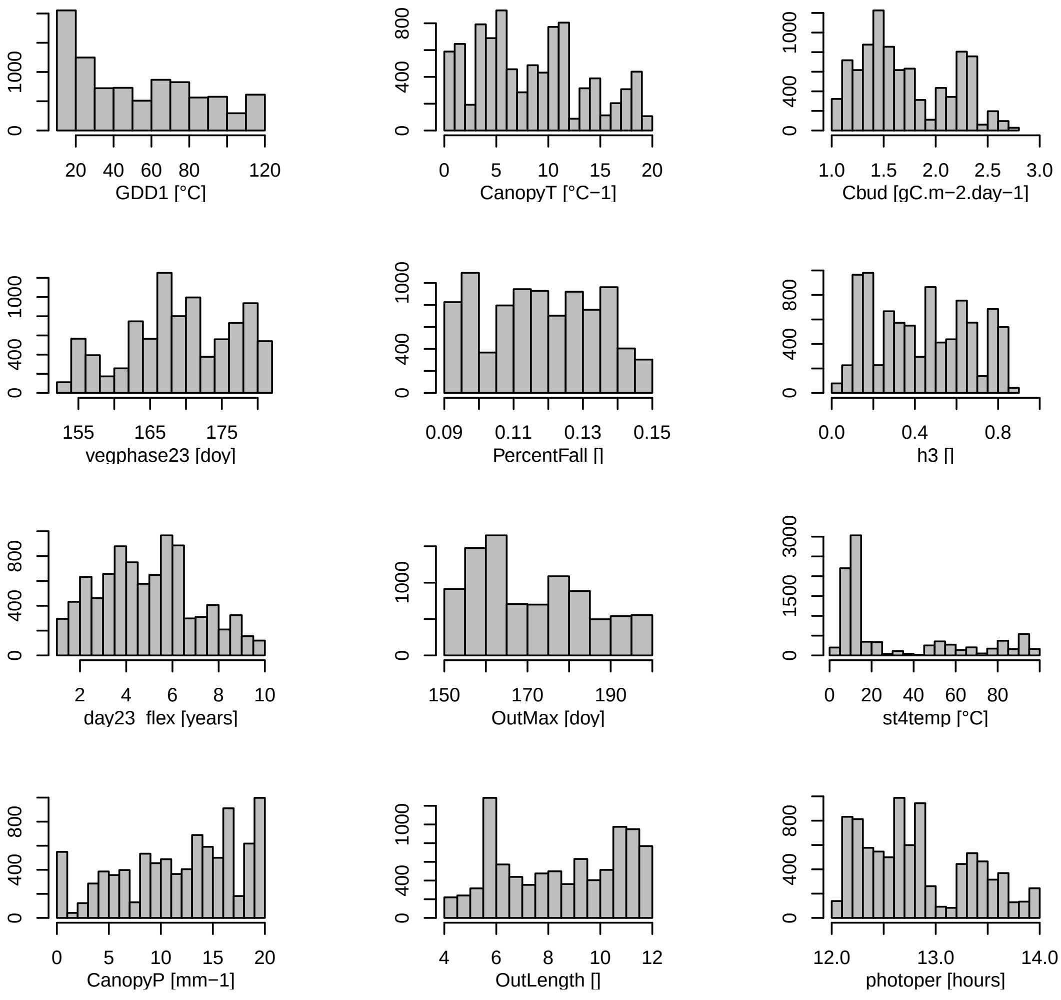

Figure S14. As in Fig. S6 at WCORILE site.

Photosynthesis parameters for WCORILE

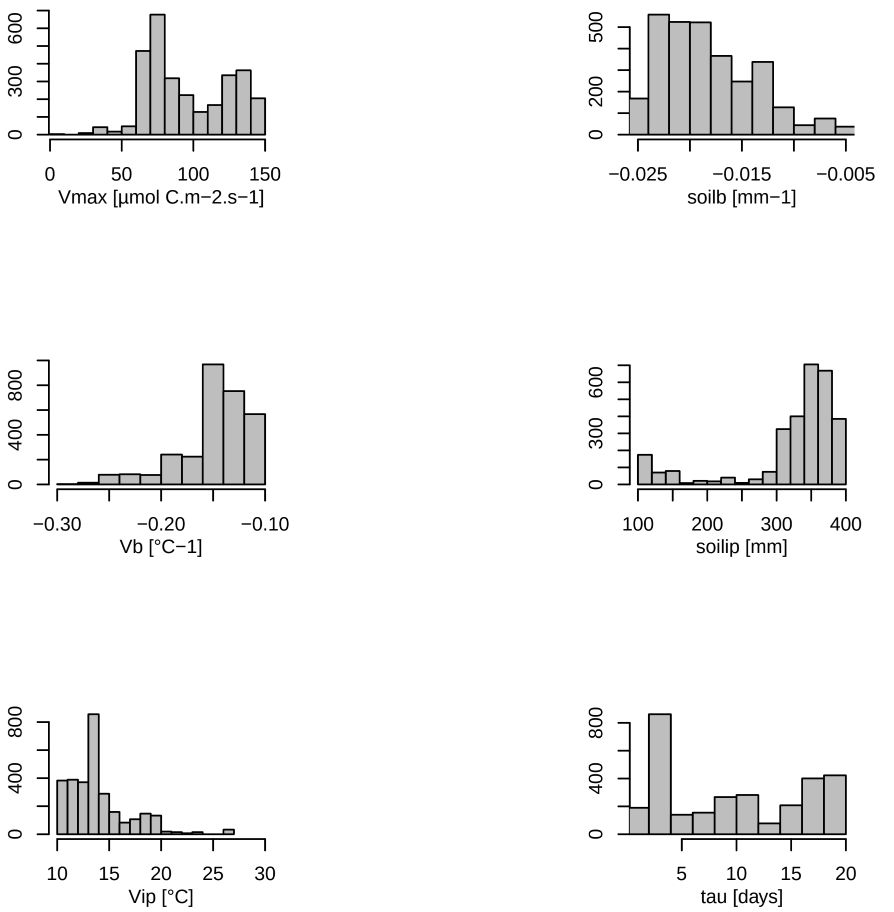

Figure S15. As in Fig. S7 at WCORILE site.

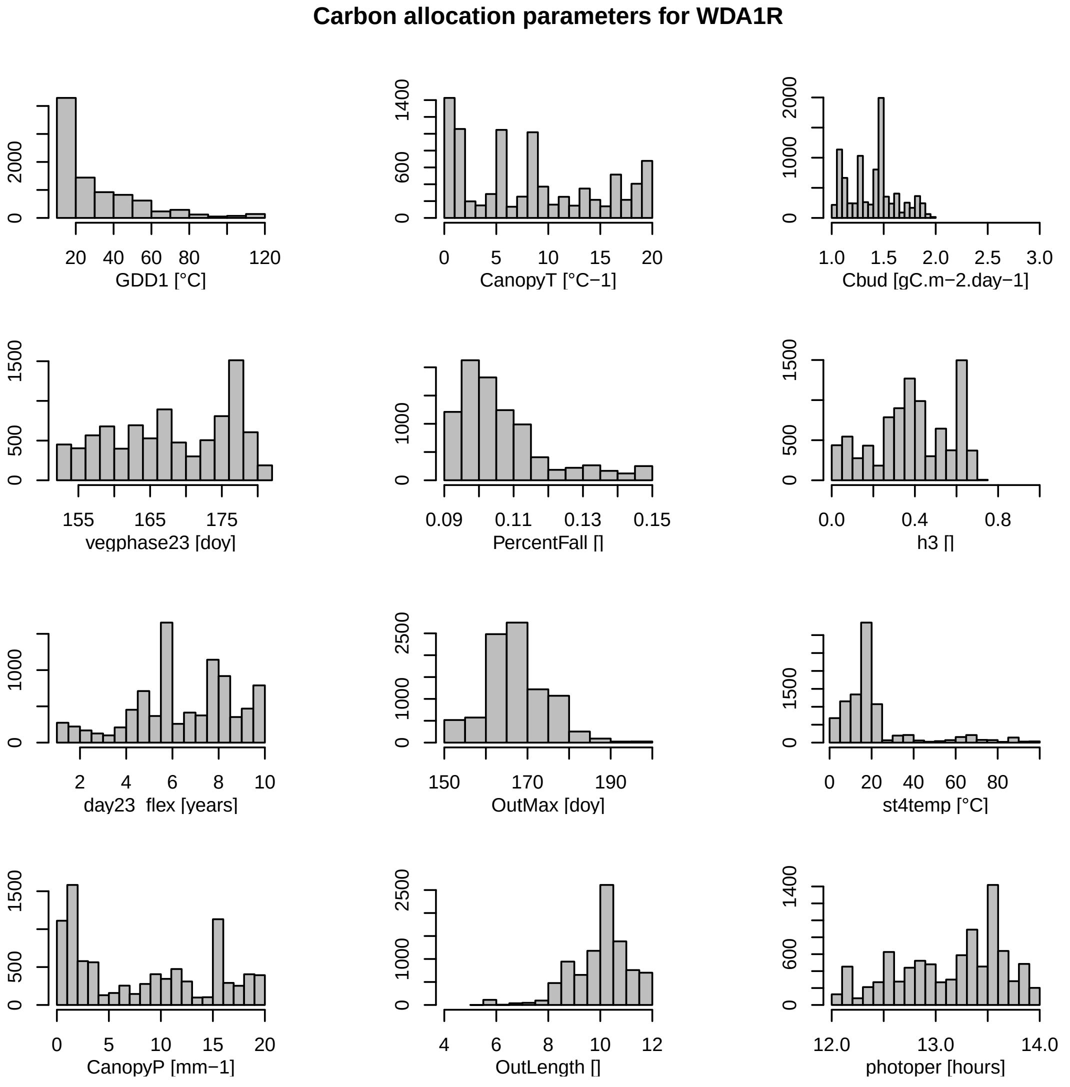

Figure S16. As in Fig. S6 at WDA1R site.

Photosynthesis parameters for WDA1R

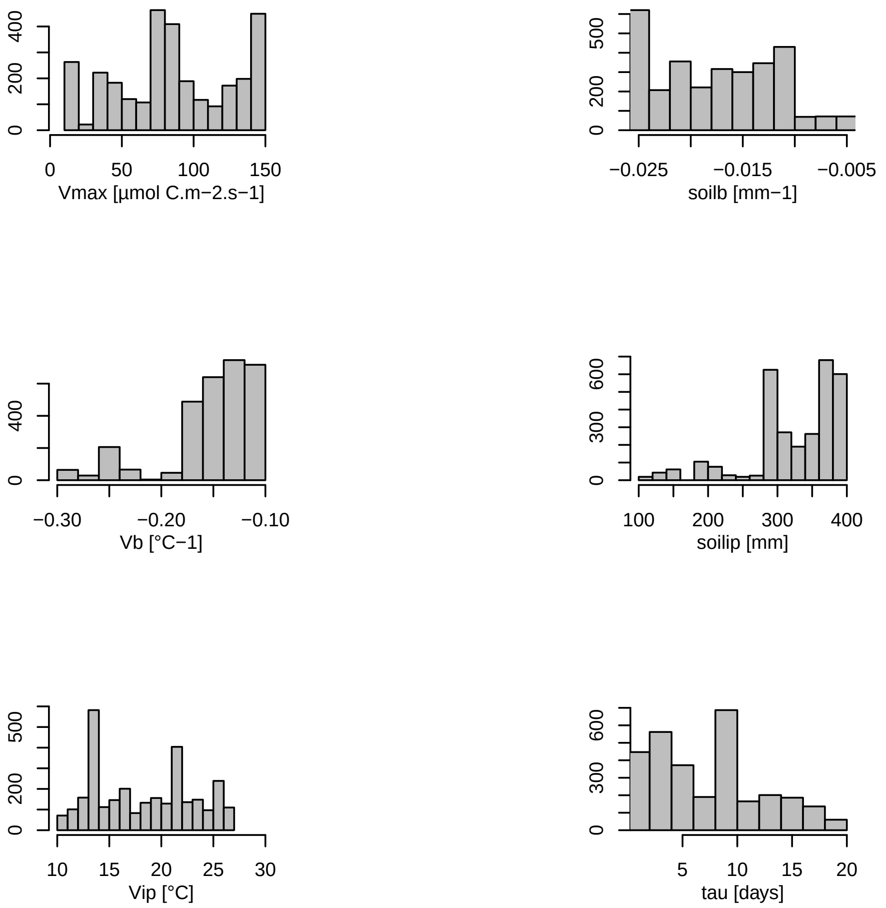

Figure S17. As in Fig. S7 at WDA1R site.

Carbon allocation parameters for WHER

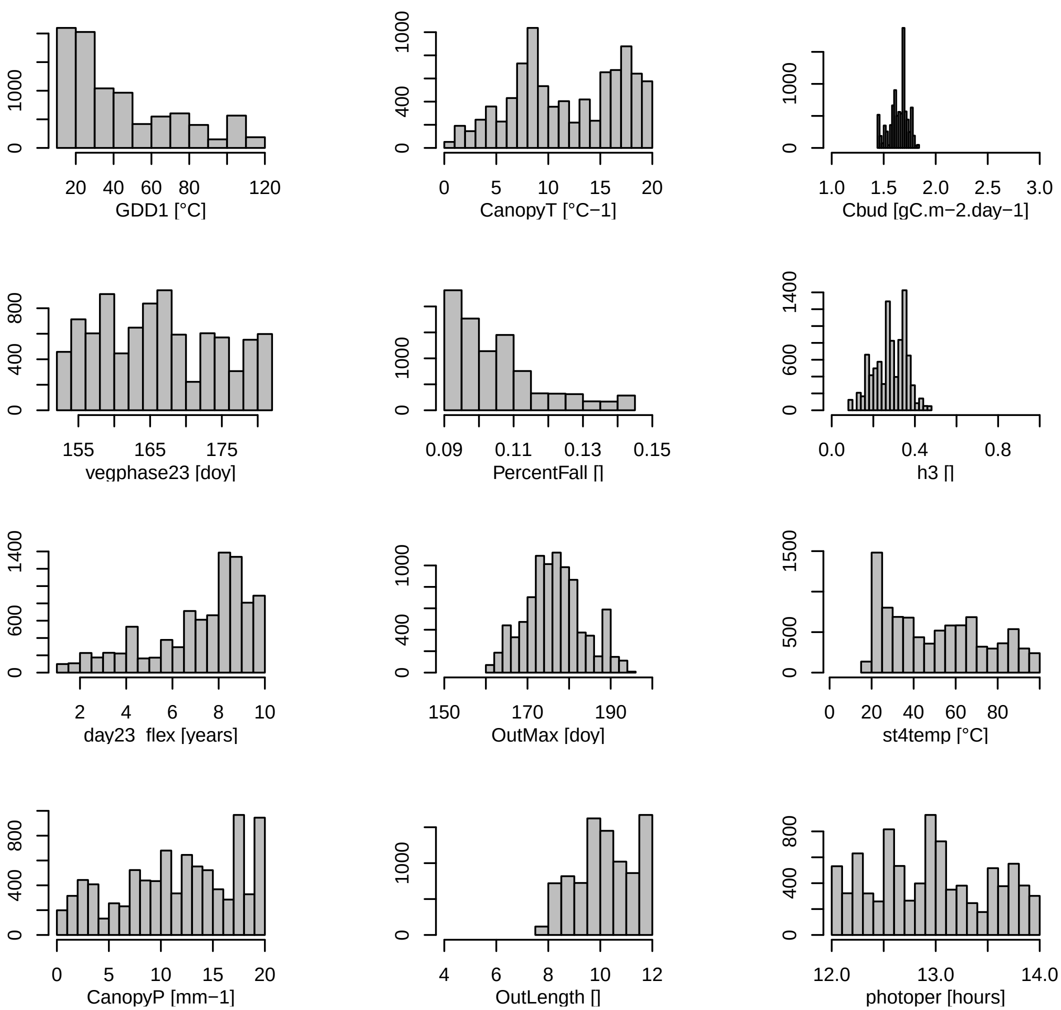

Figure S18. As in Fig. S6 at WHER site.

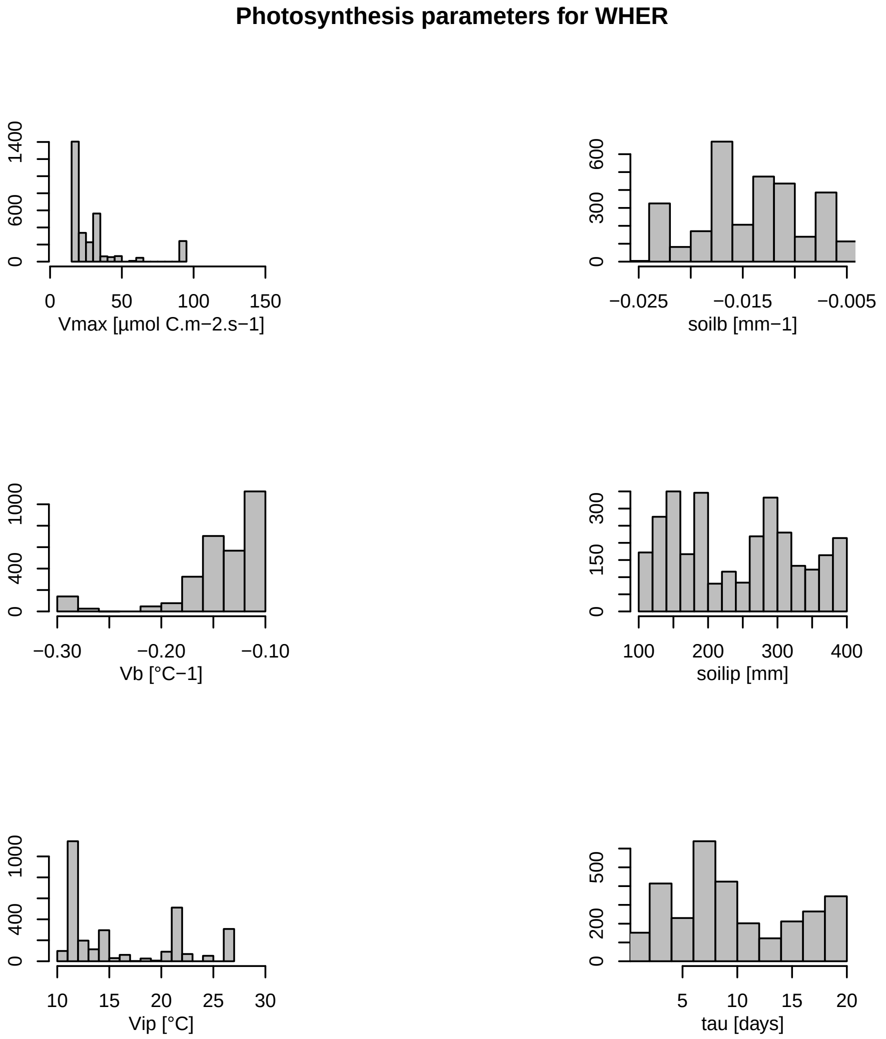

Figure S19. As in Fig. S7 at WHER site.

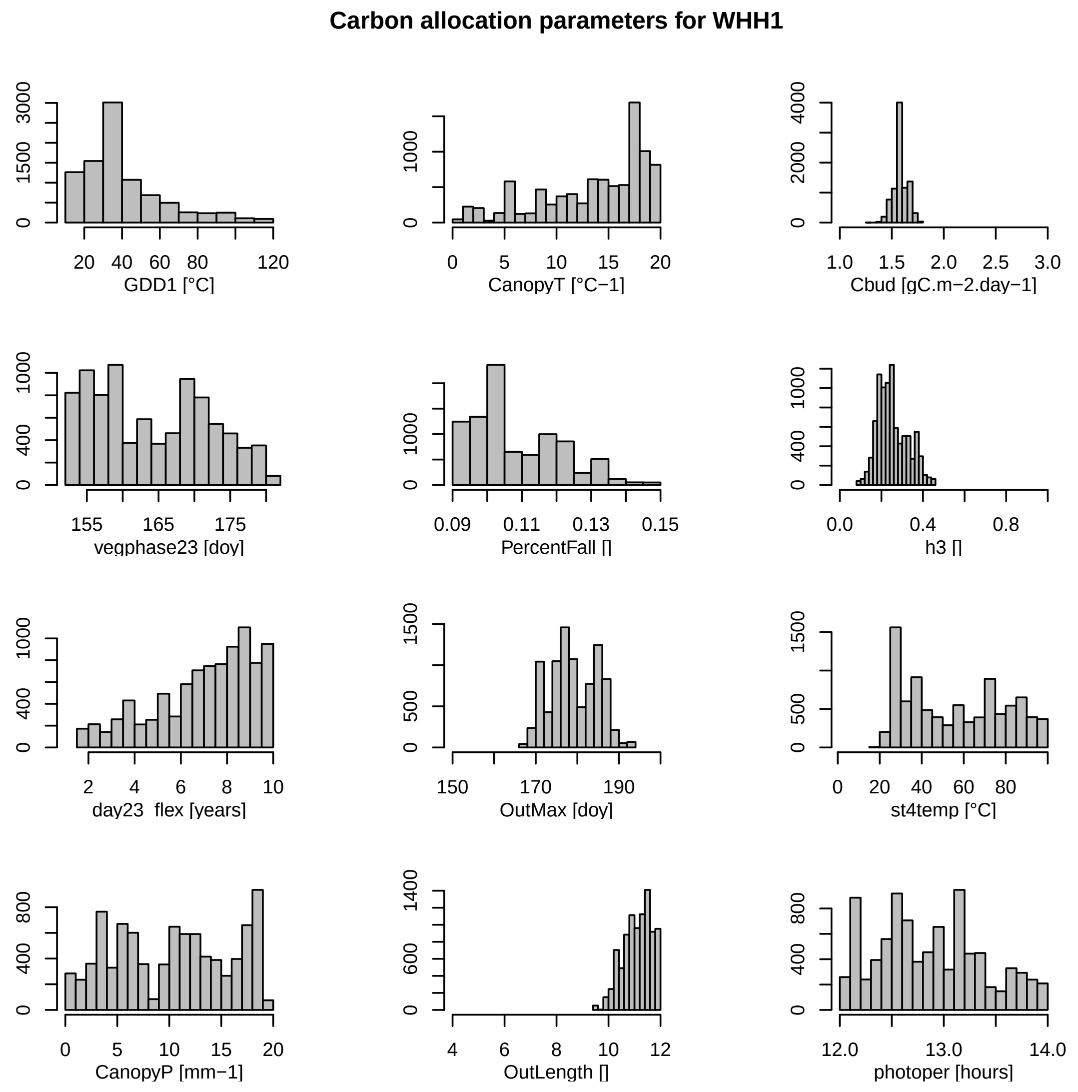

Figure S20. As in Fig. S6 at WHH1 site.

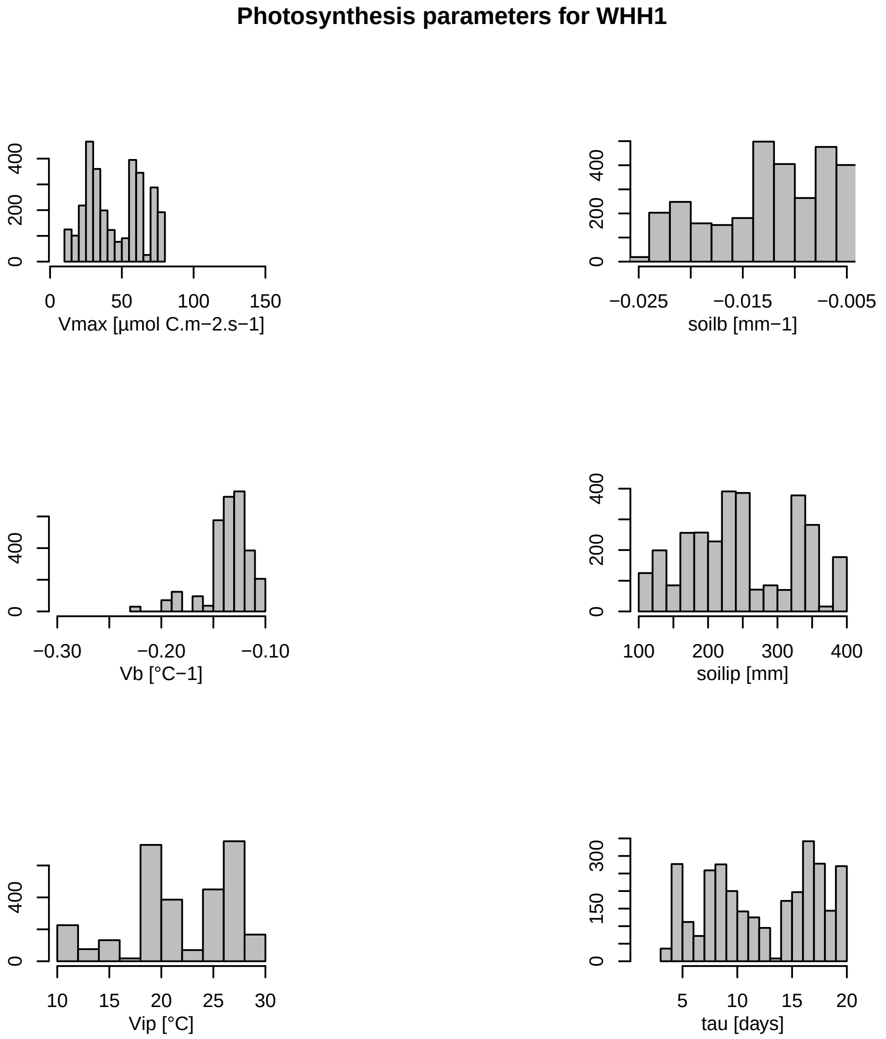

Figure S21. As in Fig. S7 at WHH1 site.

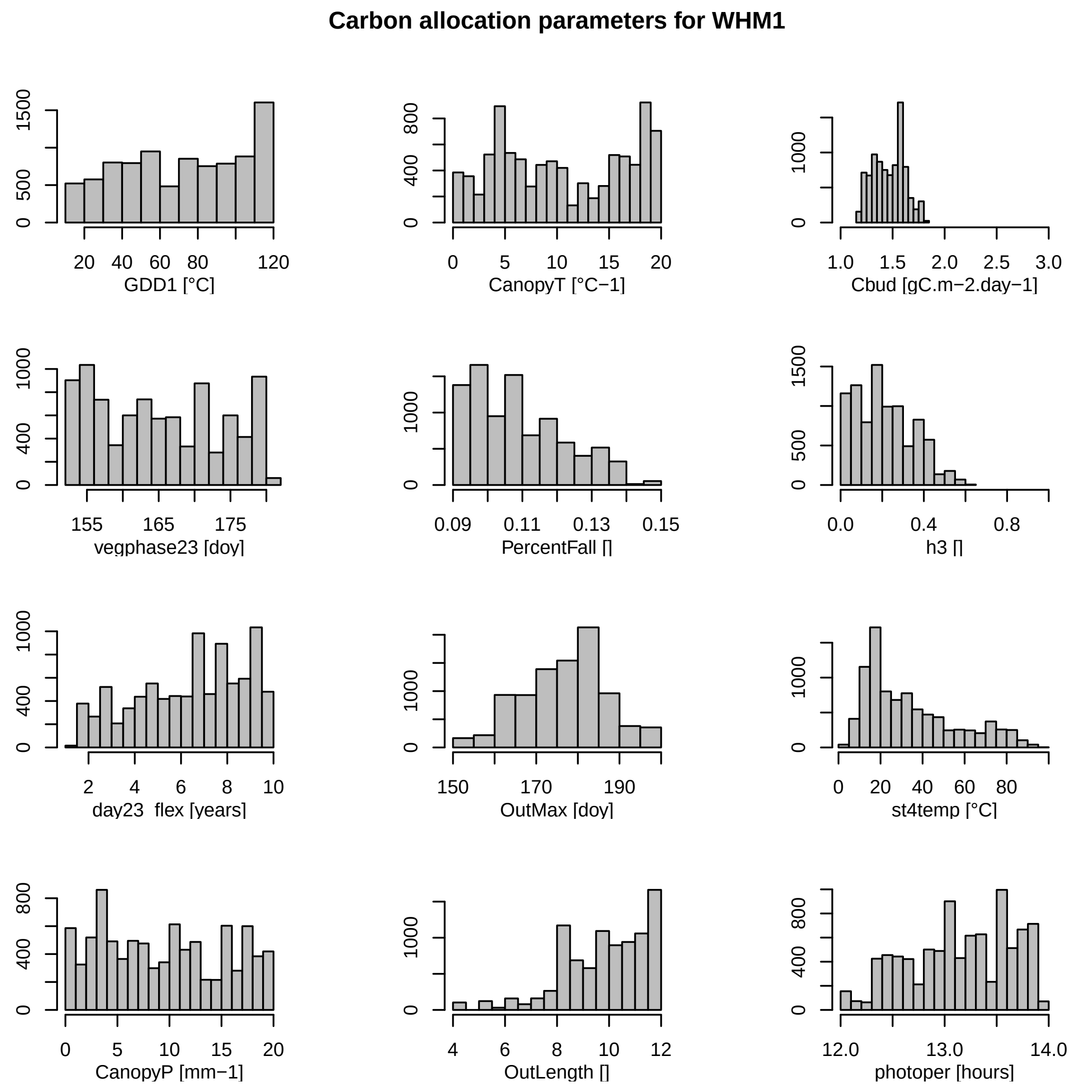

Figure S22. As in Fig. S6 at WHM1 site.

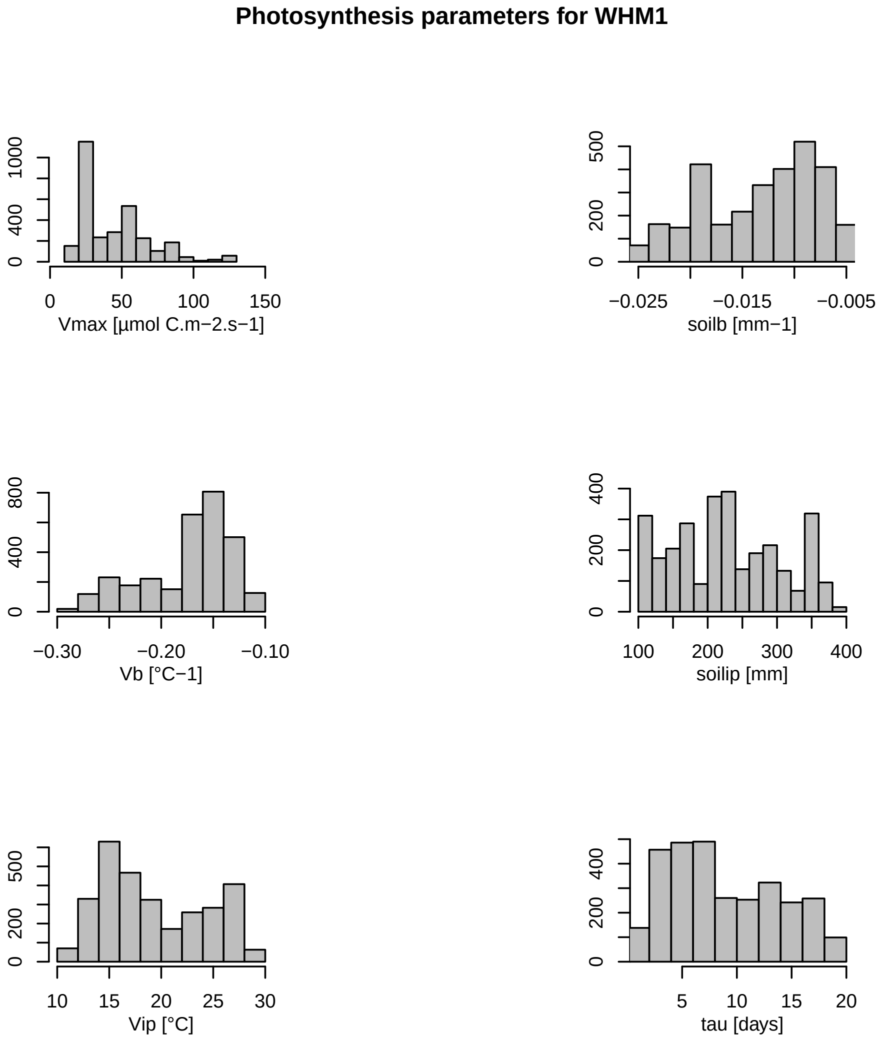

Figure S23. As in Fig. S7 at WHM1 site.

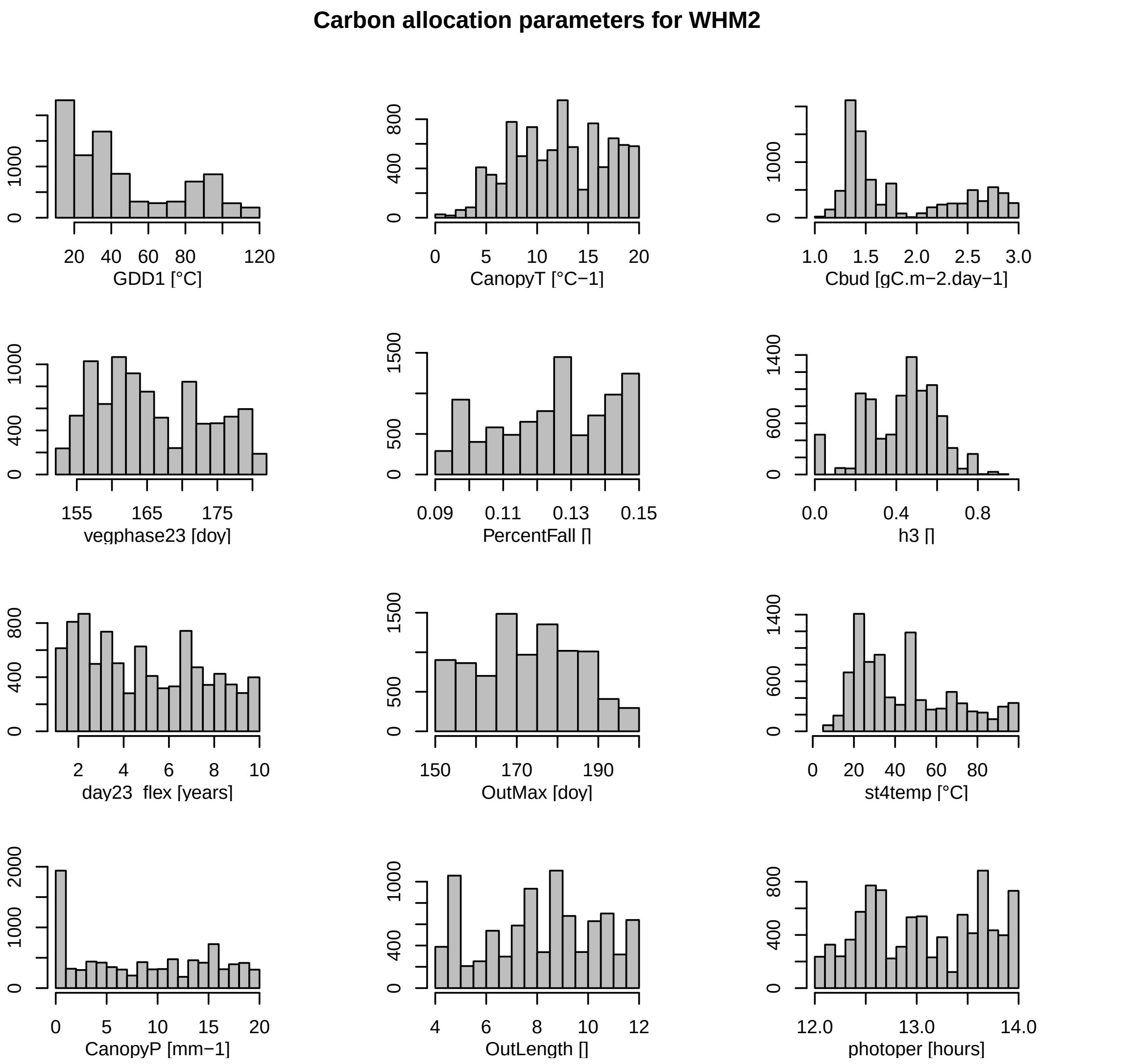

Figure S24. As in Fig. S6 at WHM2 site.

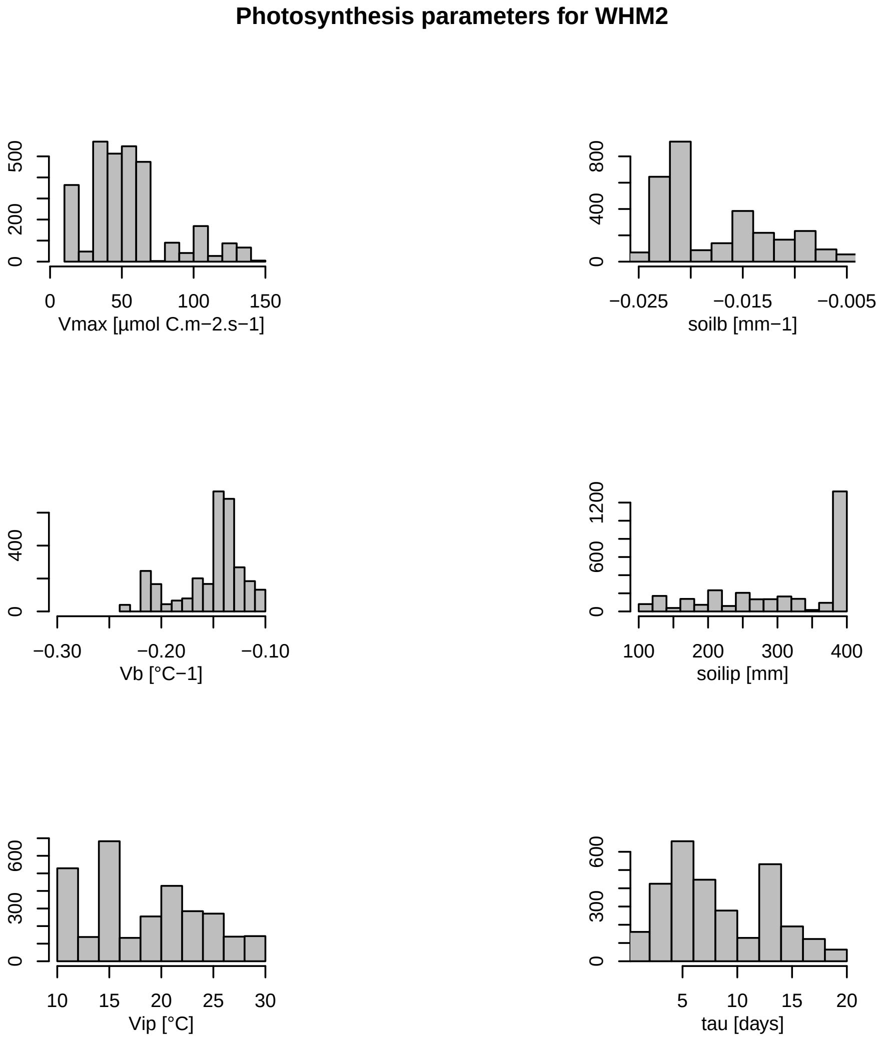

Figure S25. As in Fig. S7 at WHM2 site.

Carbon allocation parameters for WL32

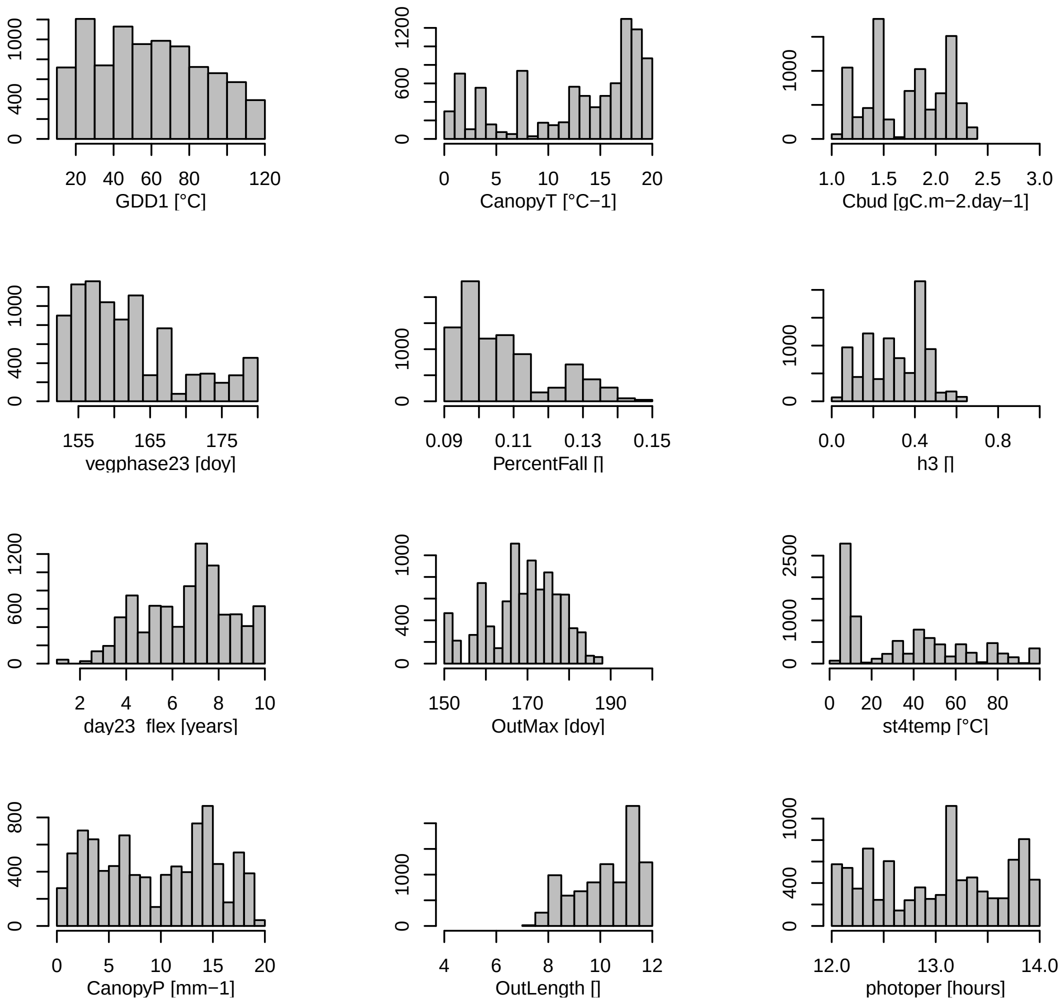

Figure S26. As in Fig. S6 at WL32 site.

Photosynthesis parameters for WL32

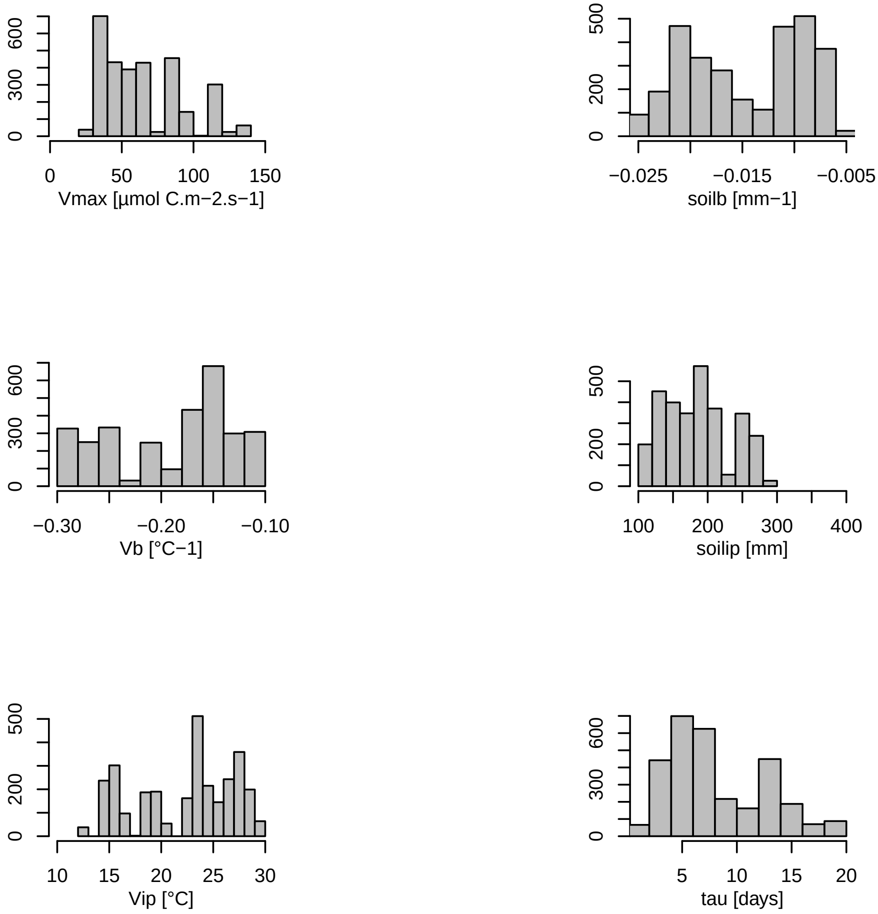

Figure S27. As in Fig. S7 at WL32 site.

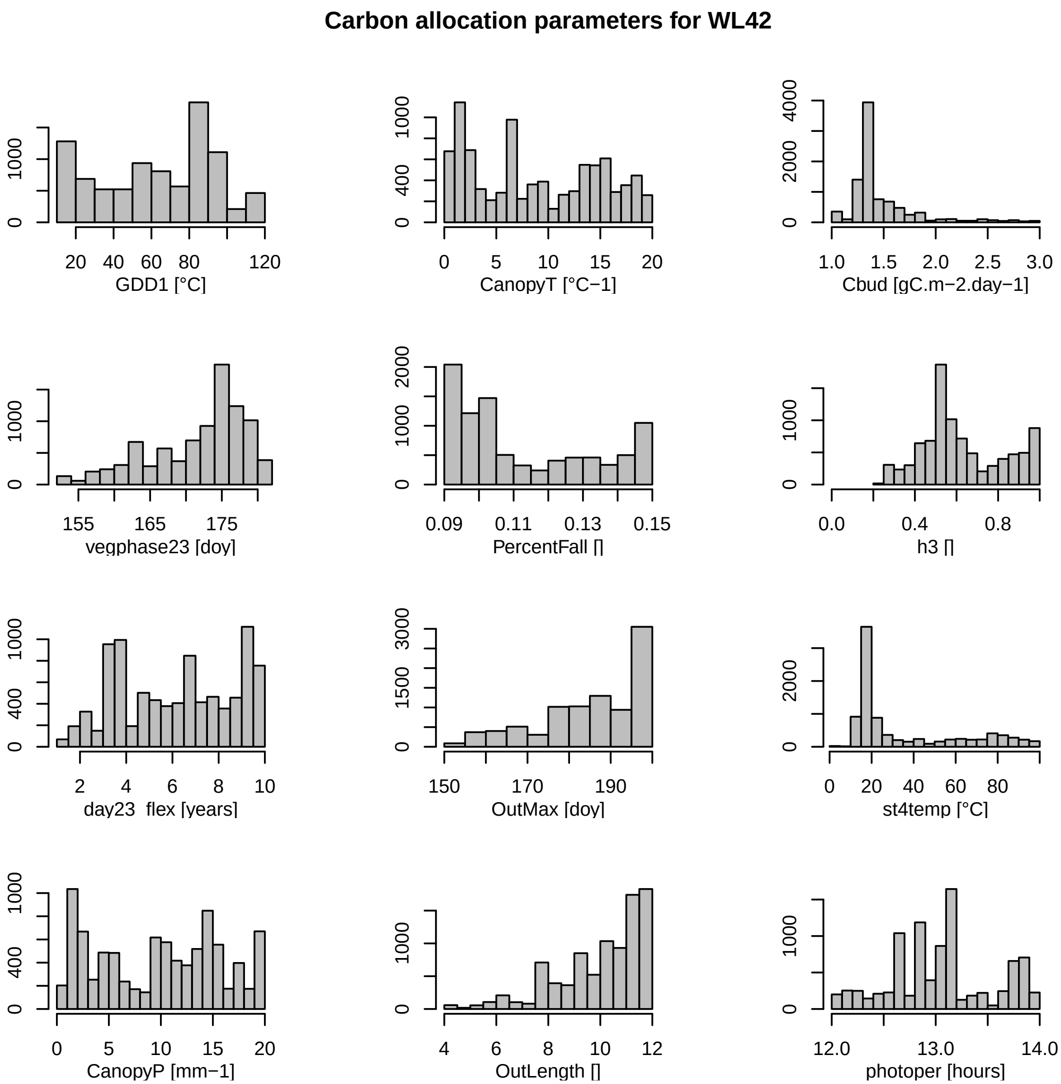

Figure S28. As in Fig. S6 at WL42 site.

Photosynthesis parameters for WL42

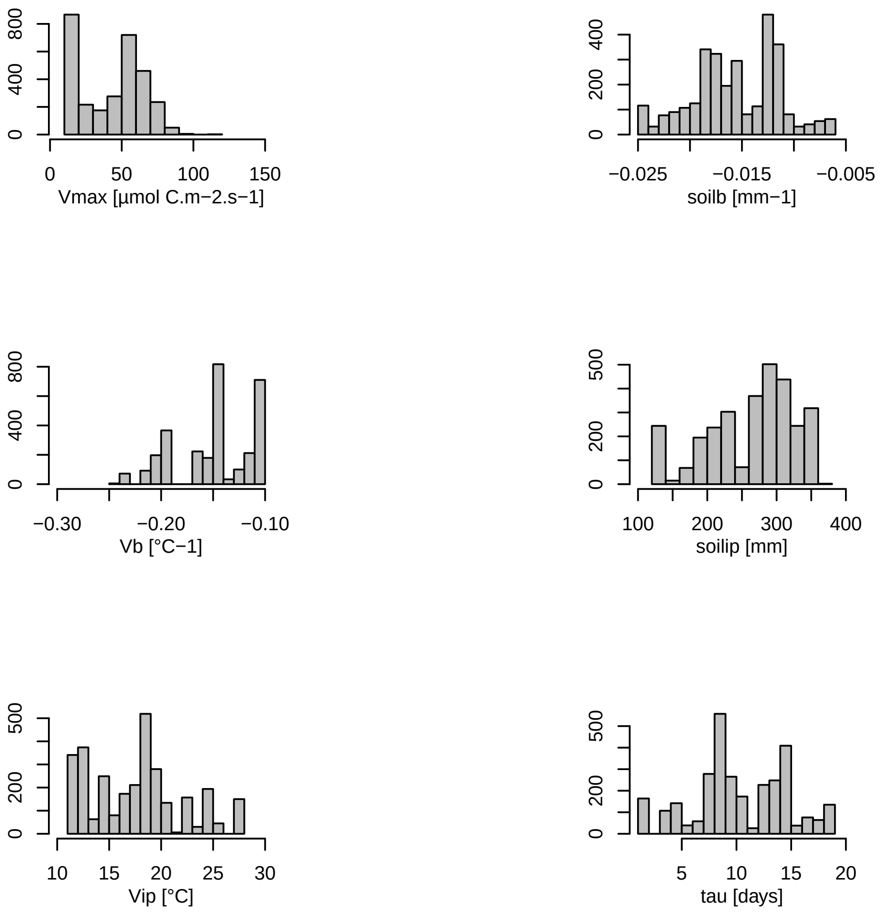

Figure S29. As in Fig. S7 at WL42 site.

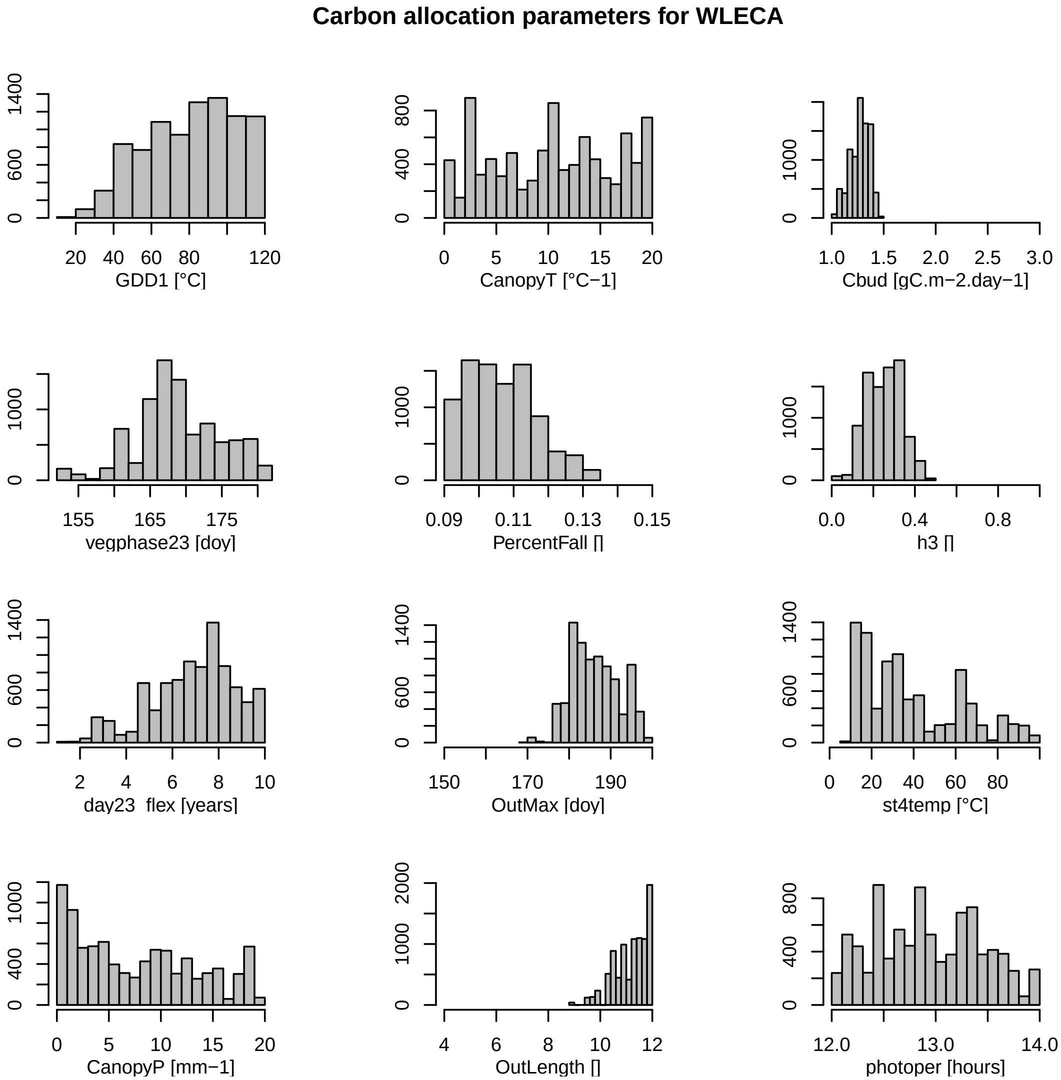

Figure S30. As in Fig. S6 at WLECA site.

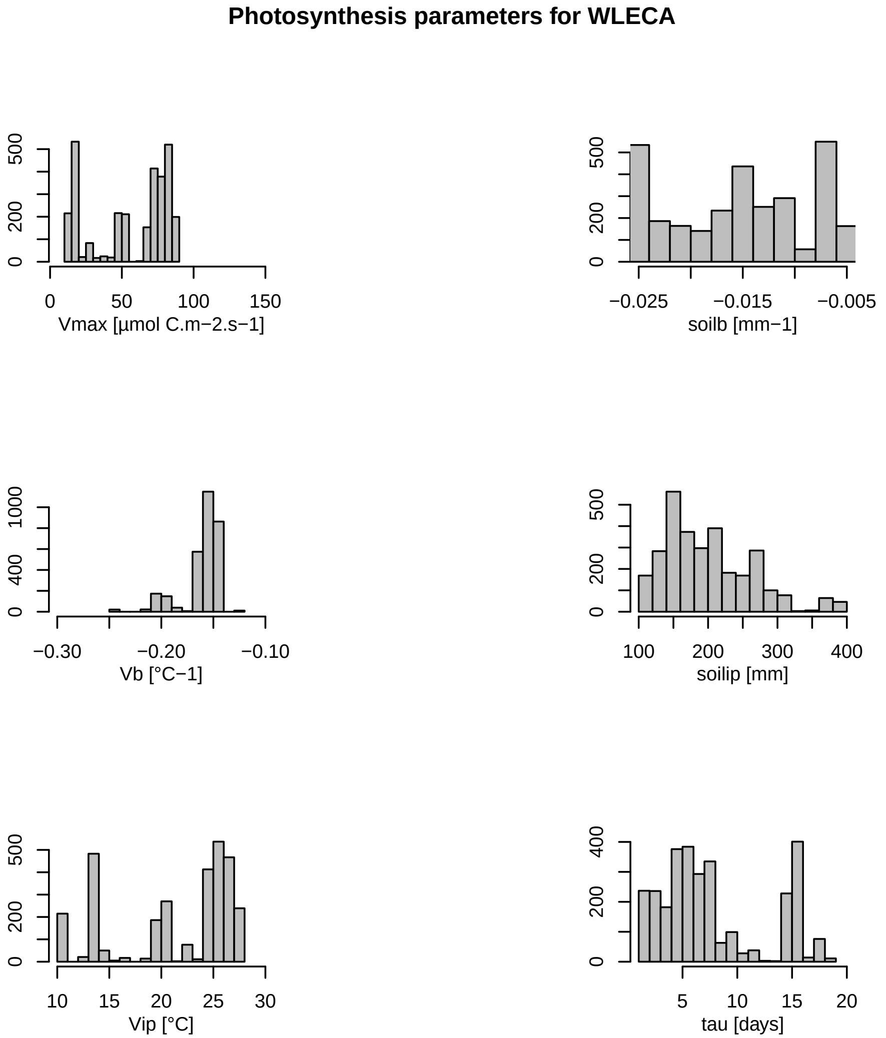

Figure S31. As in Fig. S7 at WLECA site.

Carbon allocation parameters for WNFL1V

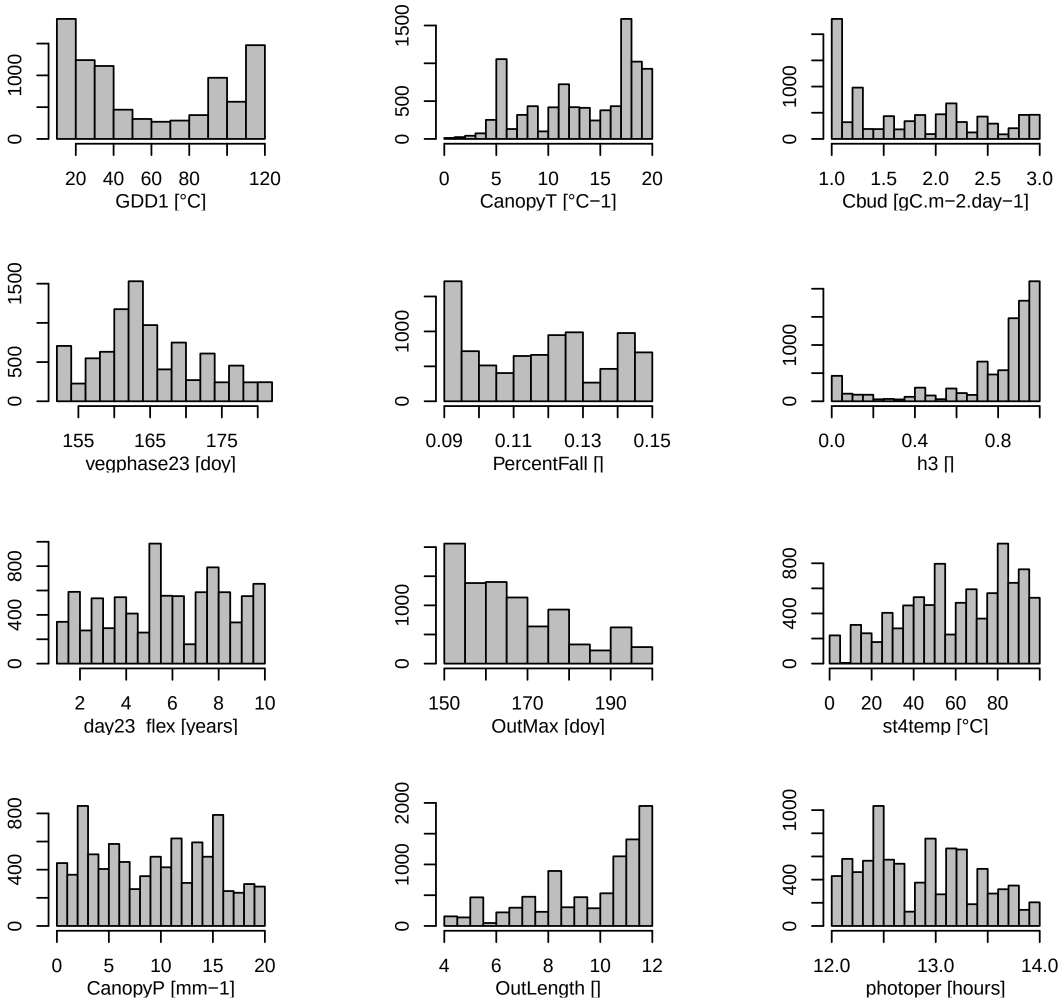

Figure S32. As in Fig. S6 at WNFL1V site.

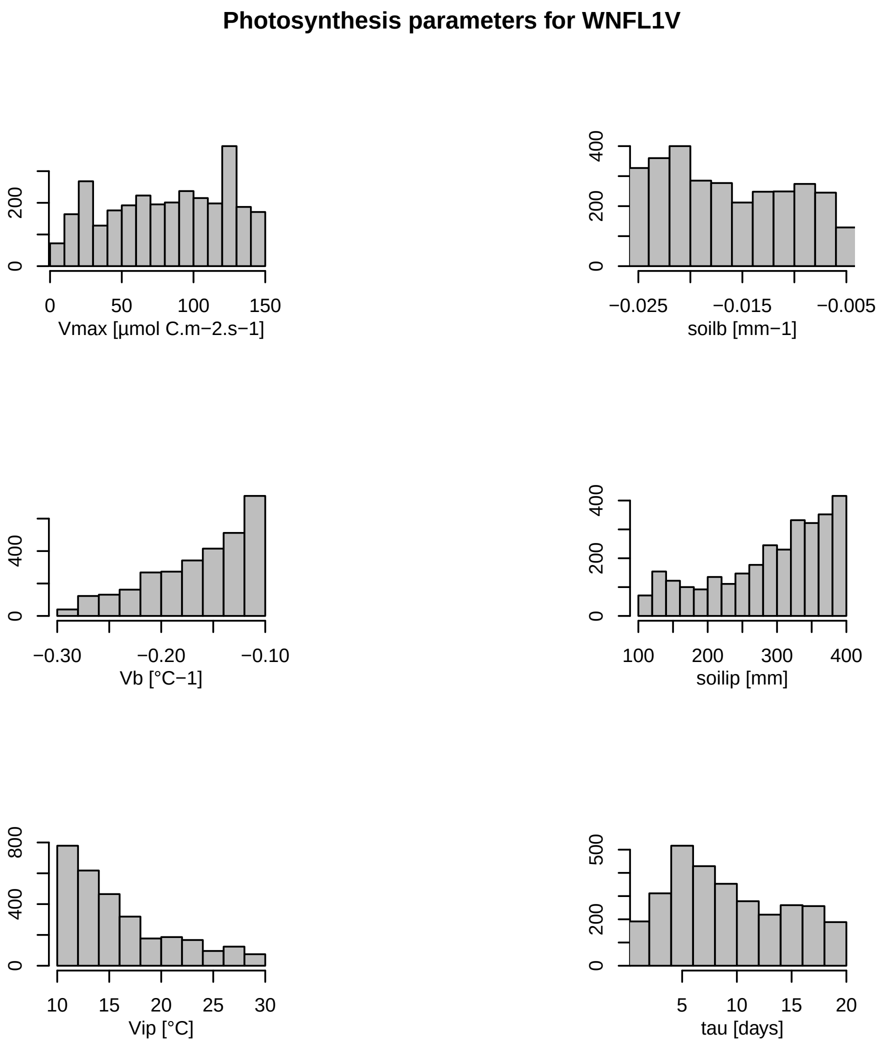

Figure S33. As in Fig. S7 at WNFL1V site.

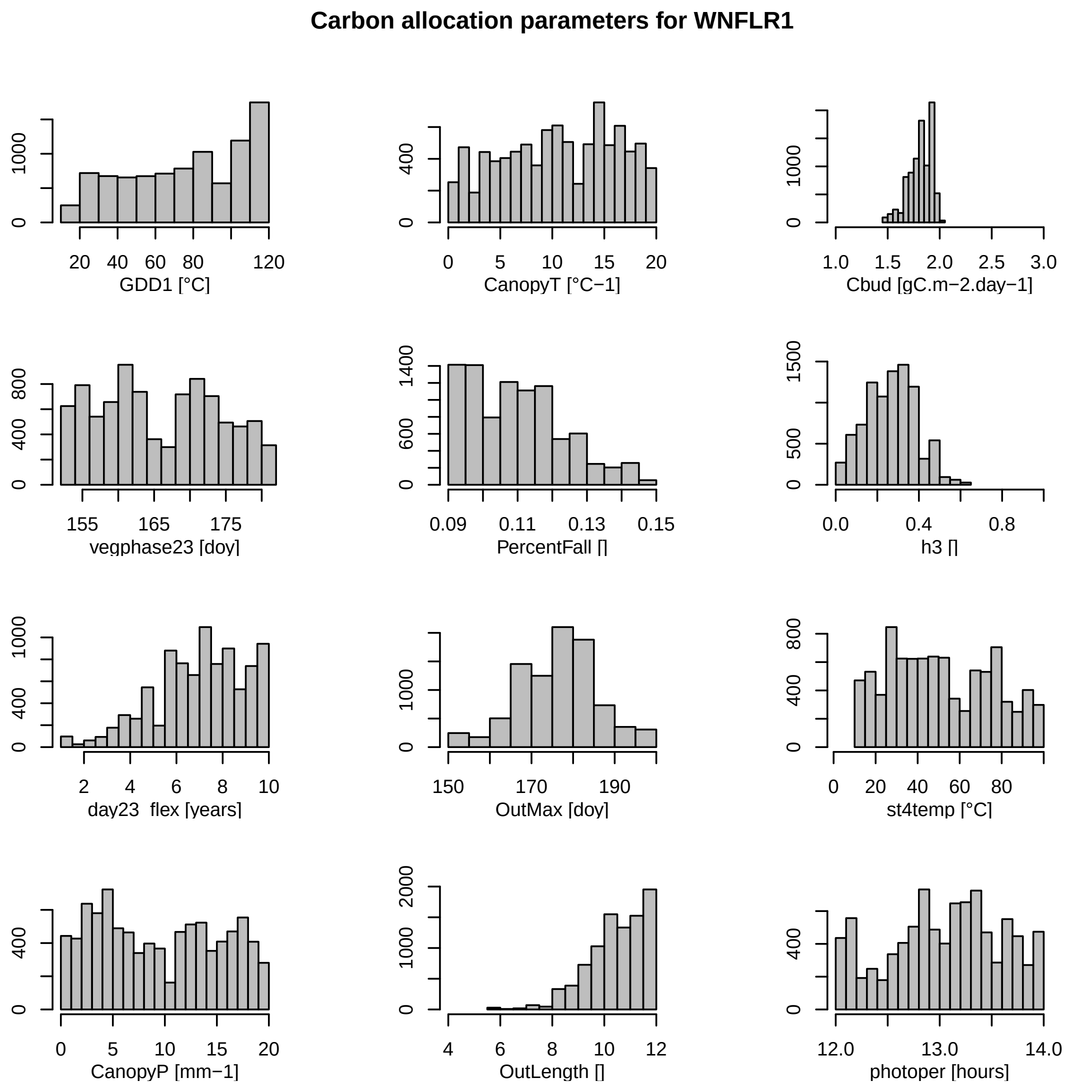

Figure S34. As in Fig. S6 at WNFLR1 site.

Photosynthesis parameters for WNFLR1

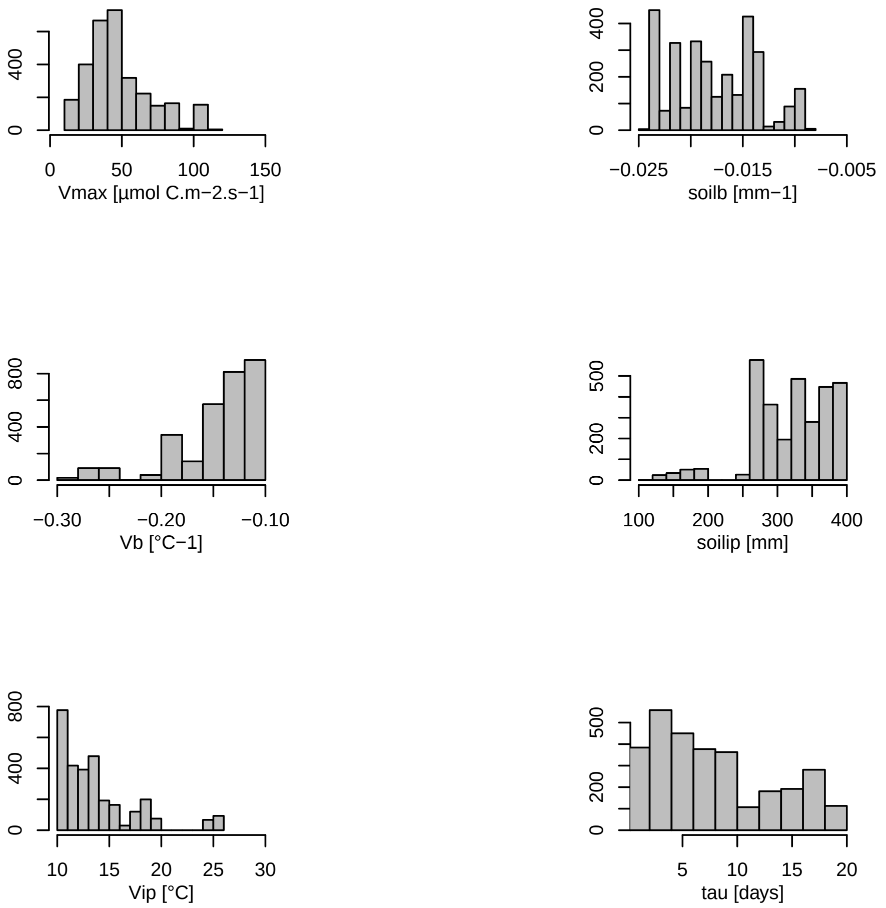

Figure S35. As in Fig. S7 at WNFLR1 site.

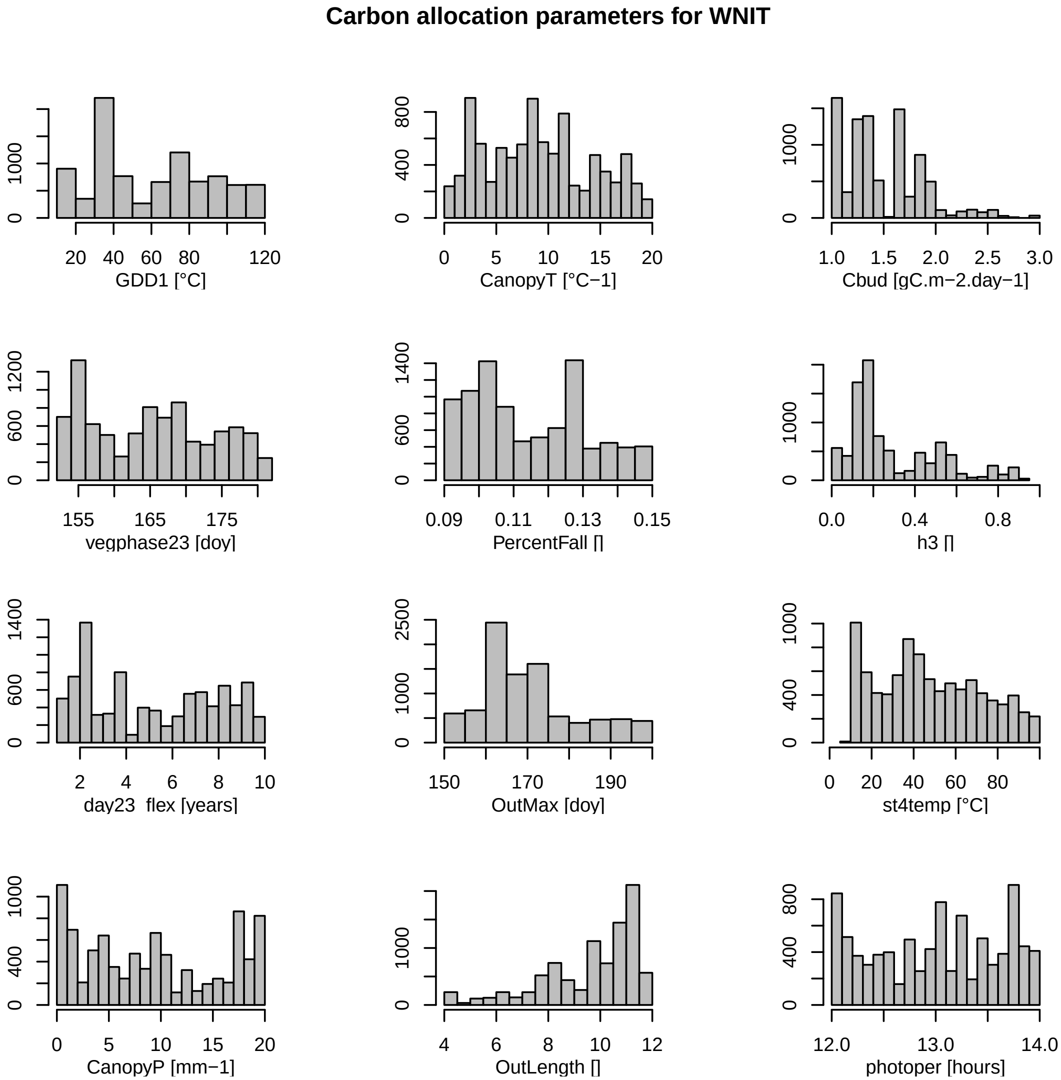

Figure S36. As in Fig. S6 at WNIT site.

Photosynthesis parameters for WNIT

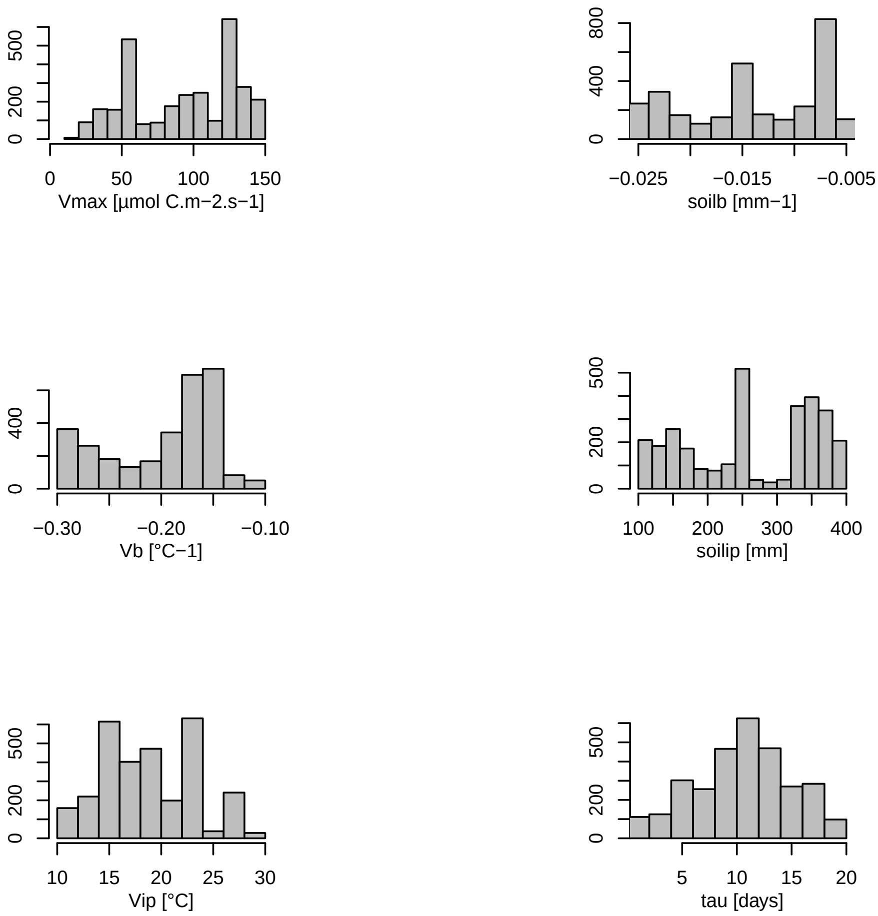

Figure S37. As in Fig. S7 at WNIT site.

Carbon allocation parameters for WPOOL

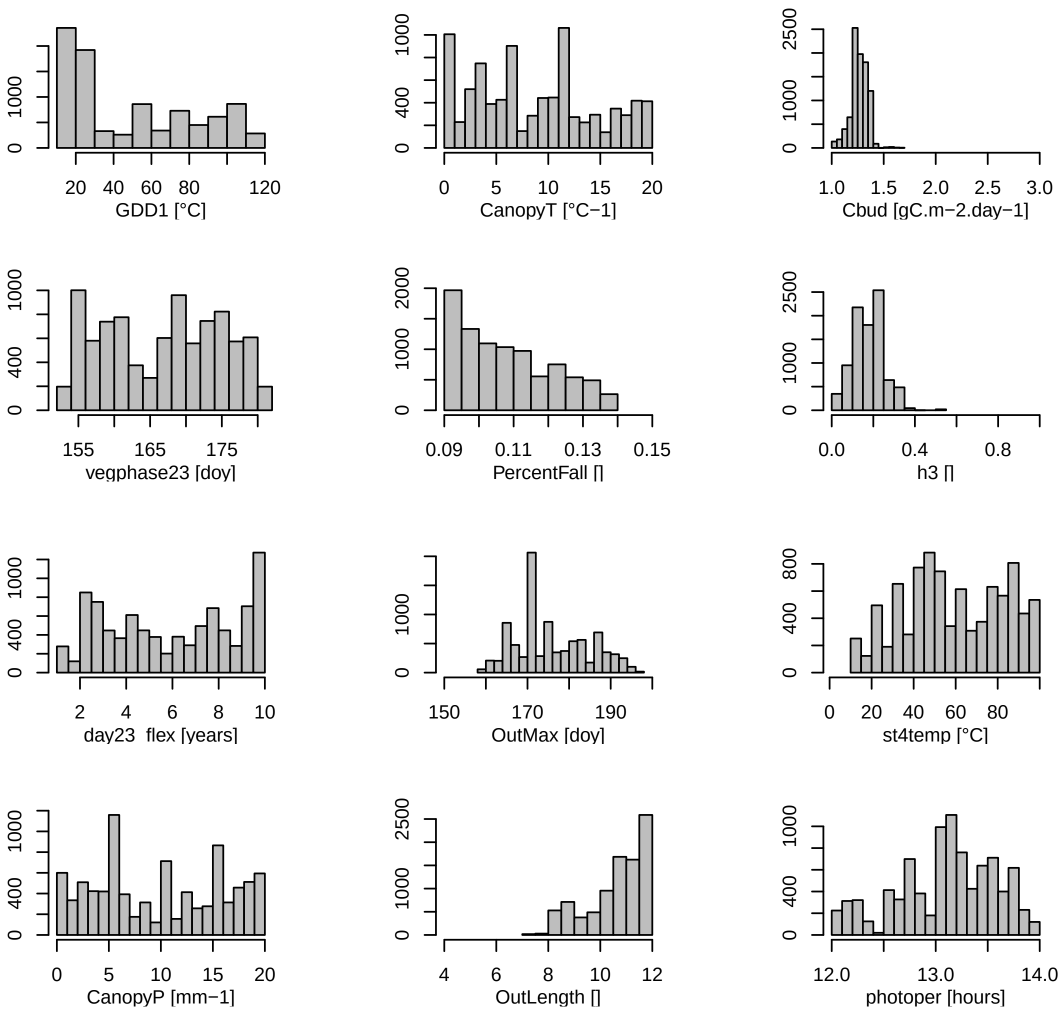

Figure S38. As in Fig. S6 at WPOOL site.

Photosynthesis parameters for WPOOL

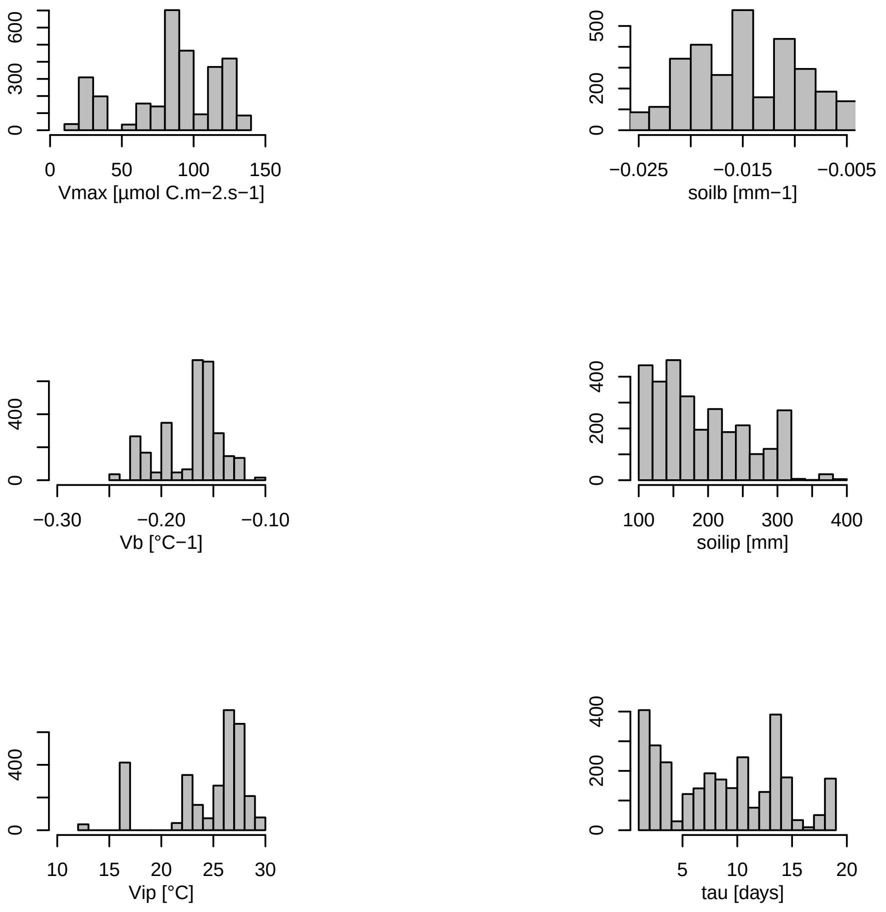

Figure S39. As in Fig. S7 at WPOOL site.

Carbon allocation parameters for WROZM

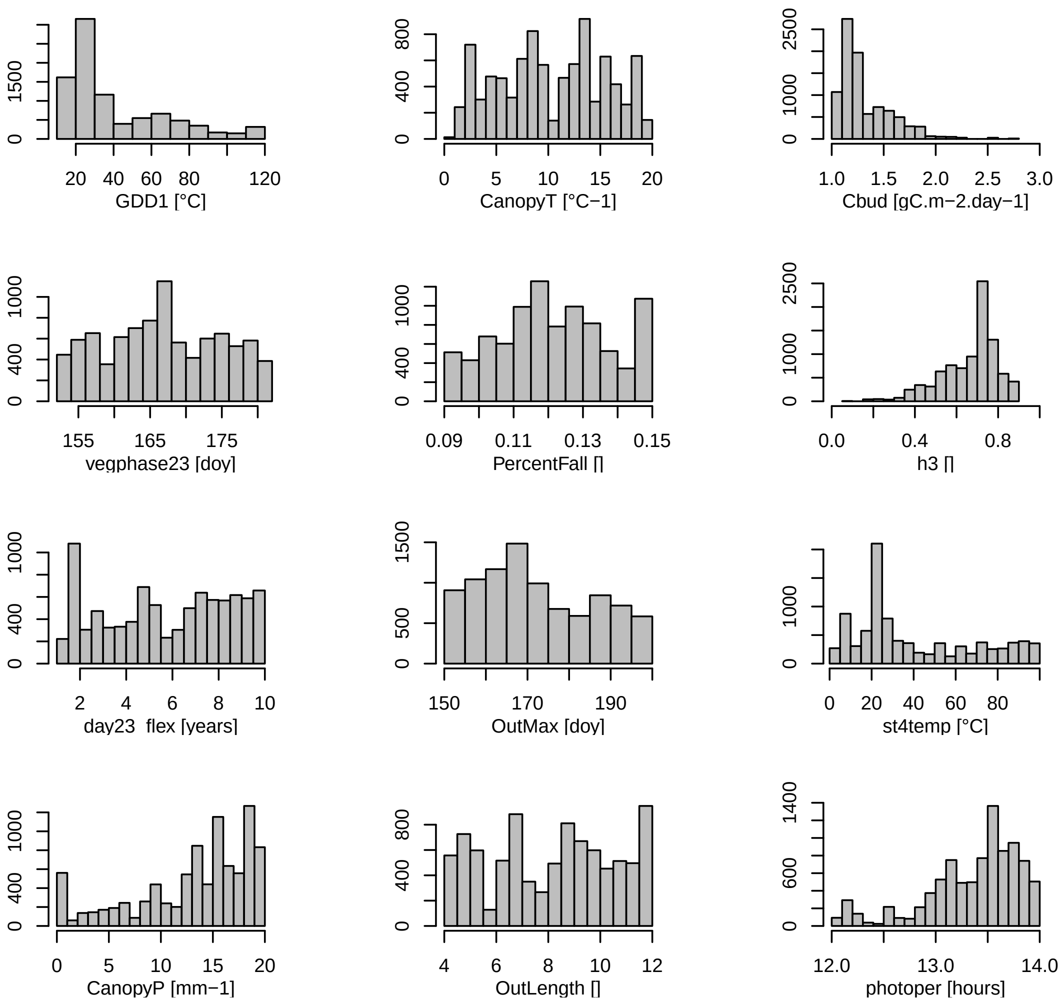

Figure S40. As in Fig. S6 at WROZM site.

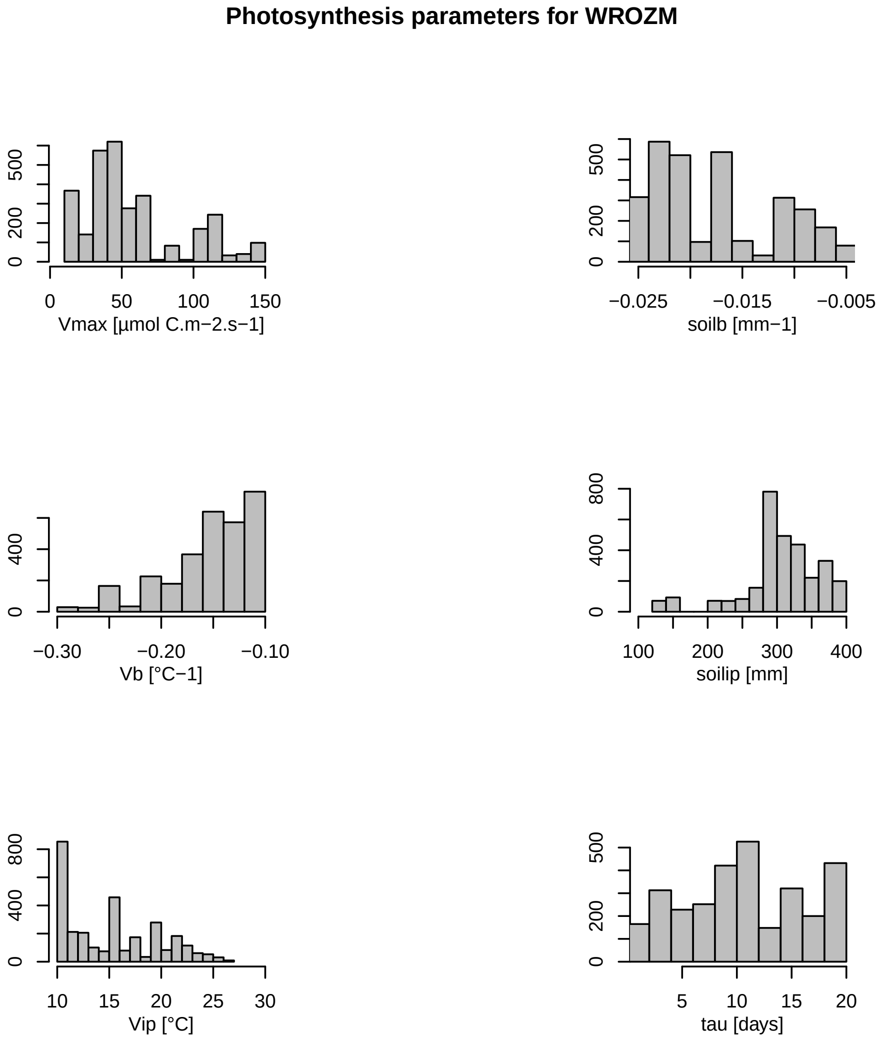

Figure S41. As in Fig. S7 at WROZM site.

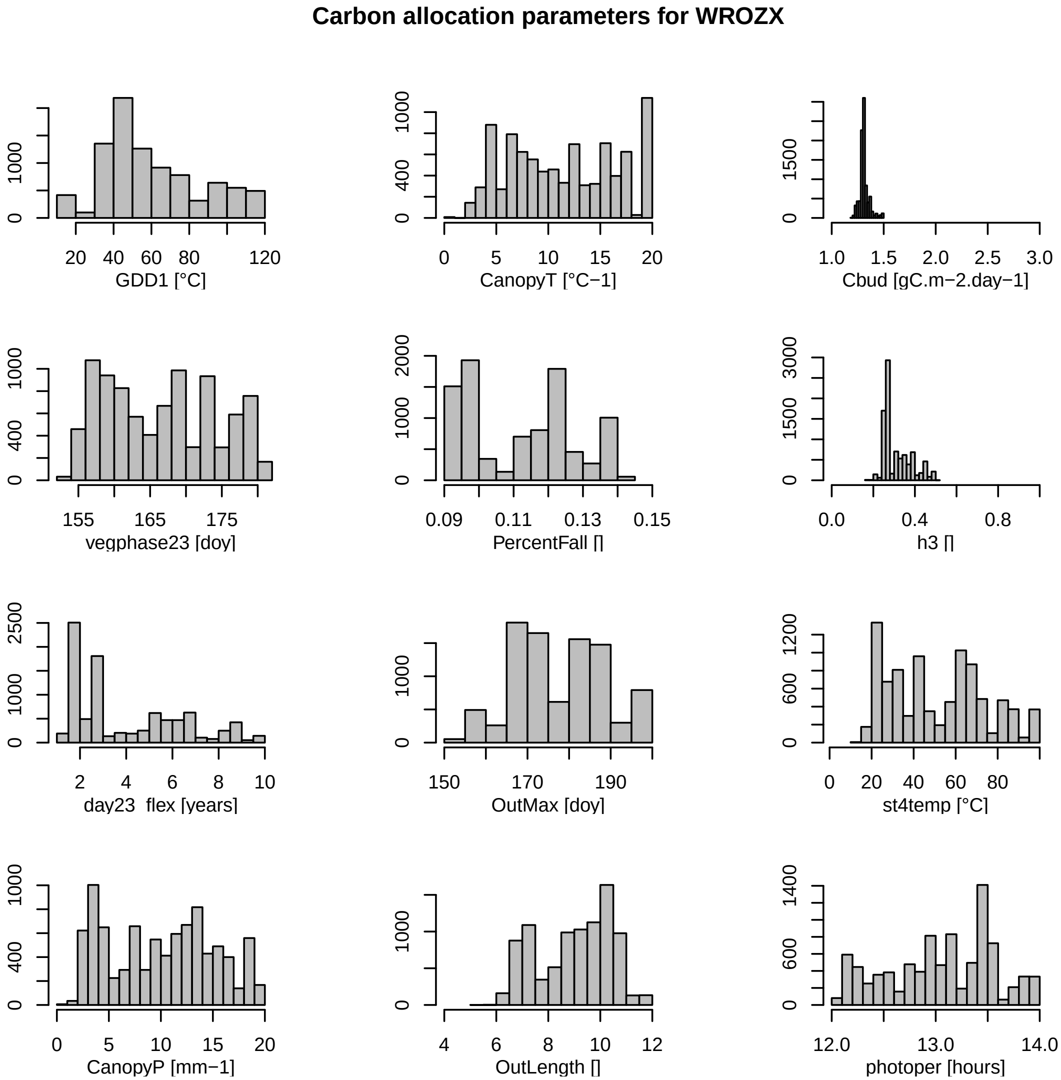

Figure S42. As in Fig. S6 at WROZX site.

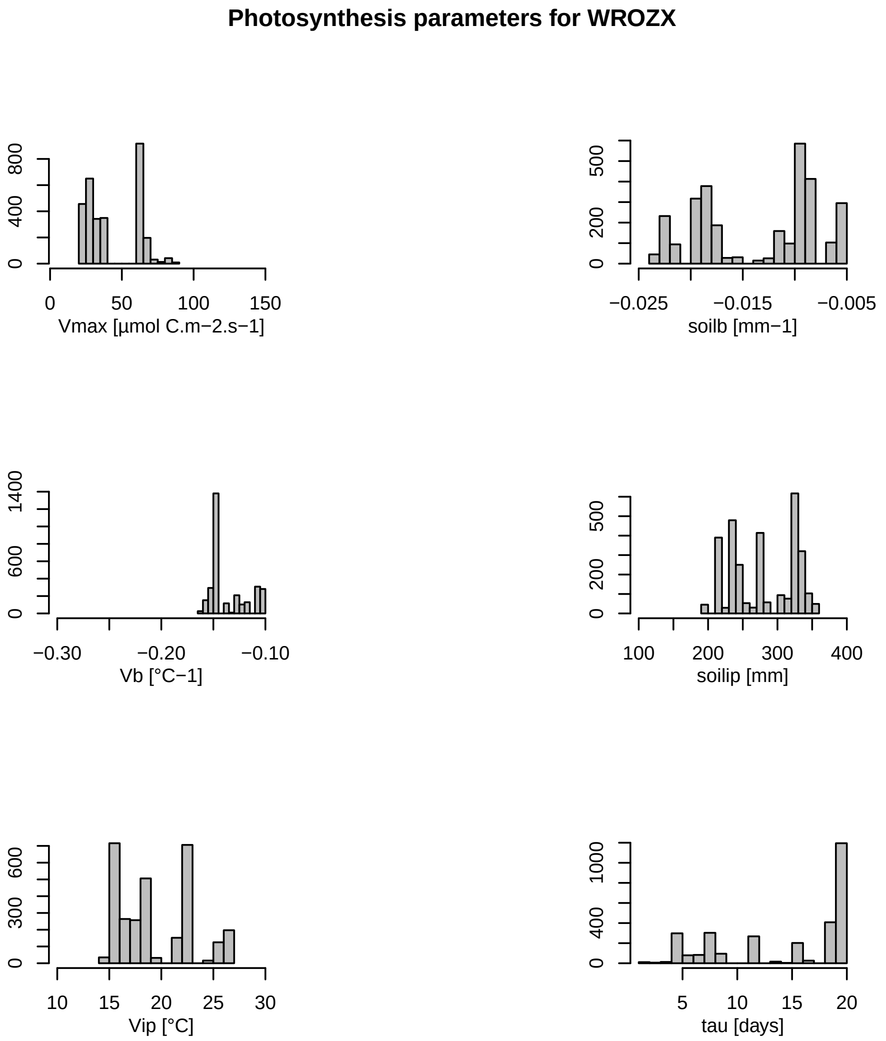

Figure S43. As in Fig. S7 at WROZX site.

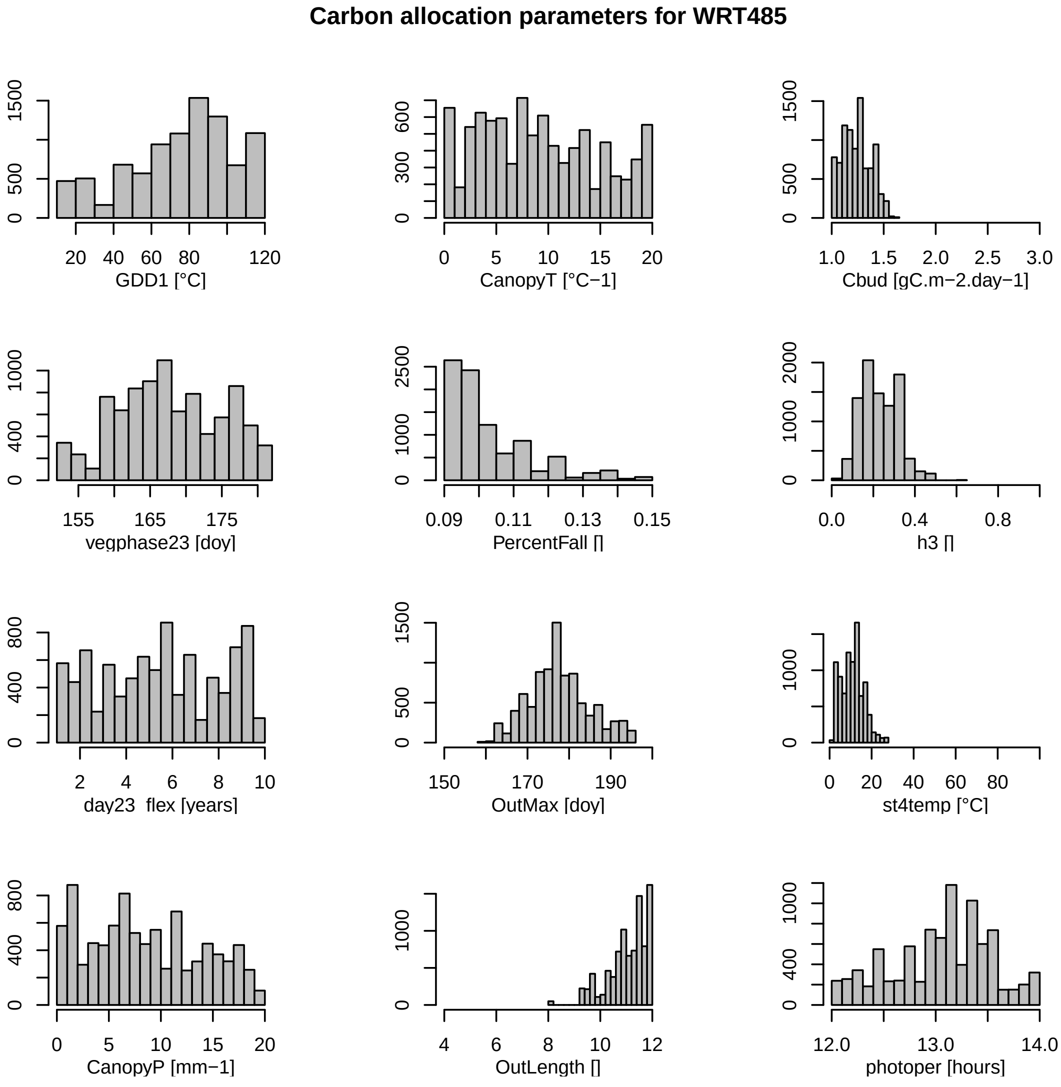

Figure S44. As in Fig. S6 at WRT485 site.

Photosynthesis parameters for WRT485

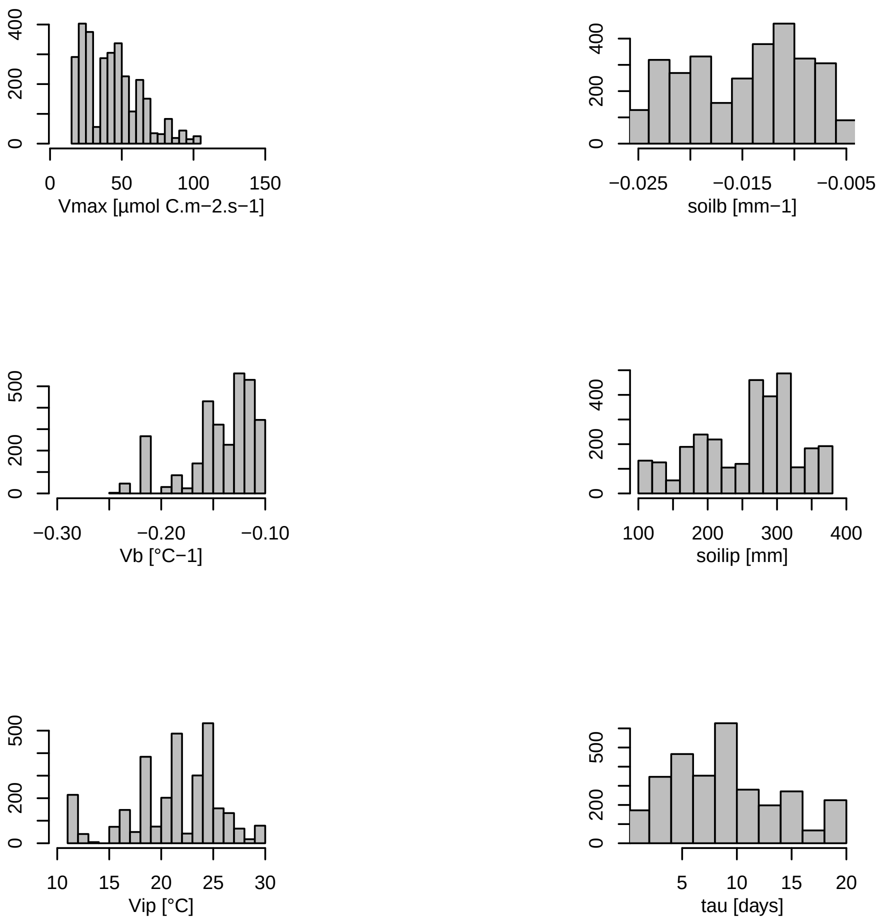

Figure S45. As in Fig. S7 at WRT485 site.

Carbon allocation parameters for WTHH

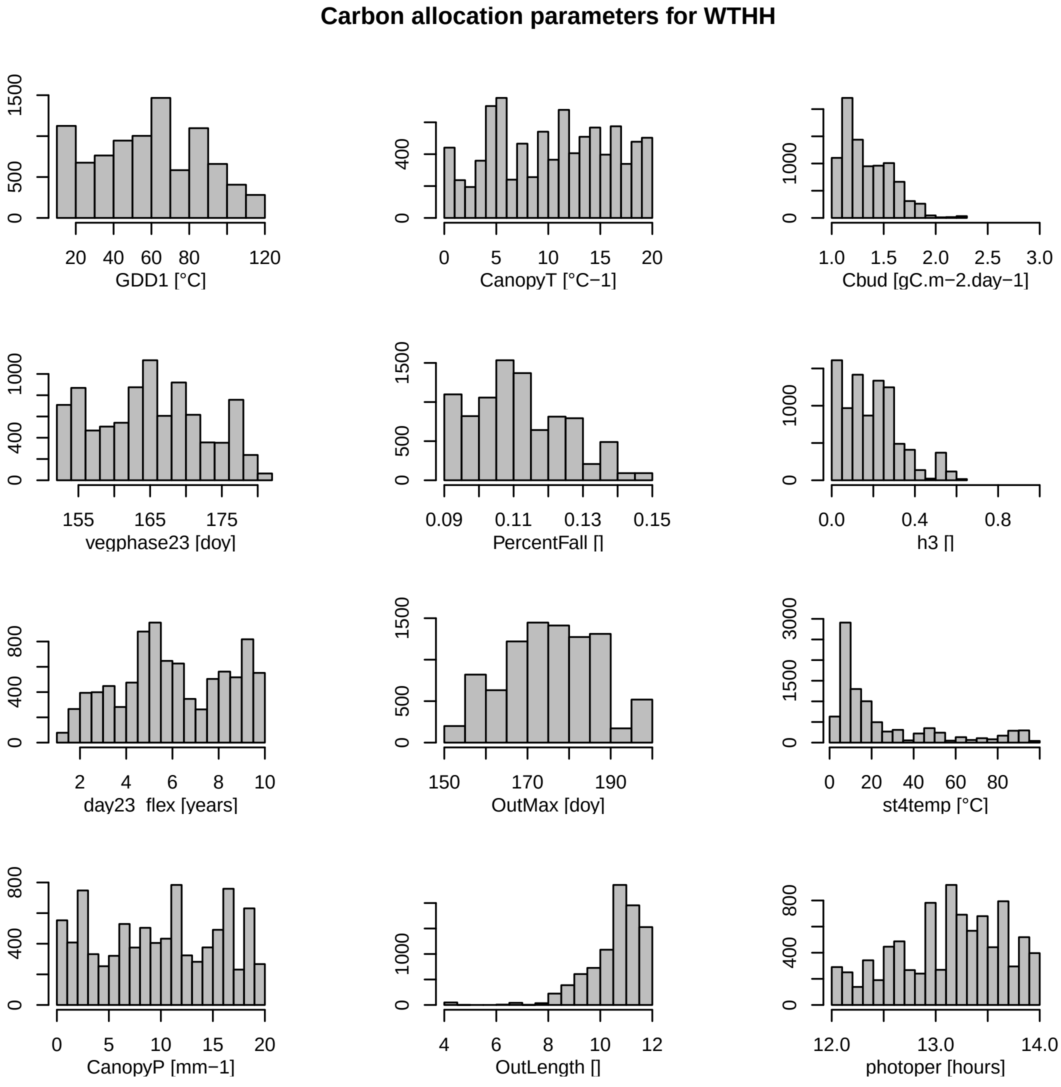

Figure S46. As in Fig. S6 at WTHH site.

Photosynthesis parameters for WTHH

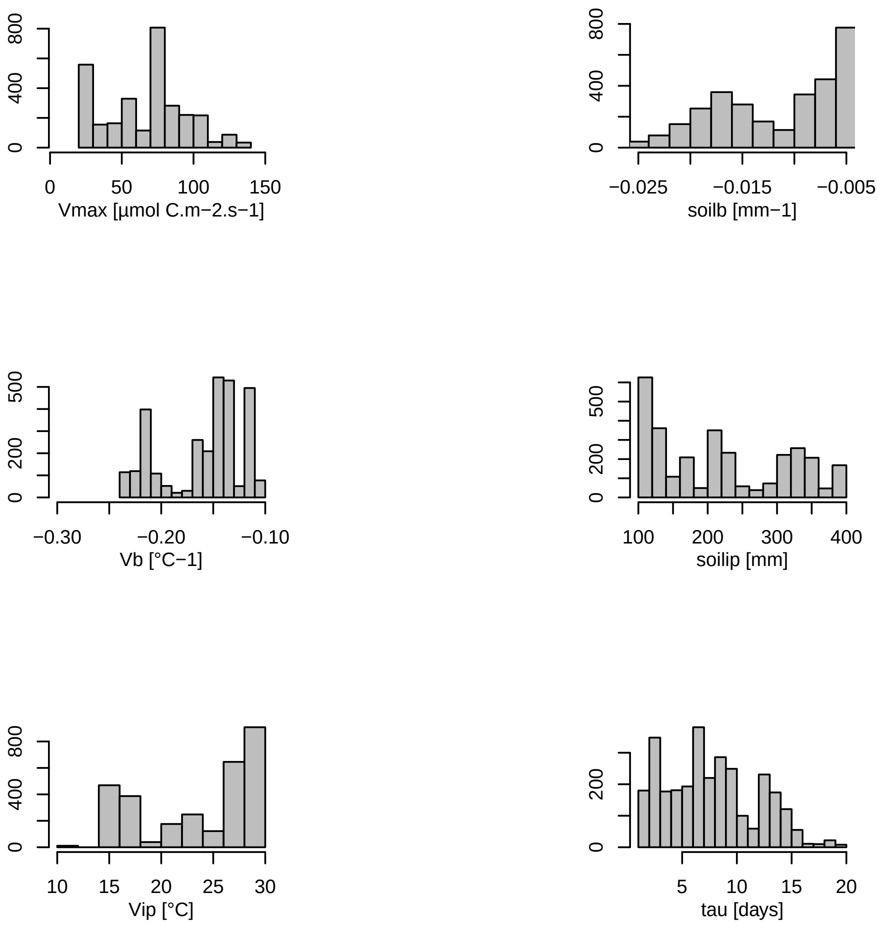

Figure S47. As in Fig. S7 at WTHH site.

Carbon allocation parameters for WROZ

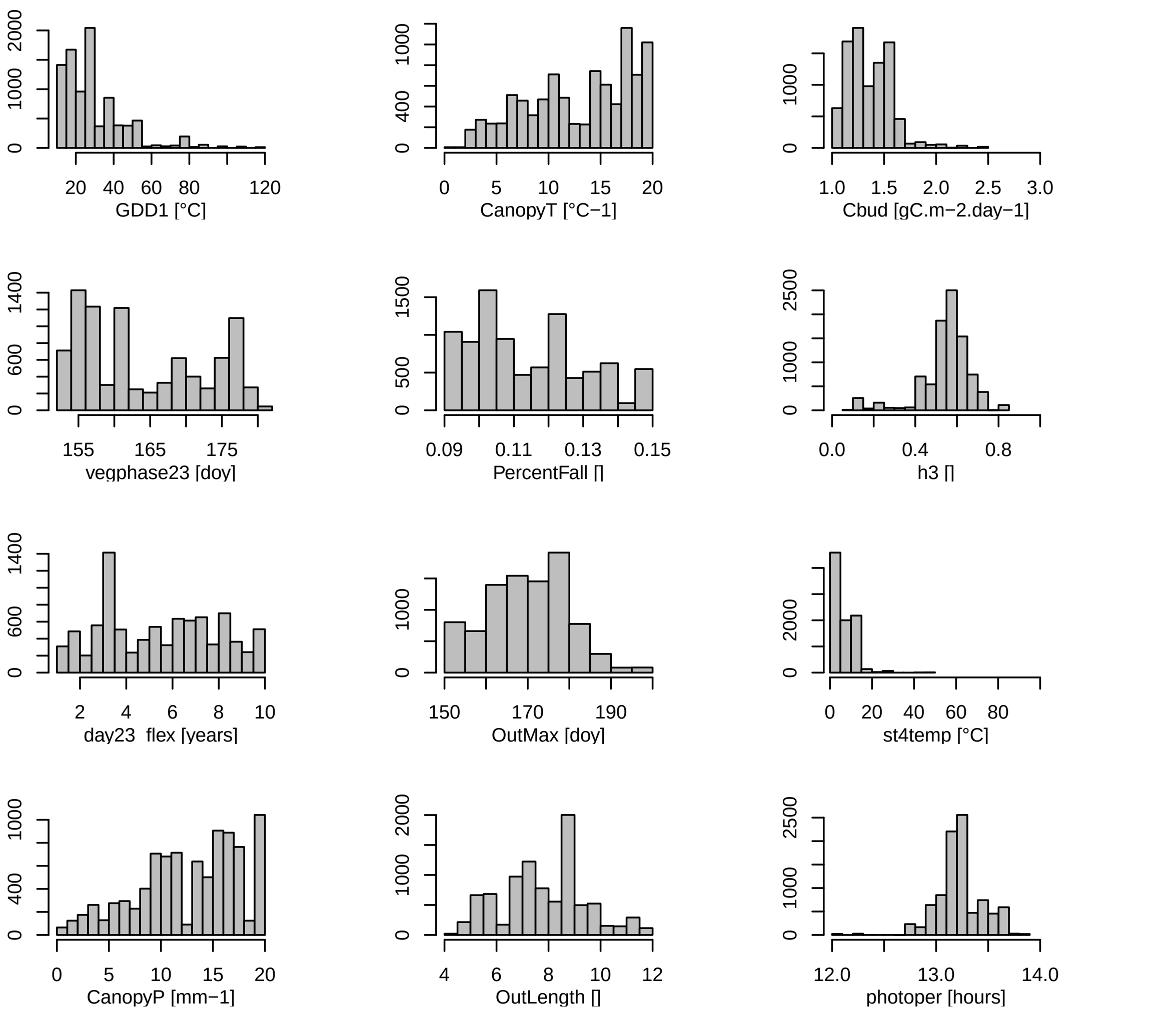

Figure S48. Posterior frequency distributions of carbon allocation parameters (Table S3) at WROZ site (NRCAN (5') climatic dataset) (Fig. 1b, Table 2) for the 1950-2000 calibration period.

Photosynthesis parameters for WROZ

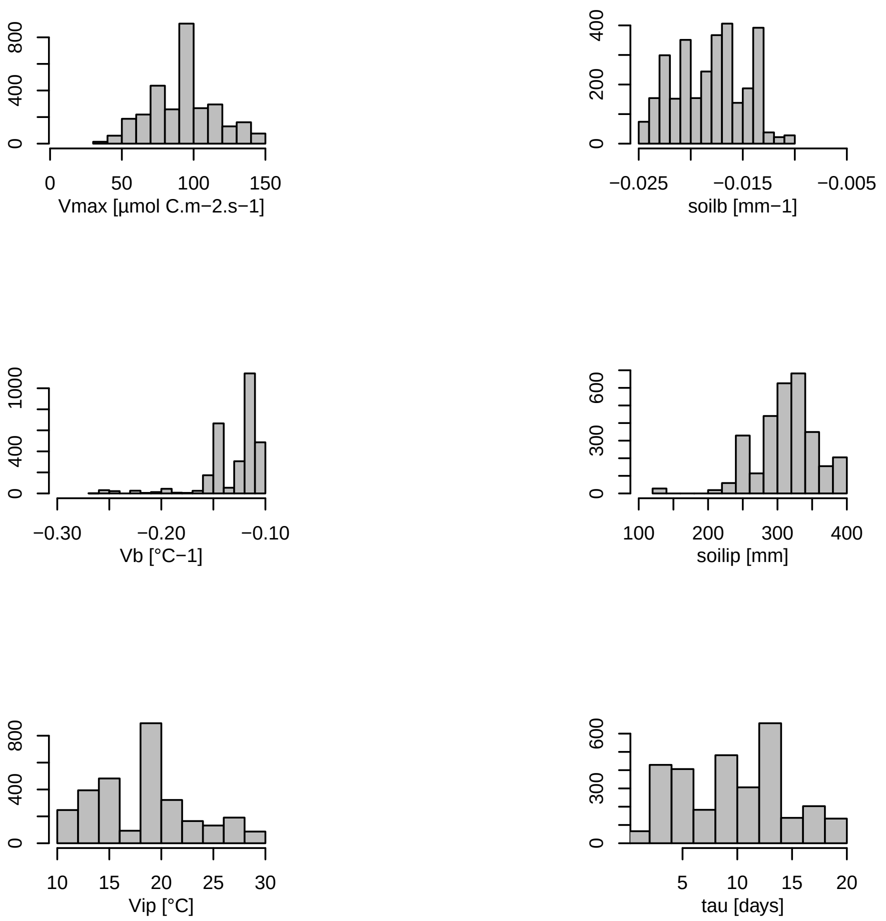

Figure S49. Posterior frequency distributions of photosynthesis parameters (Table S3) at WROZ site (NRCAN (5') climatic dataset) (Fig. 1b, Table 2) for the 1950-2000 calibration period.

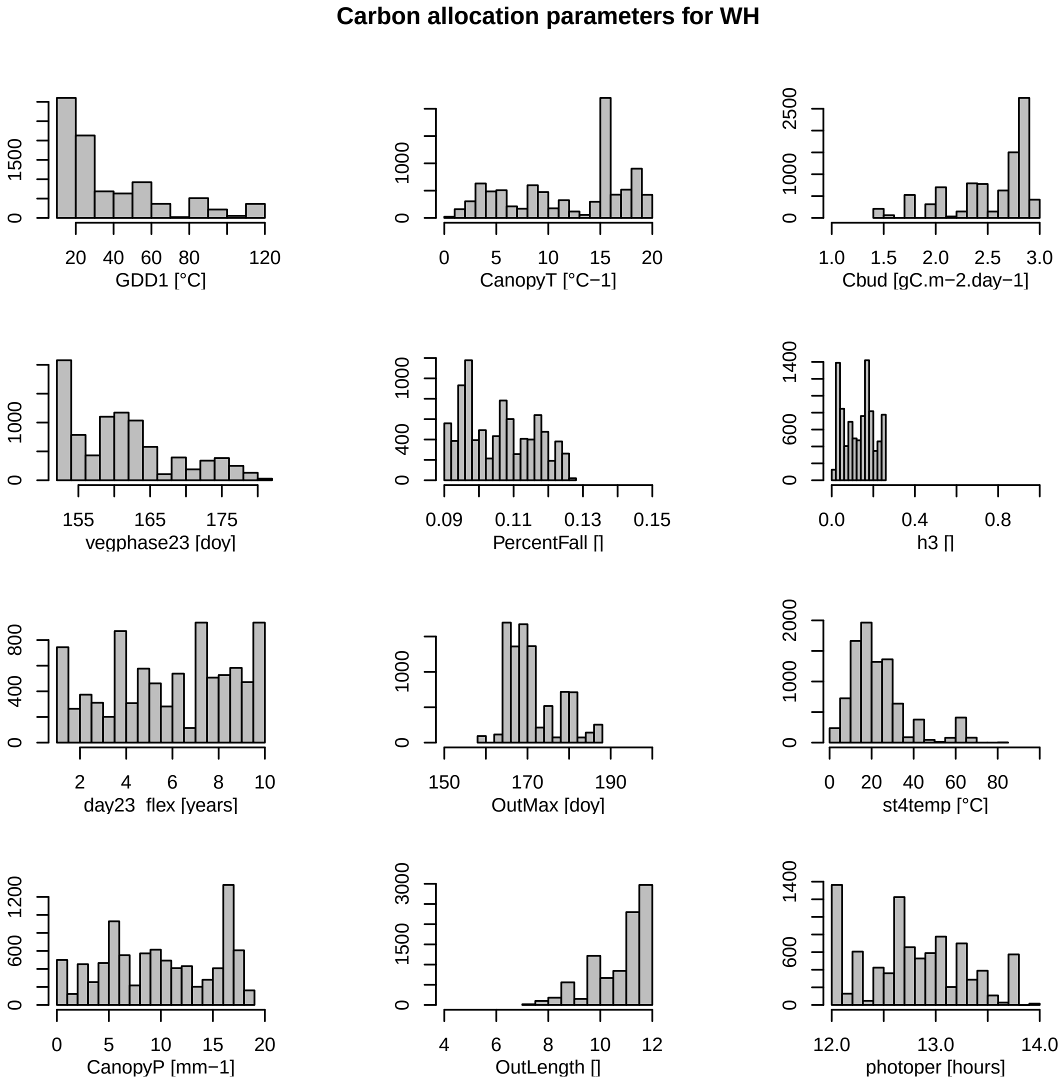

Figure S50. As in Fig. S48 at WH site.

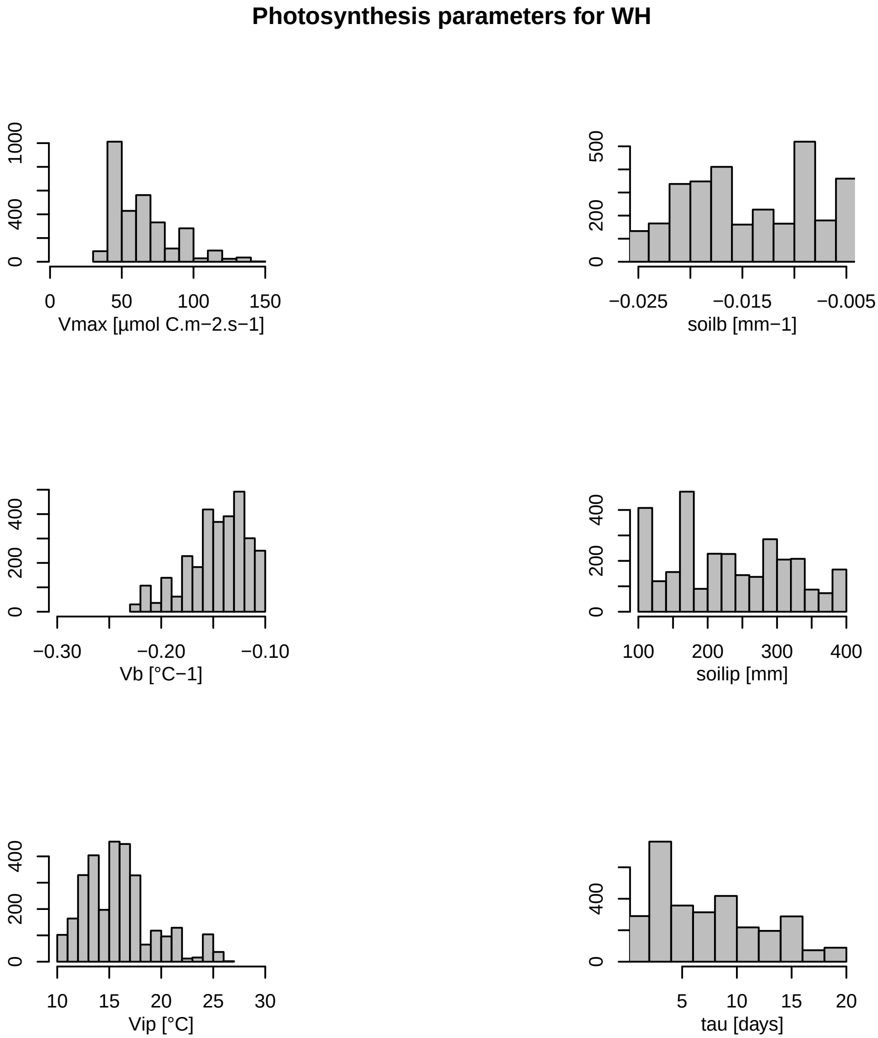

Figure S51. As in Fig. S49 at WH site.

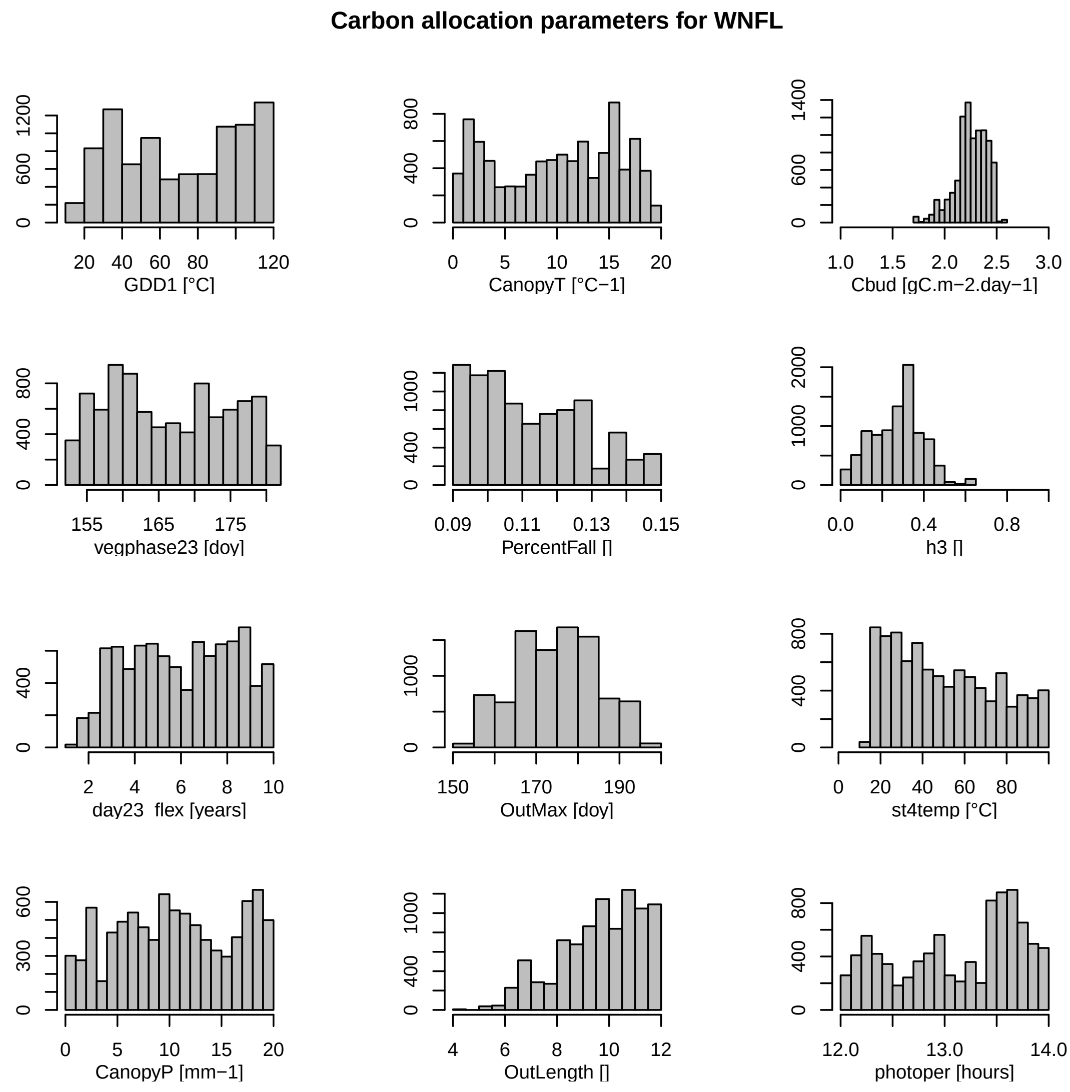

Figure S52. As in Fig. S48 at WNFL site.

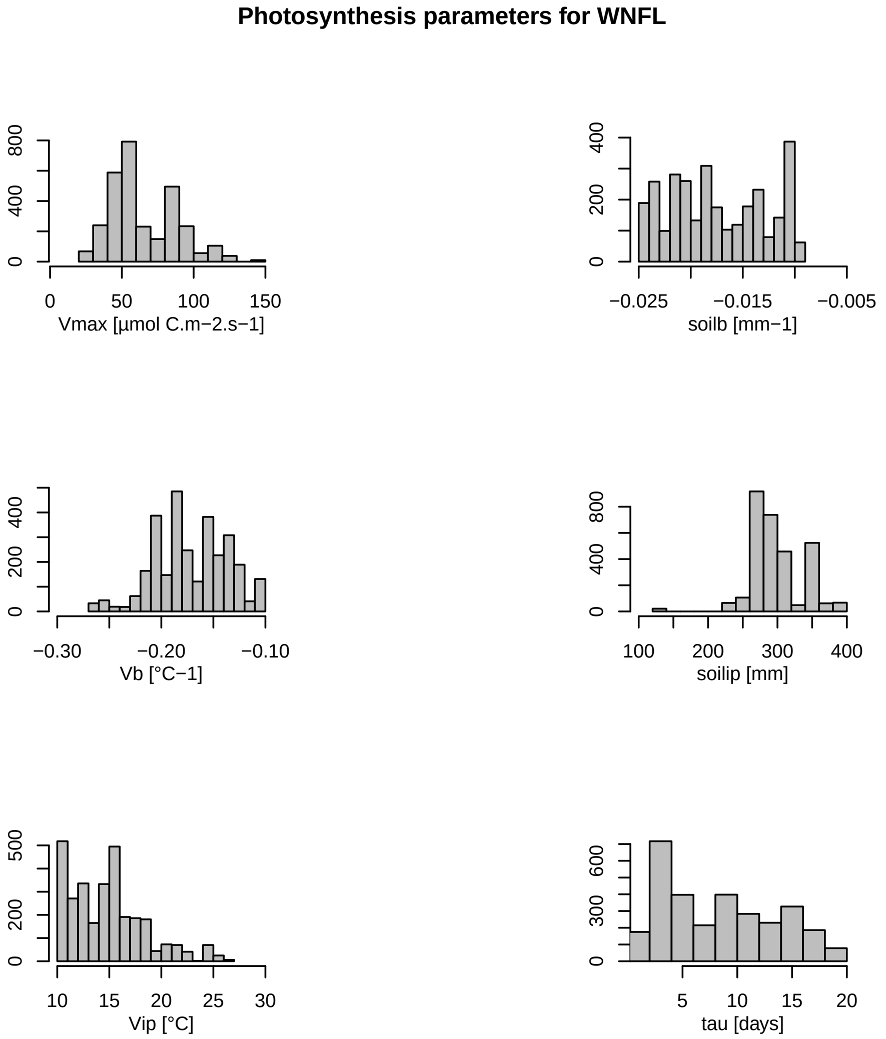

Figure S53. As in Fig. S49 at WNFL site.

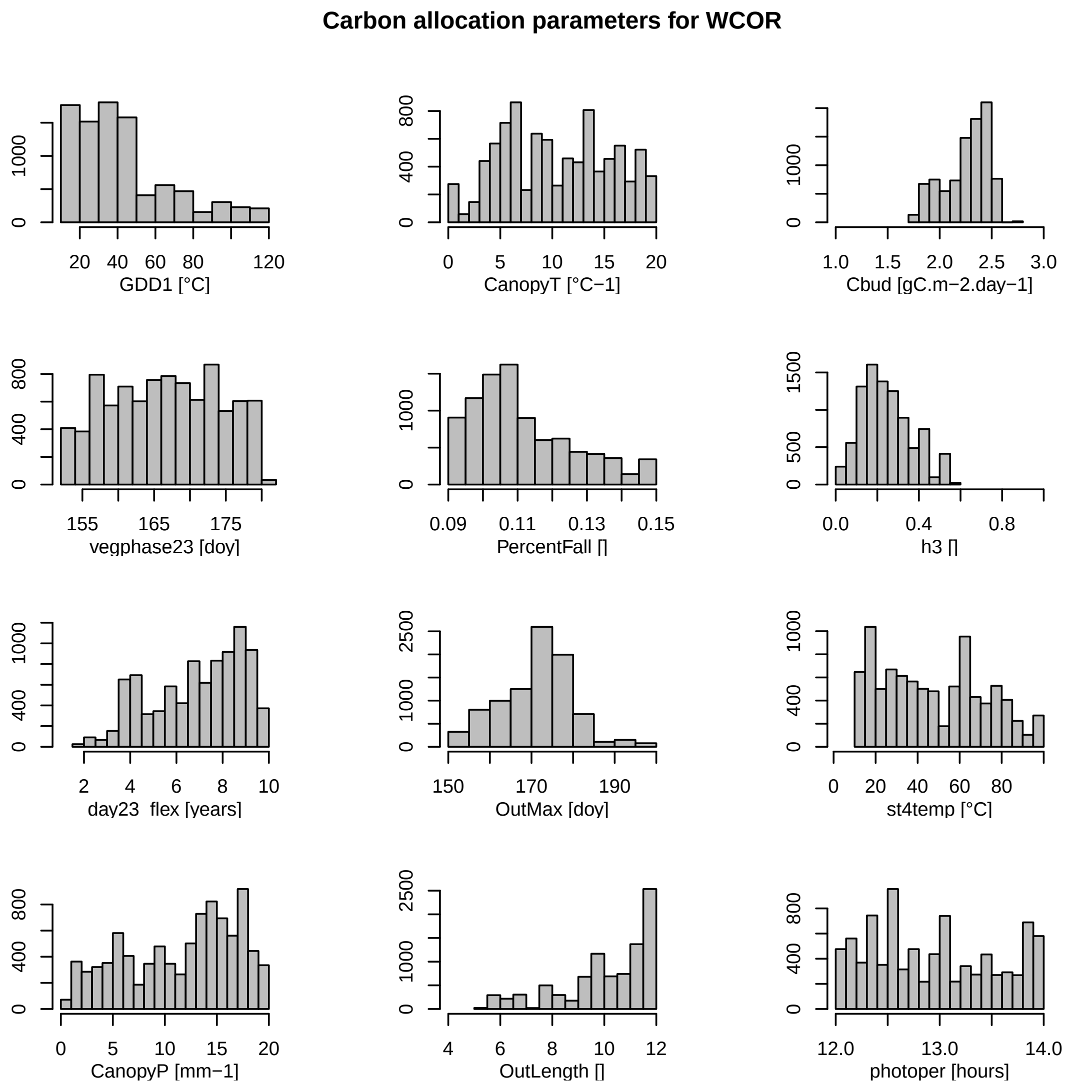

Figure S54. As in Fig. S48 at WCOR site.

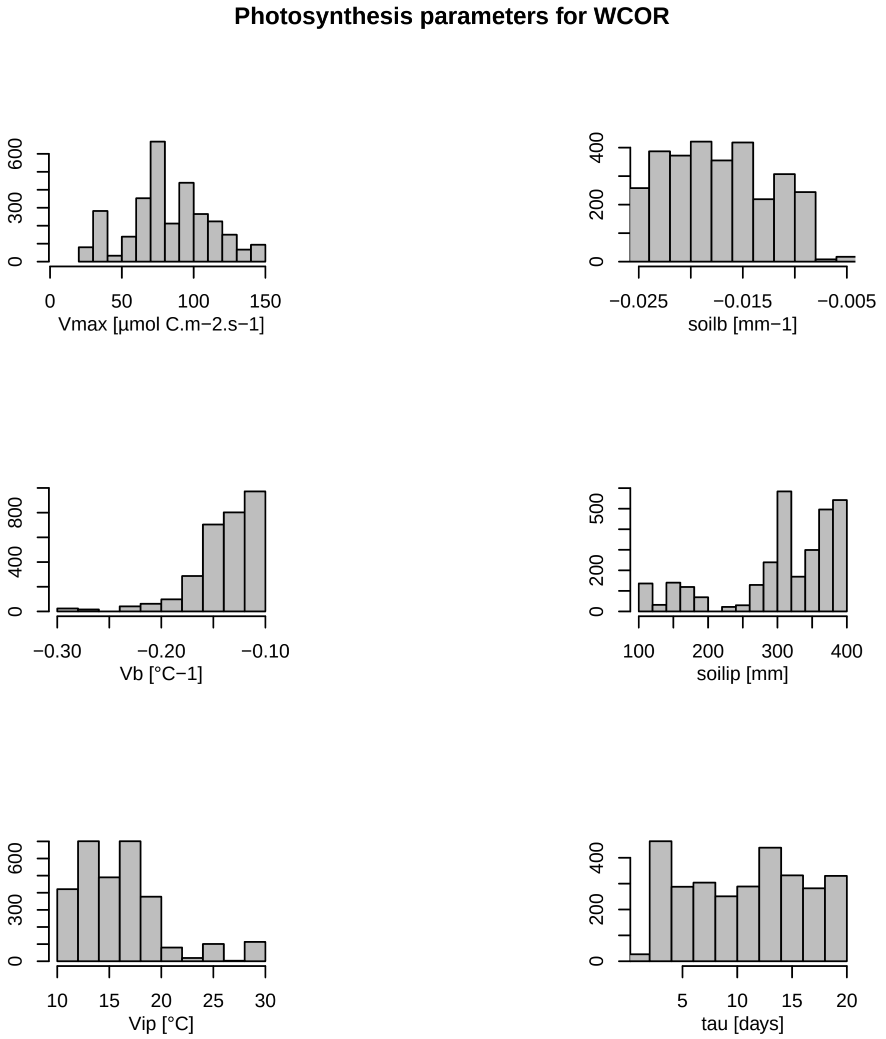

Figure S55. As in Fig. S49 at WCOR site.

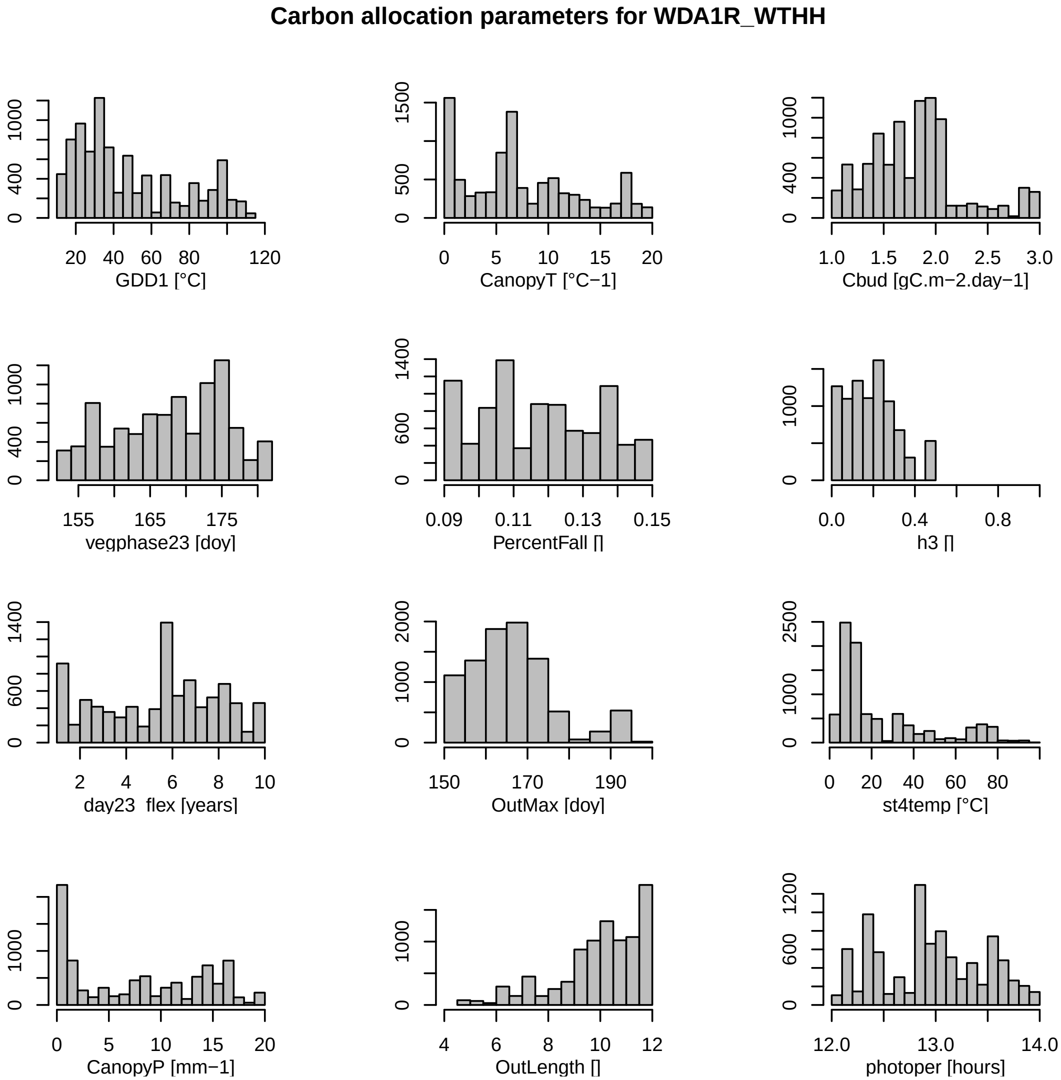

Figure S56. As in Fig. S48 at WDA1R_WTHH site.

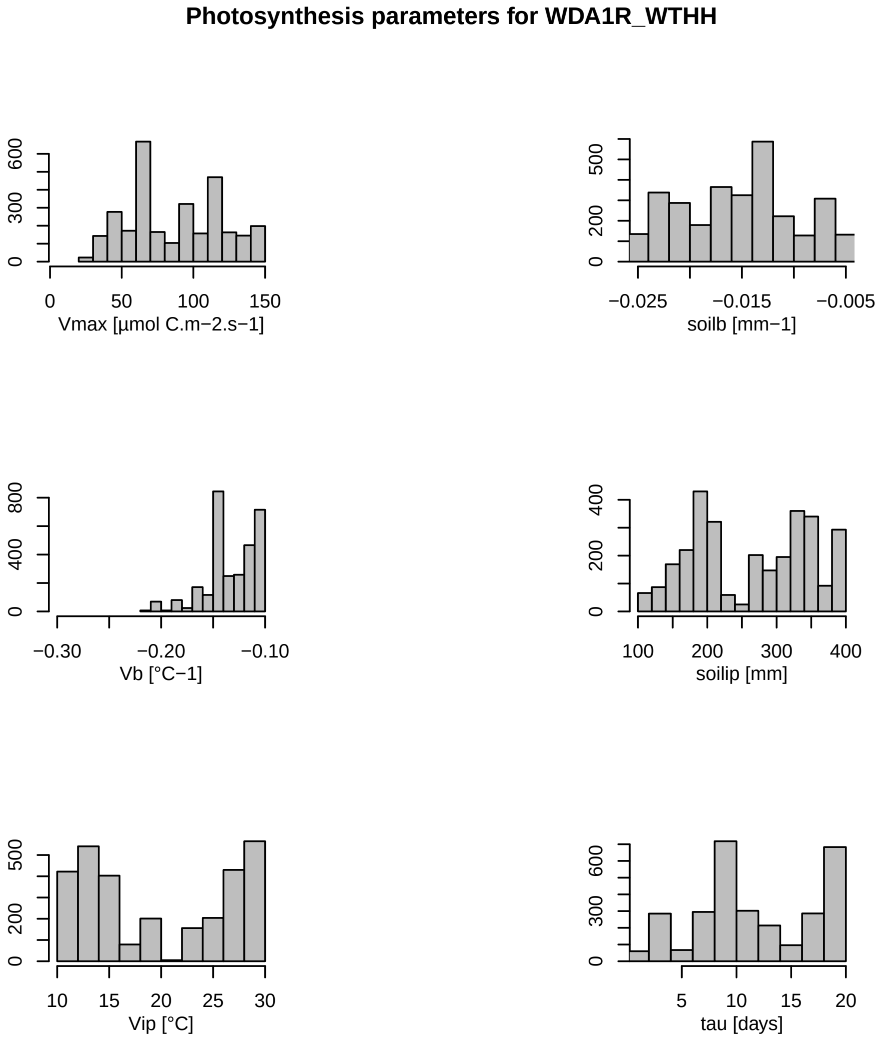

Figure S57. As in Fig. S49 at WDA1R_WTHH site.

Carbon allocation parameters for EALP

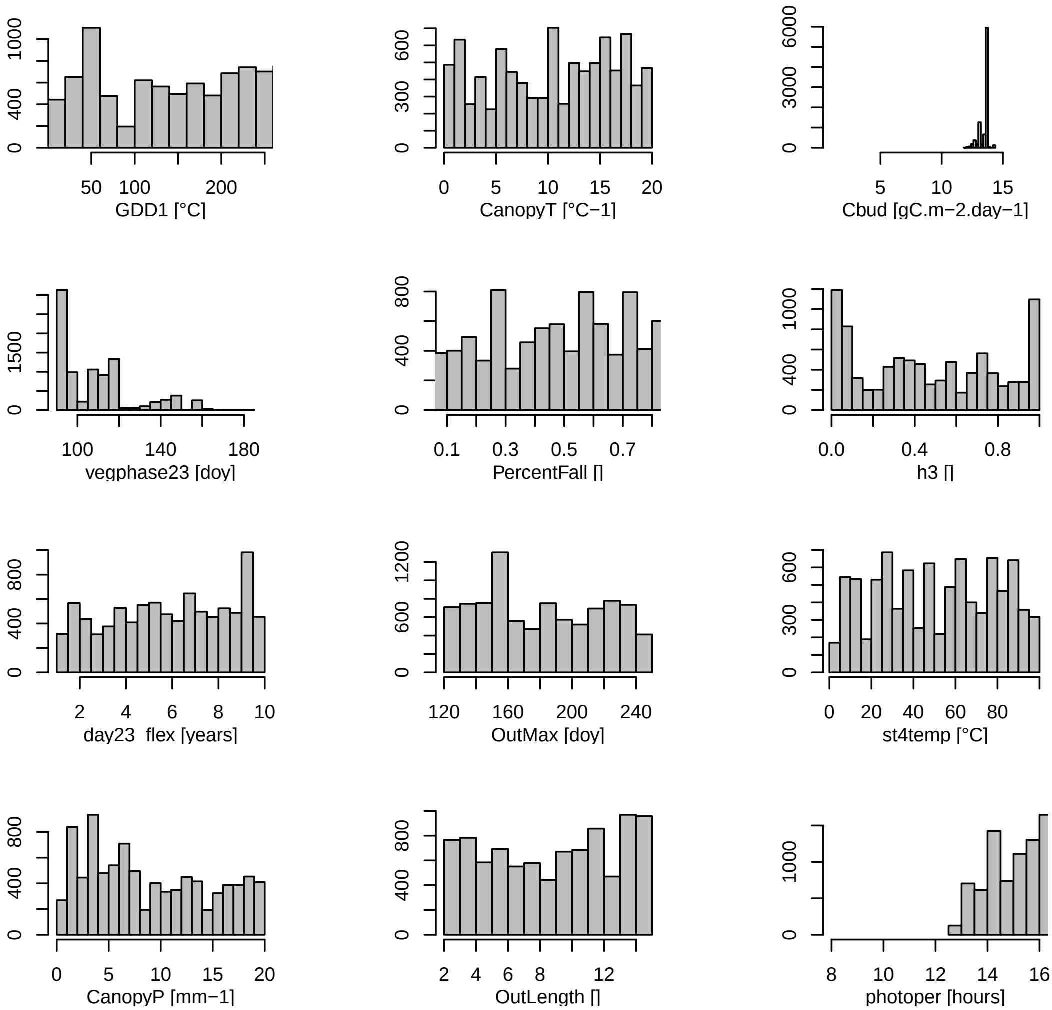

Figure S58. Posterior frequency distributions of carbon allocation parameters (Table S3) at EALP site (GHCN climate data) (Fig. 2, Table 2) for the 1950-2000 calibration period.

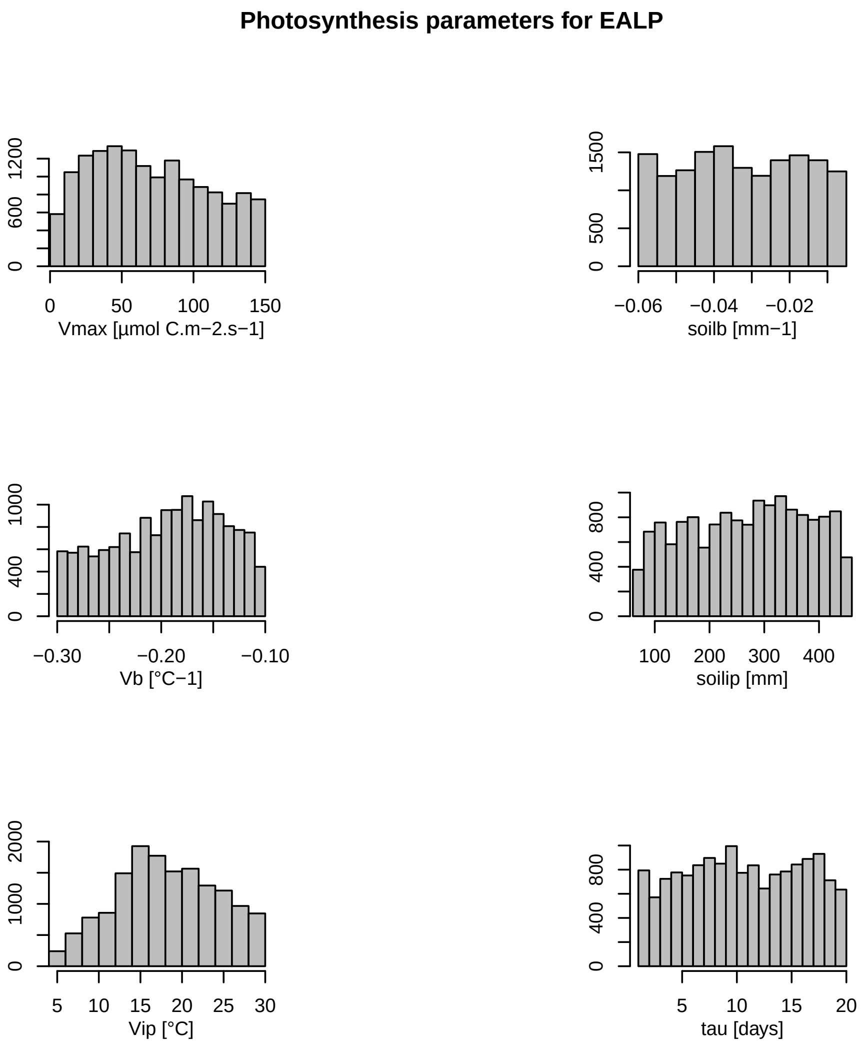

Figure S59. Posterior frequency distributions of photosynthesis parameters (Table S3) at EALP site (GHCN climate data) (Fig. 2, Table 2) for the 1950-2000 calibration period.

Carbon allocation parameters for SWIT179

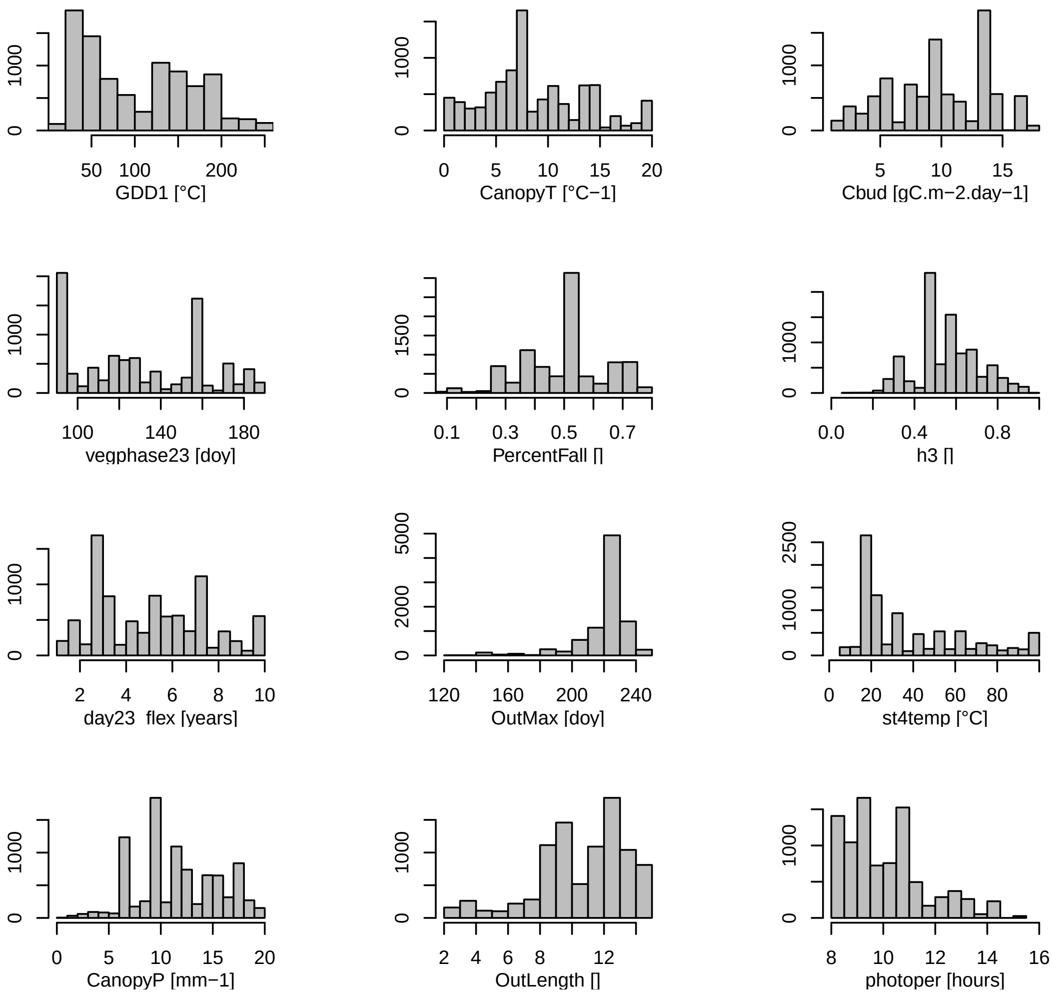

Figure S60. As in Fig. S58 at SWIT179 site.

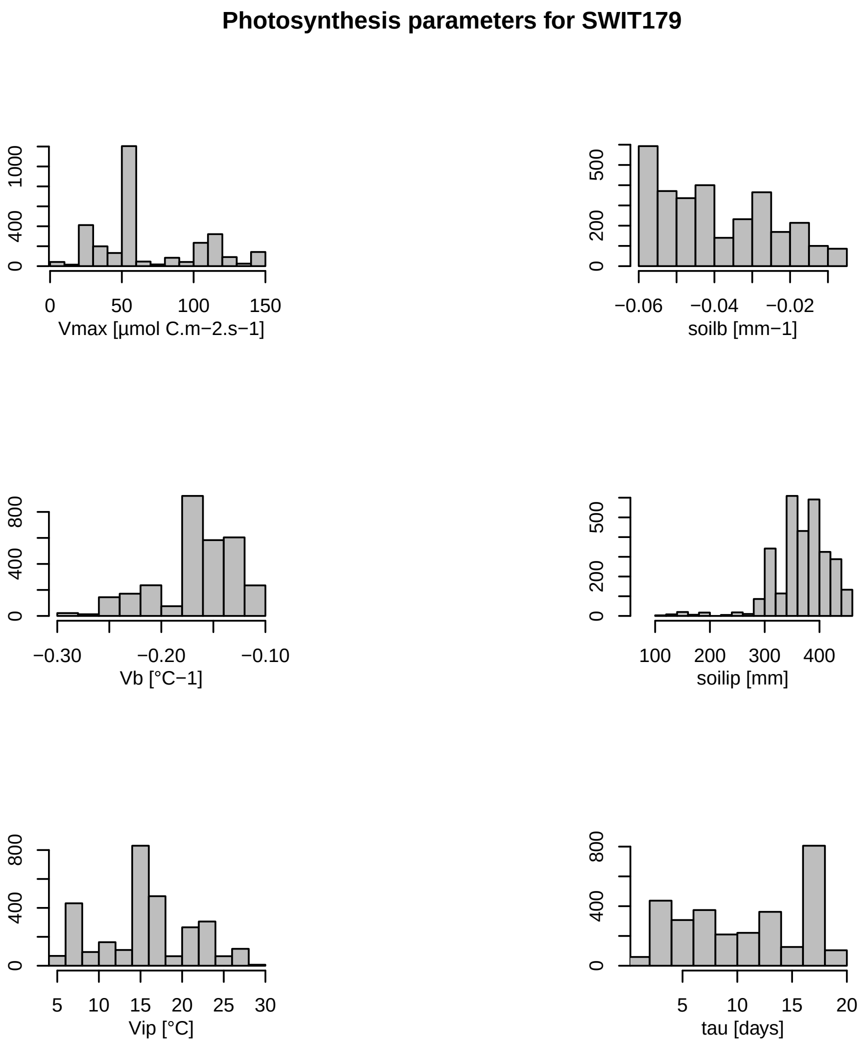

Figure S61. As in Fig. S59 at SWIT179 site.

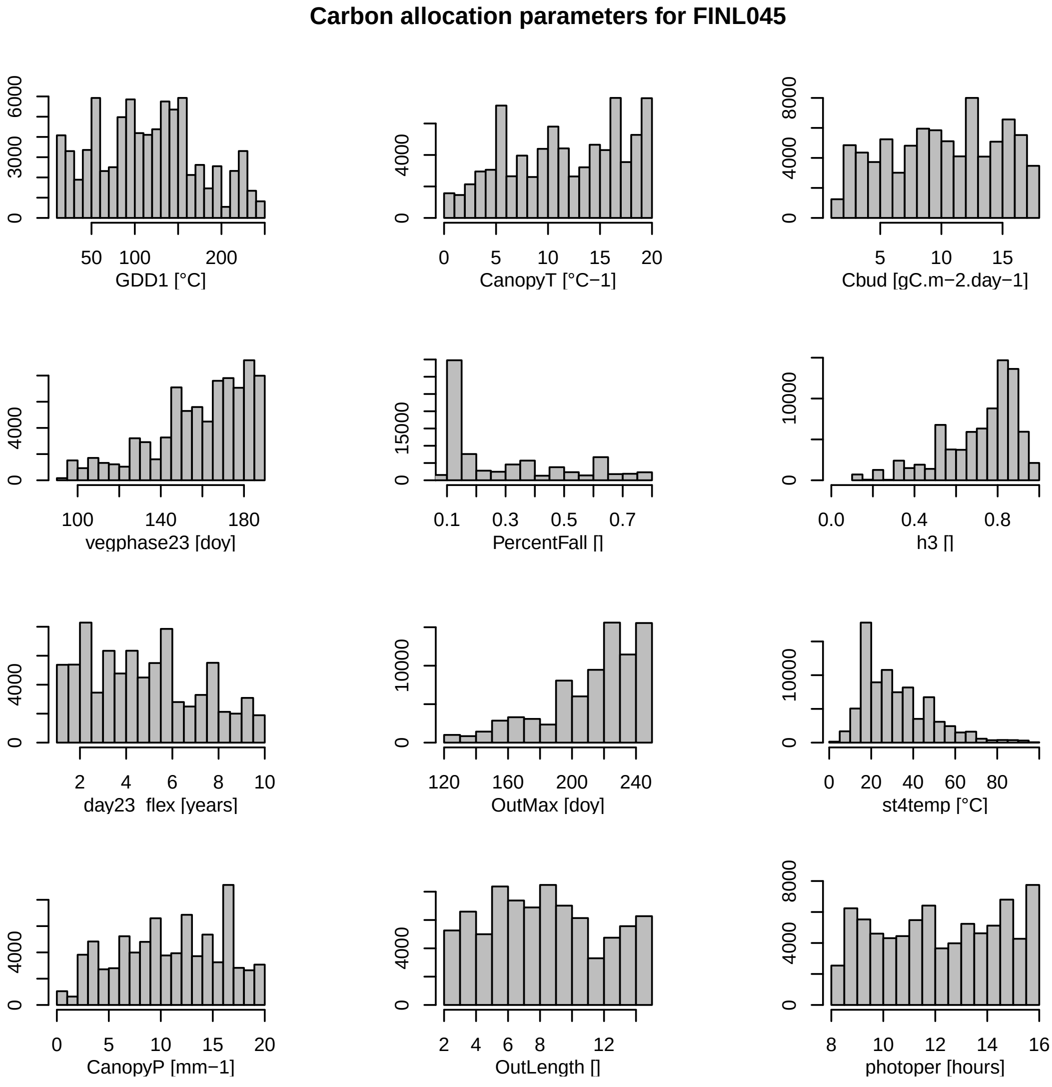

Figure S62. As in Fig. S58 at FINL045 site.

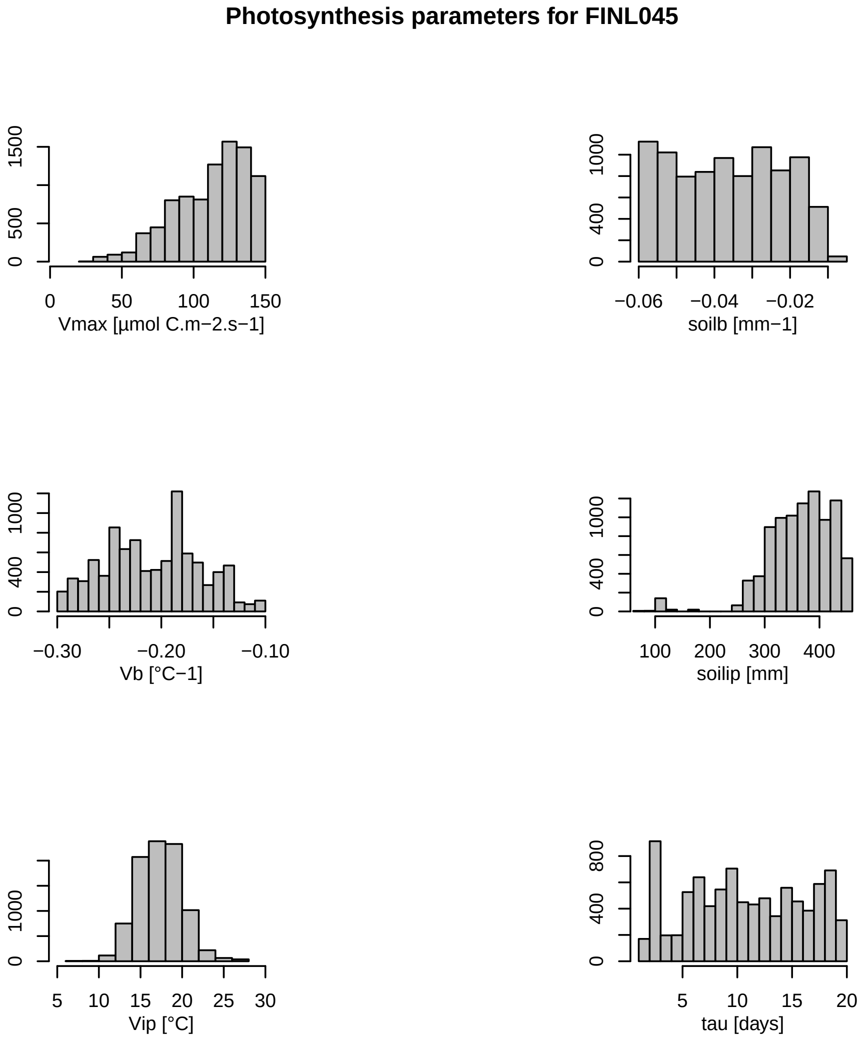

Figure S63. As in Fig. S59 at FINL045 site.